SCINTIGRAPHIC STUDIES TO EVALUATE GASTRIC FUNCTIONS

ATCHARA PROMDAUNG

**A THESIS SUBMITTED IN PARTIAL FULFILLMENT
OF THE REQUIREMENTS FOR
THE DEGREE OF MASTER OF SCIENCE
(MEDICAL PHYSICS)
FACULTY OF GRADUATE STUDIES
MAHIDOL UNIVERSITY
2011**

Thesis
entitled

SCINTIGRAPHIC STUDIES TO EVALUATE GASTRIC FUNCTIONS

……

Miss. Atchara Promdaung
Candidate

……

Asst. Prof. Chanika Sritara, M.D.
M.Sc. (Nuclear Medicine)
M.Sc. (Clinical Epidemiology)
Major advisor

……

Assoc. Prof. Chiraporn Tocharoenchai,
Ph.D. (Biomedical Engineering)
Co-advisor

……

Prof. Banchong Mahaisavariya,
M.D., Dip. Thai Board of Orthopedics
Dean
Faculty of Graduate Studies
Mahidol University

……

Lect. Puangpen Tangboonduangjit,
Ph.D. (Medical Radiation Physics)
Program Director
Master of Science Program
in Medical Physics
Faculty of Medicine
Ramathibodi Hospital
Mahidol University

Thesis
entitled

SCINTIGRAPHIC STUDIES TO EVALUATE GASTRIC FUNCTIONS

was submitted to the Faculty of Graduate Studies, Mahidol University
for the degree of Master of Science (Medical Physics)
on
January 31, 2011

……
Miss. Atchara Promdaung
Candidate

.....
Assoc. Prof. Supatporn Tepmongkol, M.D.
Member

……
Assoc. Prof. Pawana Pusuwan, M.D.
Chair

.....
Assoc. Prof. Chiraporn Tocharoenchai, Ph.D. (Biomedical Engineering)
Member

……
Asst. Prof. Chanika Sritara, M.D.
M.Sc. (Nuclear Medicine)
M.Sc. (Clinical Epidemiology)
Member

……
Prof. Banchong Mahaisavariya, M.D., Dip. Thai Board of Orthopedics
Dean
Faculty of Graduate Studies
Mahidol University

……
Prof. Rajata Rajatanavin
M.D., F.A.C.E.
Dean, Faculty of Medicine
Ramathibodi Hospital
Mahidol University

ACKNOWLEDGEMENTS

I would like to acknowledge to all those who gave me the possibility to complete this thesis.

I would like to express my sincere gratitude and deep appreciation to Asst. Prof. Chanika Sritara my advisor for her valuable supports, suggestions, comments, and review in all the time of research. I would like to thank my co-advisor, Assoc. Prof. Chiraporn Tocharoenchai for her valuable support, suggestions and helpful assistance.

Besides my advisors, I would like to thank my thesis committee, Assoc. Prof. Pawana Pusuwan, Faculty of Medicine, Siriraj Hospital and Assoc. Prof. Supatporn Tepmongkol, Faculty of Medicine, Chulalongkorn University, who asked me good questions and gave valuable comments.

I would like to thank the co-operation of both volunteers and staffs of department of Nuclear Medicine at Ramathibodi Hospital.

I would like to acknowledge to Thai Neurogastroenterology and Motility Society for supporting funds and their valuable guidance in this thesis.

I would like to thank Lect. Puangpen Tangboonduangjit, Chair of Science program in Medical Physics, Faculty of Medicine, Ramathibodi Hospital and the lectures of Medical Physics program for their valuable advice.

Finally, this thesis is dedicated to my family. Thank you for their understanding, love and care. They have always supported and encouraged me to my best in all matters of life.

Atchara Promdaung

SCINTIGRAPHIC STUDIES TO EVALUATE GASTRIC FUNCTIONS

ATCHARA PROMDAUNG 5036371 RAMP/M

M.Sc. (MEDICAL PHYSICS)

THESIS ADVISORY COMMITTEE: CHANIKA SRITARA, M.D., M.Sc. (NUCLEAR MEDICINE), M.Sc. (CLINICAL EPIDEMIOLOGY), CHIRAPORN TOCHAROENCHAI, Ph.D. (BIOMEDICAL ENGINEERING).

ABSTRACT

The objectives of this research were to study gastric emptying and gastric antral contractions through scintigraphy to check gastric emptying times in normal people among 20 Thai volunteers (10 males and 10 females in the age range of 25-64 years), who signed and agreed to participate in the study. After eating standard food (one No.1 egg, stirred and blended with 10-milliliters plain water, 5 milliliters of vegetable oil and 1mCi of ^{99m}Tc-Phytate, cooked in a microwave oven, 100 grams of steamed rice and 100 milliliters of plain water) for 10 minutes, six periodical pictures of each standing volunteer's stomach were taken in a 4 hour timeframe. The gastric emptying time in to the small intestine until the stomach emptied, was analyzed using nonlinear regression. The nonlinear regression was applied to fit the data of the food remaining in the stomach at each period with a modified power exponential function of Siegel to derive k and β values. The derived k and β were used to calculate the lag phase time and half emptying time through the maximum slope tangent Couturier method. In terms of the gastric antral contraction, data were analyzed using a Fourier transform to find the frequency and amplitude of gastric antral contractions. Findings from the study of the lag phase time and half emptying time in normal people using the cut-off value at percentiles at 2.5 and 97.5 were in the range of 5.56-38.37 and 50.49-87.48 minutes, respectively. The average frequency of gastric antral contractions in normal people at the 62nd, 92nd, and 122nd minutes were 3.2 ± 0.2, 3.1 ± 0.2, and 3.1 ± 0.2 cycles / min, respectively. Findings from the study of the amplitude, collected at the 62nd, 92nd, and 122nd minutes in normal people were in the range of 0.16–2.62, 0.17-3.51, and 0.35-1.99, respectively.

KEY WORDS: SCINTIGRAPHY / SOLID GASTRIC EMPTYING / GASTRIC ANTRAL MOTILITY

113 pages

การศึกษาการทำงานของกระเพาะอาหารโดยใช้วิธีการทางด้านเวชศาสตร์นิวเคลียร์
SCINTIGRAPHIC STUDIES TO EVALUATE GASTRIC FUNCTIONS

อัจฉรา พรหมด้วง 5036371 RAMP/M

วท.ม. (ฟิสิกส์การแพทย์)

คณะกรรมการที่ปรึกษาวิทยานิพนธ์ : ชนิกา ศรีธรา, M.Sc. (NUCLEAR MEDICINE), M.Sc. (CLINICAL EPIDEMIOLOGY), จิราภรณ์ โตเจริญชัย, Ph.D. (BIOMEDICAL ENGINEERING)

บทคัดย่อ

วัตถุประสง ค์ของการ วิจัยเพื่อ ศึกษา การย่อยอาหารแข็งใน กระเพาะ อาหาร และการเคลื่อนไหวของกระเพาะอาหารส่วนแอนทรัมโดยวิธีการ Scintigraphy ในอาสาสมัครปกติชาวไทย และหาเวลาที่ใช้ในการย่อยอาหารแข็งในคนปกติ มีอาสาสมัคร 20 ราย (เพศชาย 10 ราย และหญิง 10 ราย ช่วงอายุ 25-64 ปี) ลงนามยินยอมเข้าร่วมในการศึกษานี้ หลังจาก อาสาสมัคร รับประทาน อาหารมาตรฐาน (ไข่ไก่เบอร์ 1 จำนวน 1 ฟอง ตีผสมกับน้ำเปล่า 10 มิลลิลิตร น้ำมันพืช 5 มิลลิลิตร และสารรังสี ^{99m}Tc-Phytate 1 mCi แล้วทำให้สุกด้วยการอบในเตาไมโครเวฟ, ข้าวสวย 100 กรัม และน้ำเปล่า 100 มิลลิลิตร) เสร็จภายในเวลา 10 นาที เริ่มทำการถ่ ายภาพกระเพาะอาหาร ทันทีในท่ายืน โดยถ่ายภาพกระเพาะอาหารเป็นช่วงๆ จนถึง 4 ชั่วโมง วิเคราะห์ข้อมูลเวลาที่กระเพาะส่งอาหารเข้าไปยังลำไส้เล็กจนกระทั่งกระเพาะอาหารว่าง ด้วยการวิเคราะห์ความถดถอยไม่เชิงเส้นเพื่อทำการ fit ข้อมูลสัดส่วนอาหารที่เหลืออยู่ในกระเพาะในแต่ละช่วงเวลา ด้วย modified power exponential function ของ Siegel และใช้หาค่าพารามิเตอร์ของสมการ จากนั้นนำค่าพารามิเตอร์ที่ได้ไปใช้ในการคำนวณเวลาในการย่อยอาหารและเวลาที่อาหารผ่านกระเพาะไปได้ครึ่งหนึ่งด้วยวิธีของ Couturier สำหรับการศึกษาการเคลื่อนไหวของแอนทรัม วิเคราะห์ข้อมูล ด้วยการทำ Fourier transform เพื่อหาความถี่ และความแรงในการบีบตัวของแอนทรัม ผลการศึกษาเวลาที่ใช้ในการย่อยอาหารและเวลาที่อาหารผ่านกระเพาะไปได้ครึ่งหนึ่งในคนปกติโดย ใช้จุดตัด ณ เปอร์เซ็นไทล์ที่ 2.5 และ 97.5 ค่าที่ได้อยู่ในช่วงระหว่าง 5.56 - 38.37 และ 50.49-87.48 นาทีตามลำดับ สำหรับค่าความถี่เฉลี่ยในการบีบตัวของแอนทรัมของ คนปกติ ซึ่งทำการเก็บข้อมูลในนาทีที่ 62, 92 และ 122 มีค่าเท่ากับ 3.2 ± 0.2 , 3.1 ± 0.2 และ 3.1 ± 0.2 รอบ/นาทีตามลำดับ และความแรงในการบีบตัวของแอนทรัม ในนาทีที่ 62, 92 และ 122 อยู่ในช่วงระหว่าง 0.16-2.62, 0.17-3.51 และ 0.35-1.99 ตามลำดับ

113 หน้า

CONTENTS

LIST OF TABLES

LIST OF TABLES (cont.)

LIST OF FIGURES

LIST OF FIGURES (cont.)

LIST OF FIGURES (cont.)

LIST OF FIGURES (cont.)

LIST OF FIGURES (cont.)

LIST OF FIGURES (cont.)

LIST OF ABBRAVIATIONS

Abbreviations	Term
ADM	Intraluminal antral manometry
CONT	Controls
DAS	Dynamic antral scintigraphy
DD	Diabetics with delayed gastric emptying
DN	Diabetics with normal gastric emptying
EGG	Cutaneous electrogastrography
keV	Kilo electron volt
MS	Maximum slope tangent
ROI	Region of interest
SD	Standard deviation
$T_{1/2}$	Emptying haft-time
TLAG	Lag phase time
T_{RE}	Real emptying time or Constant emptying time
V-P	Vagotomy and pyloroplasty
g	Gram
cc.	Cubic Centimeter
mCi	milliCurie
DICOM	Digital Imaging and Communications in Medicine
TIFF	Tagged Image File Format
GIF	Graphics Interchange Format
JPEG	Joint Photographic Experts Group
BMP	Bitmap
FITS	Flexible Image Transport System
bit	Binary digit

LIST OF ABBRAVIATIONS (cont.)

Abbreviations	Term
NIH	National Institutes of Health
MATLAB	Matrix Laboratory

CHAPTER I
INTRODUCTION

Gastric emptying scintigraphy is a nuclear medical procedure to diagnose and check gastric malfunctions through lag phase time and emptying half-time, $T_{1/2}$ to identify gastric functionality. Gastric emptying time refers to the time the stomach dispatches food mixed with enzyme which makes food smaller in size to small intestines until the stomach is empty. Gastric emptying scintigraphy using a gamma camera is considered a gold standard approach as it offers accurate quantitative data and physiologic liquid and solid foods can be examined with a non-invasive method (1, 2).

Findings from gastric emptying scintigraphy through a gamma camera depend on such factors as food qualities, liquid or solid, food composition, meal volume (3), body position (4), smoking (5), gender (6-12), phase of menstrual cycle (13-14), time of day. Interpreting gastric emptying findings depends of the technique applied (15), and each examination should base on the same standard to avoid errors from the examination technique (16). There was a study to find the standard solid gastric emptying value in 123 strong, multi-national volunteers by eating eggs labeled with radioisotope, 2 slices of bread, strawberry jam and water (17). However, the test meal used is not common to most Thai people. This research aims to find the normal value of solid gastric emptying using a test meal most Thai people eat daily, namely, rice and eggs labeled with radioisotope. The eggs are cooked in a microwave oven. The study was performed in Thai normal healthy volunteers using the gastric emptying scintigraphy, a nuclear medical technique.

Findings from other researches show that diabetic patients who suffer from dyspepsia may have abnormal gastric antral contraction, leaving food in the stomach for a long time. Other researchers have studied gastric antral motility through the gastric emptying scintigraphy jointly with a Fourier algorithm and data derived are analyzed in terms of frequency and amplitude (antral motility parameters). The data

derived will explain gastric antral contraction. As information about gastric antral contraction is not much available, a study of antral contraction in Thai normal healthy volunteers will serve as basis to evaluate diabetic patients who suffer from dyspepsia.

It is also appropriate to explore the relationship between the lag phase time and emptying half-time, $T_{1/2}$ as well as antral contraction. Literature review shows that the studies on this have been scarce, none in Thai subjects. Subsequently, the researcher firmly believes this research will serve as basic information for other researchers to further work on gastric functionality.

CHAPTER II
OBJECTIVES

The objectives of this study are:

2.1 To study solid gastric emptying and gastric antral motor activity measured by gastric scintigraphy in Thai healthy volunteers.

2.2 To define frequency and range of amplitude of antral contraction.

CHAPTER III
LITERATURE REVIEWS

3.1 Normal gastric physiology

The stomach is a J-shaped muscular pouch, located in the upper abdomen. It has three major roles. First, it provides a reservoir for food; second, it breaks down solid food into small particles that when combined with its secretion of gastric juice form a semiliquid mixture called chyme; and third, it controls the rate of emptying of gastric content into the duodenum.

Anatomically, the stomach is divided into three regions as shown in Figure 3.1(A) (18): the fundus (proximal portion to the gastroesophageal junction), the corpus (between the gastroesophageal junction and the incisura angularis), and the antrum (between the incisura angularis and the duodenum).

Physiologically, the human stomach consists of two integrated but electromechanically distinct parts as shown in Figure 3.1(B) (18): the proximal stomach that encompasses the fundus and the orad corpus, and the distal stomach that includes the mid and caudad corpus, and the proximal, middle, and distal antrum. The proximal portion of the stomach is a reservoir for solid and liquid food. It controls emptying by generating a pressure gradient between the stomach and the duodenum. The distal stomach is the prime propeller, grinder, and siever of solid food and is characterized by phasic peristaltic waves that spread out circumferentially from the corpus to the pylorus at a rate of three contractions per minute.

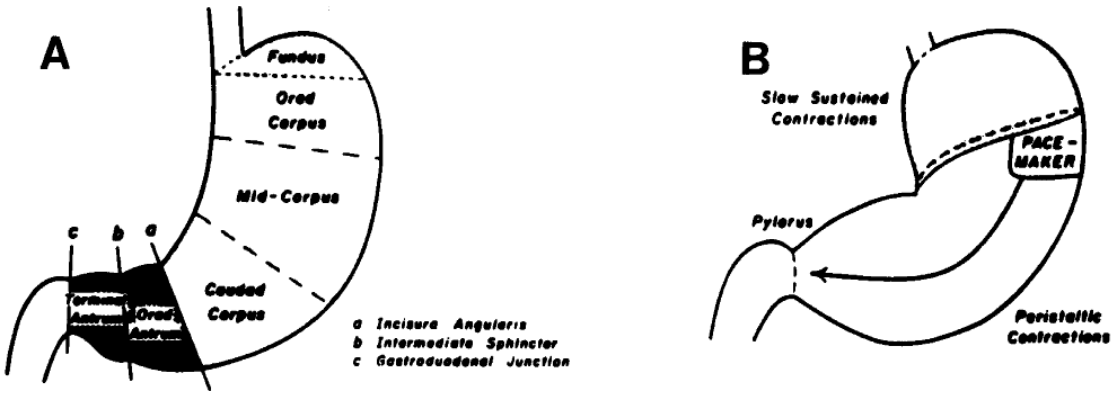

Figure 3.1 Anatomy and electrophysiology of the stomach. (A) The classical division of the stomach into its anatomical parts. (B) The two distinct electrophysiological entitles (18).

3.2 Emptying of Solids

The gastric emptying curve for solid food is sigmoidal in shape and characterized by the following as shown in Figure 3.2 (18): (1) an initial lag phase during which no or little solid is emptied; (2) a prolonged phase with a constant emptying rate; and (3) a late, much slower phase when the stomach is nearly empty.

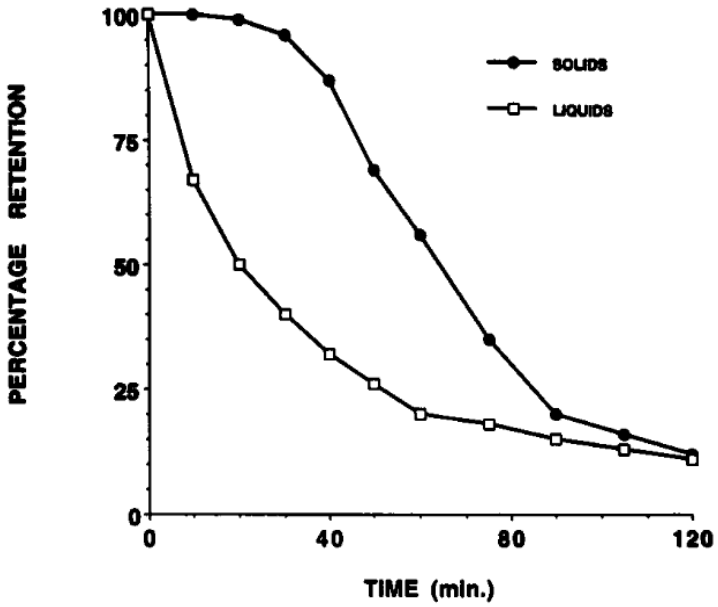

Figure 3.2 Gastric emptying curves for solids and liquids. In normal subjects, solid emptying is sigmoidal in shape with an initial lag phase with no or little emptying, followed by a linear phase with constant emptying rate and a much slower late phase. Liquid curve follows a single exponential course (18).

The rate of solid emptying is determined by the physical characteristics, caloric density, caloric content, and distribution, osmolality, acidity, viscosity and volume of the test meal, which trigger gastric and duodenal receptors and activate the feedback mechanisms. These mechanisms allow for a constant amount of calories to be delivered per minute to the duodenum (18).

3.3 Analysis of gastric emptying data

3.3.1 Standardization Issues

Before analysis of gastric emptying curves can begin, both time and fraction remaining must be well defined (19). First, what is time 0? Is it the start of meal ingestion or is it the point at which consumption of the meal has finished? For liquid meals the difference is small. For solid meals, the difference may be as much as 10 min, and the length of time required to eat the meal may vary considerably from subject to subject. For uniformity, time 0 is always defined as the point at which meal ingestion begins. Since counting takes time, the time of the resulting estimate of fraction remaining should be defined as the middle of the counting interval (for a 1 min count beginning at 10 min, the time should be recorded as 10.5 min).

According to Couturier et al. (20) normalizing the data by the time activity curve maximum value, which is not necessarily the value at time zero, is an acceptable solution to fit any time activity curve, even with a self-attenuation phenomenon.

3.3.2 Choosing a Method of Analysis

Gastric emptying patterns are determined by the interaction of a variety of biologic factors: propulsive forces, inhibitory feedback, central nervous system input, the anatomical structure of the operated or unoperated stomach, and so on. However, these factors do not have a clear picture of the individual factors or the way in which they work, so the choice of a model for gastric emptying cannot be made on a biologic basis (19).

Elashoff et al. (19) outlined the following set of characteristics which any mathematical curve used to analyze gastric emptying data should satisfy.

1. The mathematical curve should have as few parameters as possible.

2. The parameters should have clear graphical interpretations. Changes in the value of a parameter should have an obvious relationship to changes in the shapes of the observed emptying curves.

3. The curve should provide a good fit to the data points observed for individual subjects for a wide range of types of subjects and types of meals. That is, it should be flexible.

4. The curve should always give values for fraction remaining between 0.0 and 1.0 even when extrapolated to time 0 or to longer times than any measured.

5. The curve should be restricted to give a fraction remaining of 1.0 at time zero.

3.3.3 Mathematical Curves

There are many approaches for approximating emptying of solid meal components. The first is to use a single straight line, but the straight line does not satisfy conditions 3, 4, and 5. Extrapolated values will be nonsense and there are many emptying patterns far different from a straight line. Furthermore, this line does not correctly describe both phases of gastric emptying, in particular the lag phase.

The exponential, $f = ae^{-kt}$, has been widely used in gastric emptying studies. The fraction of the meal remaining in the stomach at time t is f, a is the fraction present at time 0, e is the constant 2.718, and k is a rate parameter. The parameter k has a simple relationship to the time at which one-half the meal present at time zero has emptied [$t_{1/2} = (\log_e 2)/k$]. A widespread problem in the use of the exponential has been the failure to restrict the curve to go through 100% at zero time. When this is not done, the estimated $t_{1/2}$ will not correspond to the time at which 50% of the meal has emptied. If the exponential is restricted by fixing a = 1.0, then criteria 4 and 5 are satisfied. Substituting $(\log 2)/t_{1/2}$ for k, the equation can be mathematically written as

$$f = e^{-\log 2\ (t\ /\ t1/2)} \qquad (1)$$

or as

$$f = 2^{-\ (t\ /\ t/2)} \qquad (2)$$

However, describing the initial lag phase accurately is impossible with an exponential function and the method of analysis should take into account the whole emptying curve rather than focusing separately on specific time points or only a part of the emptying curve. Plotting the emptying curves for each individual is the best way to examine, understand, and display the details of the emptying process. For these reasons, Elashoff et al. (19) made the parameters directly interpretable and the

relationship to the simple exponential clear. The equation can be mathematically written as

$$f = 2^{-(t/t1/2)\beta} \quad (3)$$

and refer to it subsequently as the power exponential curve. The new parameter, β, determines the shape of the curve. For β =1, the power exponential is the same as the restricted simple exponential. For a curve with an initial lag in emptying, β is > 1.0 (the solid curves in Figure 3.3). This type of curve is often seen for solid meals, where the initial lag phase may represent the time to grind the food into smaller particles. A value of β < 1.0 describes a curve with a very rapid initial emptying followed by second slower emptying phase (the dashed curves in Figure 3.3). Such a pattern is often seen for operated subjects with liquid meals.

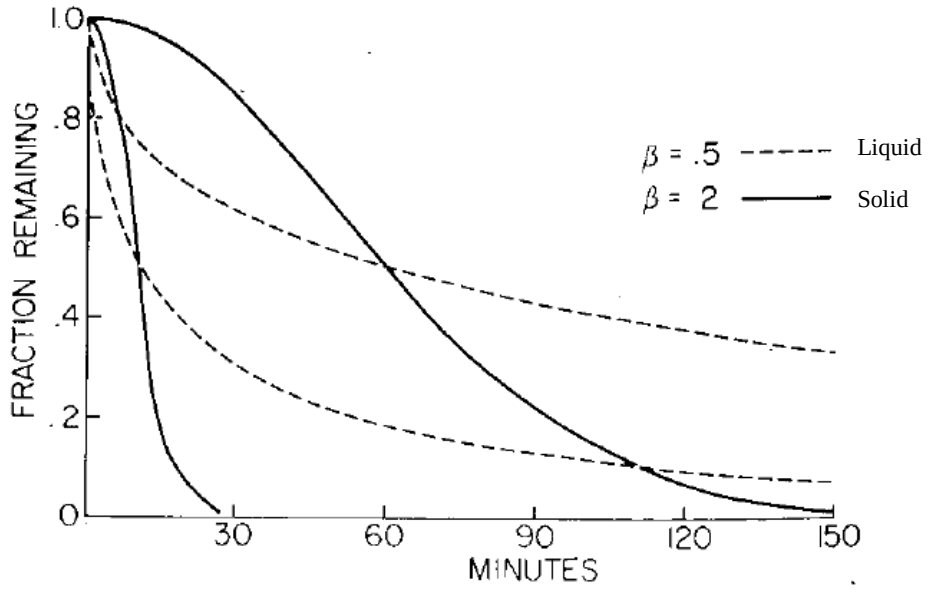

Figure 3.3 Power exponential emptying, $f = 2^{-(t/t1/2)\beta}$ with $t_{1/2}$ = 10, 60 min; β = 0.5,2

Elashoff et al. (19) investigated the use of the power exponential for analysis of gastric emptying data. They reanalyzed five gastric emptying studies by using the power exponential. The data for each subject were fit using a nonlinear least squares computer program and reported R^2 values as an index of whether or not a curve provides a good fit to the data. R^2 should be high (above 0.9). Low values of R^2 might indicate reflux, inadequate time sampling, or errors in the measurement of

emptying, as well as inadequacies in the curve being fit. For each individual, the estimated curve should be plotted with the observed points and examined for evidence of a consistent tendency for poor fit in a particular part of the curve. For nonlinear curves, R^2 can be defined by using the formula as written in equation (4).

$$R^2 = 1 - \frac{Residual\ sum\ of\ squares}{Total\ sum\ of\ squares} \quad (4)$$

The data as shown in Figure 3.4 and 3.5 are typical of results in these studies as a whole. Table 3.1 shows data from two studies of the emptying of 10 mm cubes of labeled chicken liver; β was > 1.0 for all subjects, indicating that emptying was not exponential in pattern but showed a slow early phase followed by a speeding up of emptying.

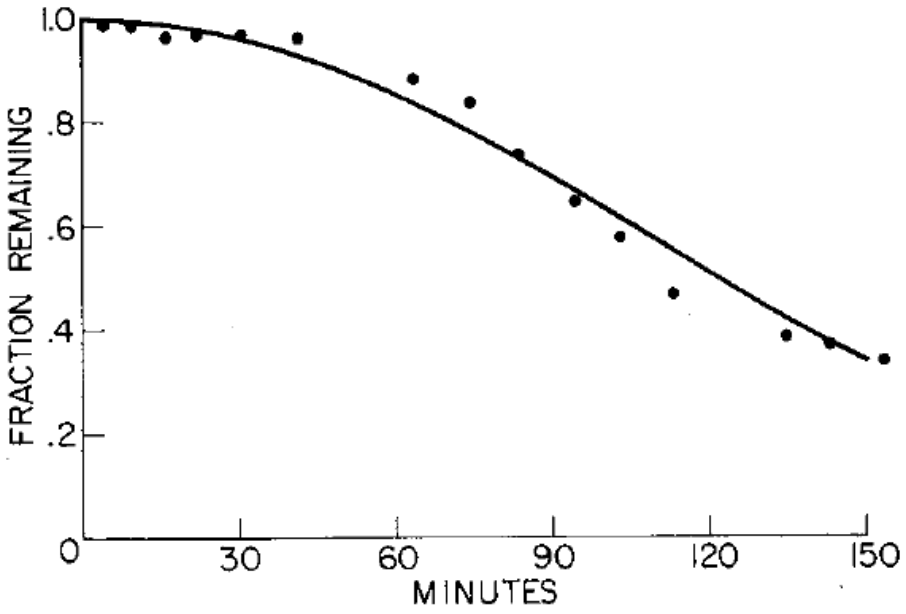

Figure 3.4 Emptying of 10 mm labeled chicken liver with 0.25 mm chicken liver in beef stew in a normal subject, ($t_{1/2}$ = 121, β = 2.1, R^2 = 0.99 for power exponential; $t_{1/2}$ = 126, R^2 = 0.86 for simple exponential)(19).

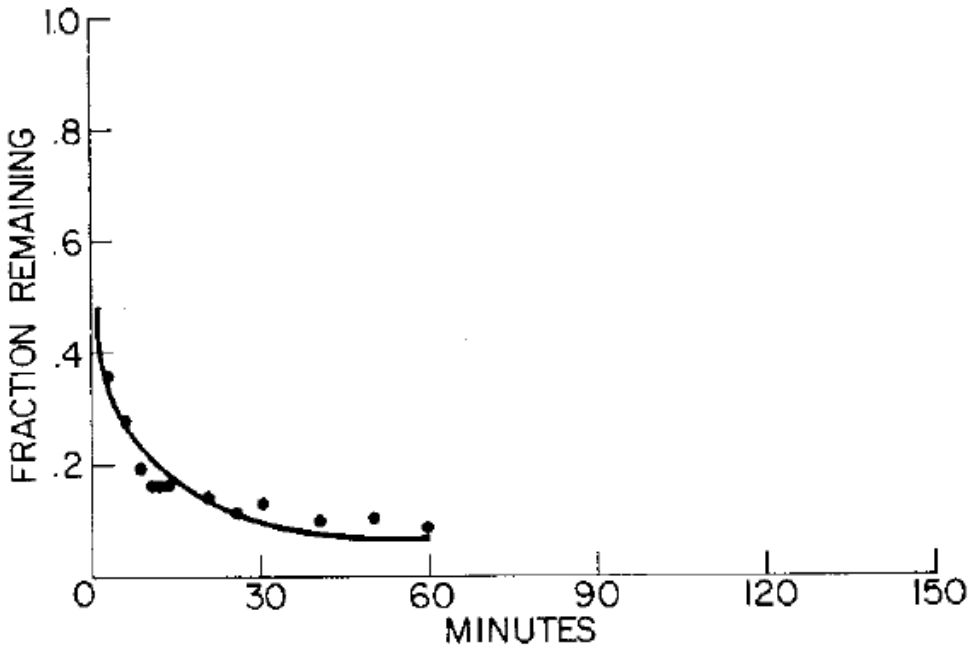

Figure 3.5 Emptying of labeled glucose solution meal for a subject with a vagotomy and pyloroplasty ($t_{1/2}$ = 0.7, β = 0.31, R^2 = 0.92 for power exponential; $t_{1/2}$ = 3, R^2<0 for simple exponential fit)(19).

Table 3.1 Emptying of labeled 10 mm cubes of chicken liver in normal subjects (19).

Meal	n	$t_{1/2}$	β	min R^2
26 g 10-mm cubes of liver[a] with 0.25-mm particles of liver in 213 g stew and 200 ml water	8[c]	110 (43)	1.81 (0.36)	0.94
30 g 10-mm cubes of liver[b] with 75 g noodles and 200 ml water	8	86 (14)	1.86 (0.62)	0.92

Values are means of parameters for power exponential model. Numbers in parentheses are standard deviations. [a]Labeled with indium (^{113m}In) in 4 subjects and technetium (^{99m}Tc) in 4 subjects. [b]Labeled with ^{113m}In. [c]Three subjects participated in both studies

Table 3.2 shows data from a meal of 400 ml of glucose solution labeled with technetium. For normal subjects, the simple exponential would have provided a good description of emptying (average β is near 1.0). However, patients with a vagotomy and pyloroplasty (V-P) showed very rapid initial emptying often followed by a long period of slow emptying; β ranged from 0.33 to 0.85, significantly lower than for normal subjects.

Table 3.2 Emptying of 400 milliliters of ^{99m}Tc labeled glucose solution (19).

Subjects	n	$t_{1/2}$	β	min R^2
Normals	6	43 (18)	1.12 (0.39)	0.95
V-P patients	6[a]	1.6 (0.7)	0.50 (0.22)	0.86

Values are means of parameters of the power exponential model. Numbers in parentheses are standard deviations. [a]One V-P patient with $t_{1/2}$ = 15 min and β = 0.47 was excluded from the summary.

This abnormality of emptying in subjects who have undergone ulcer operations is not confined to liquids. Table 3.3 shows the results for a meal of ^{123}I-labeled starch balls in water. Although average values for $t_{1/2}$ were close to an hour for V-P patients as well as for normal subjects, the average β for V-P patients was significantly lower than for normal subjects. In this instance, fitting of the simple exponential would have failed to demonstrate an important difference in the emptying pattern of subjects who have undergone ulcer operations. Use of the parameter β allowed discrimination between the emptying patterns of normal subjects and operated subjects even though the half-emptying times were similar.

Table 3.3 Emptying of 33 grams of ^{123}I labeled starch balls in 400 milliliters water (19).

Subjects	n	$t_{1/2}$	β	min R^2
Normals	6	64 (23)	1.38 (0.44)	0.91
V-P patients	6[a]	63 (31)	0.86 (0.21)	0.83

Values are means of parameters of power exponential model. Numbers in parentheses are standard deviations. [a]One V-P patient who had emptied only 15% of the meal by 180 min was excluded from the summary.

Elashoff et al. (19) conclude that a power exponential function has provided a reasonably good description of a wide variety of emptying patterns for different meals for operated patients as well as for normal subjects. Furthermore, this function can describe both phases of gastric emptying.

Siegel et al. (21) evaluated the ability of a modified power exponential function to define the emptying parameters of two different solid meals. Dual labeled meals were administered to 24 normal volunteers. The subjects received meals consisting of either Tc-99m in vivo labeled chicken liver or Tc-99m-egg, which have different densities, and In-111-DTPA in water. Immediately after ingestion of the dual labeled meal, the subjects were placed supine under a large field of view gamma camera fitted with a medium energy collimator and interfaced to a nuclear medicine computer system. Twenty percent energy windows were set with peaks set at 140 keV for Tc-99m and 247 keV for In-111. Images were obtained for one minute in both energy windows at 15 minute intervals for 150 minutes. The emptying curves were biphasic in nature as shown in Figure 3.6. For solids, this represented an initial delay in emptying or lag phase followed by an equilibrium emptying phase characterized by a constant rate of emptying. The curves were analyzed using a modified power exponential function. This function can be mathematically written as

$$y(t) = 1 - (1 - e^{-kt})^{\beta} \qquad (5)$$

y(t) is the fractional meal retention at time t.

k is the gastric emptying rate in min^{-1}.

β is the extrapolated y-intercept from the terminal portion of the curve.

t is the time interval in minutes

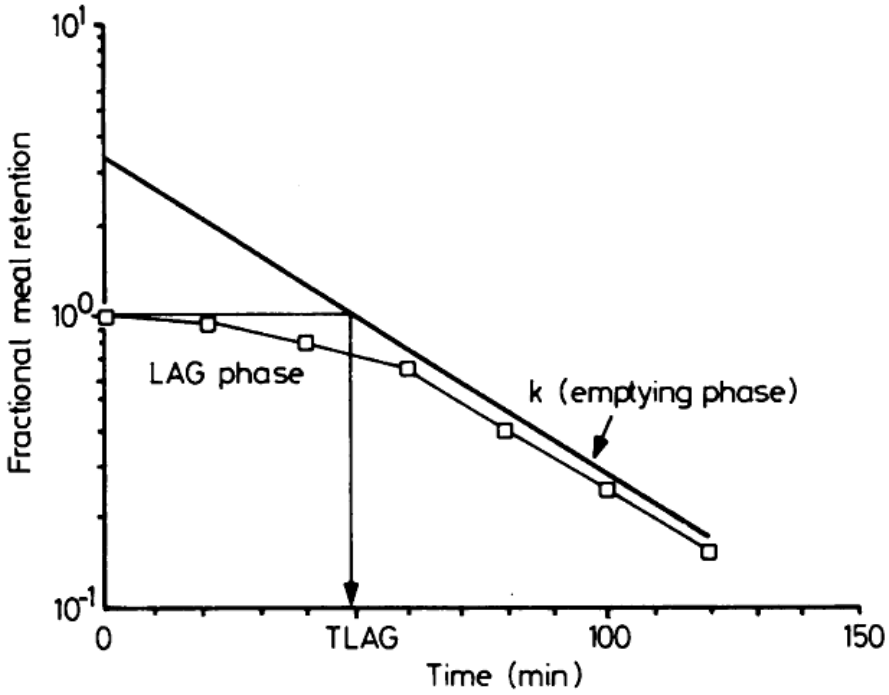

Figure 3.6 Fit of function $y(t) = 1 - (1 - e^{-kt})^{\beta}$ to a typical solid emptying curve. Graph illustrates the two distinct portions of solid emptying, namely, the lag phase, as indicated by TLAG, and the emptying phase, which is characterized by the emptying rate, k (21).

The results of curve fitting with $y(t) = 1 - (1 - e^{-kt})^{\beta}$ are shown in the Table 3.4. There was no significant difference in the emptying rate (k) for liquid and late solid meal components within or between meals. There was, however, a significantly increased β for solid chicken liver compared with solid egg ($p<0.01$) indicating a longer initial slow emptying phase as shown in Figure 3.7. This is best seen by comparing the lag times (TLAG) for these two solid meals (62±5 min and 31±2 min for chicken liver and egg, respectively). The measured half-emptying times ($t_{1/2}$) were 94.1±14.2 min and 77.6±11.2 min for chicken liver and egg, respectively, and are significantly different ($p<0.01$). The length of the lag phase and half-emptying time increased with solid food density. After the lag phase, both solids had similar emptying rates, and these rates were identical to those of the liquids.

Table 3.4 Gastric emptying curve analysis with $y(t) = 1 - (1 - e^{-kt})^{\beta}$ (21).

	Egg meal (n = 14)		Chicken liver (n = 10)	
Parameter	**Liquid**	**Solid**	**Liquid**	**Solid**
Emptying rate (k)	-0.0164±0.0007	-0.0142±0.0009	-0.0172±0.0010	-0.0155±0.0013
β	0.70±0.04	1.54±0.09	1.02±0.07	2.62±0.34
Lag phase (T_{LAG})	-	31±2 min	-	62±5 min

Results expressed as mean ± SD

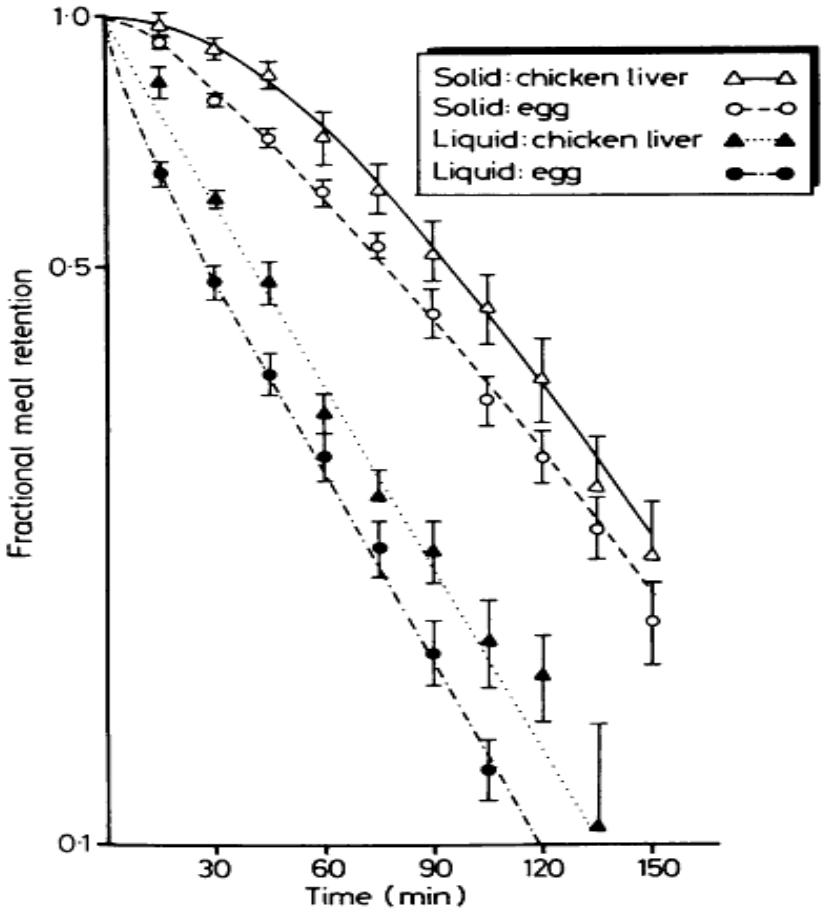

Figure 3.7 The mean ± SD fractional meal retention values for 24 subjects receiving either ^{99m}Tc-egg sandwich (n=14) or ^{99m}Tc in vivo labeled chicken liver (n=10) and ^{111}In-DTPA water on a semilogarithmic plot (21).

A test to determine the digestion of eggs and chicken liver in vitro was carried out. Two tablespoons of each Tc-99m-labelled solid food was chopped into 3 mm cubes and suspended in 25 ml gastric juice from human volunteers. The suspension was then shaken in a 37˚C water bath. Initially and at hourly intervals, 5 ml samples were removed and poured through a 5 ml syringe barrel plugged with glass wool. Saline was used to wash the solids remaining on the glass wool filters which only allowed particles finer than 1 mm to pass through. Solids and filtrates were then countered in a well counter. The counting of the solid residuals and filtrates from the in vitro experiments indicated that the egg was broken down to smaller particle sizes more rapidly than the chicken liver. At times 0, 1 h, 2 h, and 3 h the percent of the food containing particles larger than 1 mm were 99%, 98%, 97%, and 98% for the in vivo labeled chicken liver and 98%, 30%, 28%, and 6% for the egg meal. In vitro experiments indicated that the egg meal disintegrated much more rapidly than the chicken liver under mechanical agitation in gastric juice, lending further support to the hypothesis that the initial lag in emptying of solid food is due to the processing of food into particles small enough to pass the pylorus.

Siegel et al. (21) conclude that the modified power exponential model permits characterization of the biphasic nature of gastric emptying allowing for quantification of the lag phase and the rate of emptying for both solids and liquids. The length of the lag phase is affected by meal volume and density, while the latter linear phase is independent of these parameters.

Couturier et al. (20) proposed an improved approach which describes the power exponential function by two straight lines and estimated of lag phase and constant emptying times from the Elashoff (19) and Siegel (21) power exponential functions. The Elashoff and Siegel power exponential functions have been widely used to fit time activity curve of gastric emptying. The time activity curve is described by these two functions with two parameters, either $T_{1/2}$ and α or β and k:

$$e(t) = 2^{(-t/t/2)\alpha} \quad (6)$$

$$s(t) = 1-(1-e^{-kt})^{\beta} \quad (7)$$

The stomach requires time to grind the solid component of a meal into small particles before they pass through the pylorus towards the duodenum. This called the ‘lag phase’ and is affected by size of the solid particles and by the volume or density of the meal. This first phase is followed by a second process of constant emptying. The power exponential parameters do not provide an easy understanding of these two independent processes. Indeed, α, β and k have no dimension or physiological significance and $T_{1/2}$ (half-emptying time) depends on both grinding time and constant emptying time. For this reason, it is clinically useful to calculate lag phase and constant emptying times from the power exponential parameters, which are independent of each other and describe independently both phases of gastric emptying. Lag phase and constant emptying times were estimated using a maximum slope tangent method. This approach consisted in describing the power exponential function by two straight lines. The first line is the line of 100% retention rate and the second line is tangent to the maximum slope of the power exponential function (theoretical curve in Figure 3.8). The intersection of this tangent and the abscissa defines the constant gastric emptying time. The intersection of the 100% retention value line and the tangent defines the lag phase time.

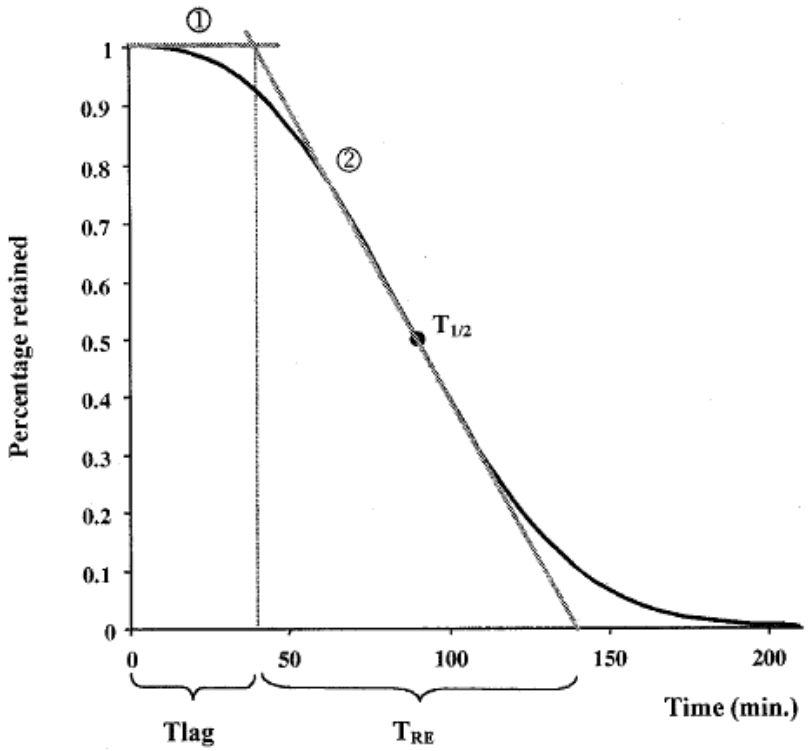

Figure 3.8 Power exponential function described by two straight lines. The first line is horizontal and represents the lag phase. The second line is a tangent and represents constant gastric emptying. The time at the intercept of these two lines marks the end of the lag phase and the start of the constant emptying phase. The intercept of the tangent with the abscissa defines the end of the real emptying time, T_{RE} (20).

The Elashoff parameters α and $T_{1/2}$ and the Siegel parameters β and k were determined by a non-linear least-squares fitting algorithm. Lag phase and constant emptying times were estimated from model parameters by using a maximum slope tangent method. The formulae are given below:

Maximum slope tangent (MS)

Couturier Elashoff's model

The lag phase is $T_{lag}(MS)_{(E)} = \left[\frac{\alpha y_m - 1}{(\alpha - 1)y_m}\right] t_m$ (8)

The real emptying time is $T_{RE}(MS)_{(E)} = \frac{t_m}{(\alpha - 1)y_m}$ (9)

Where $t_m = t_{1/2}\left(\frac{\alpha - 1}{\alpha \ln 2}\right)^{1/\alpha}$ and $y_m = \exp\left(\frac{1-\alpha}{\alpha}\right)$ (10)

Couturier Siegel's model

The half-emptying time is $T_{(1/2)S} = -\mathrm{Ln}\left(1 - 2^{(-1/\beta)}\right) \Big/ k$ (11)

The lag phase time is $T_{lag}(MS)_{(S)} = \frac{Ln\beta}{k} - \left(\frac{\beta - 1}{k\beta}\right)$ (12)

The real emptying time is $T_{RE}(MS)_{(S)} = \frac{1}{k}\left(\frac{\beta - 1}{\beta}\right)^{1-\beta}$ (13)

Couturier et al. (20) studied 132 patients (78 women, 54 men; mean age 42.55±15.26 years) and 15 controls (5 women, 10 men; mean age 31.03±5.74 years). Fifty-seven of the 132 patients had non-ulcerous dyspepsia, four ulcerous dyspepsia, 26 type I diabetes mellitus, 41 gastro-esophageal reflux, three constipation and one scleroderma. The patients and controls underwent gastric emptying scintigraphy. All examinations were performed in the morning after an overnight fast. The patients and controls ingested the same test meal, which was calibrated at 370 kcal and contained a well-cooked omelette made with an egg, in which the albumin was labeled with 1mCi of ^{99m}Tc-sulphur colloid, a slice of ham, two pieces of buttered toast (10 g of butter),

orange juice (100 ml). The first static acquisition was performed 10 min after the beginning of the meal in an anterior view and was followed 1 min later by a posterior view. The duration of each acquisition was 1 min. The interval between sets of antero-posterior acquisitions was 15 min. The acquisitions were stopped when the gastric activity rate was one-third of the initial maximum activity.

Couturier et al. (20) fitted gastric emptying experimental data derived from 147 individuals by the mathematical functions of Elashoff and Siegel. In all cases, there were no differences between the shapes of the two curves fitted for the same set of experimental data as shown in Figure 3.9. Therefore, the quality of fit was equivalent for both mathematical functions.

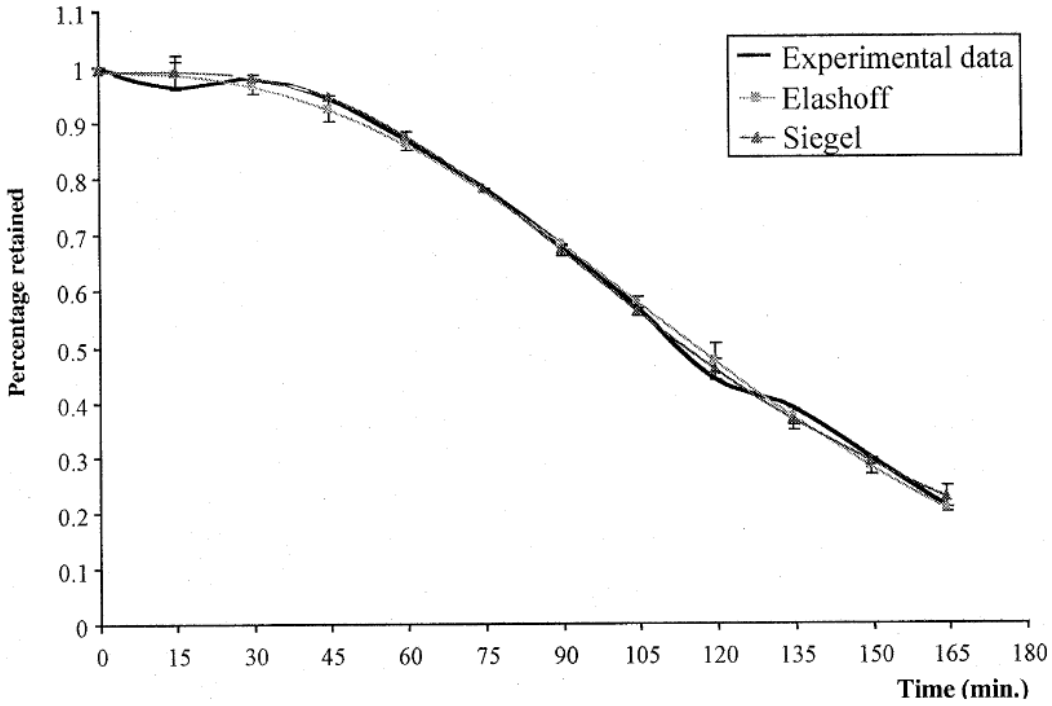

Figure 3.9 Time activity curve accurately described by the mathematical models of Elashoff (squares) and of Siegel (triangles) (20).

Table 3.5 displays descriptive statistics for the results of the controls and patients. All parameters are expressed as the mean and standard deviation (mean ± SD). Table 3.6 displays the mean values of all parameters for both mathematical functions, the mean difference between these two mathematical models and their standard deviation. The 95% confidence interval was met by all parameters.

Table 3.5 Gastric emptying parameters in controls and in patients (20).

	Controls		**Patients**	
	Elashoff	**Siegel**	**Elashoff**	**Siegel**
$T_{1/2}$ (min)	82.21±18.74	81.29±19.95	99.46±30.54	98.52±31.15
α	2.26±0.46	-	2.15±0.73	-
β	-	4.48±2.40	-	6.39±14.73
k (1/min)	-	0.0242±0.010	-	0.0208±0.009
Tlag (MS) (min)	29.33±13.83	24.02±11.53	31.83±20.12	32.14±18.09
T_{RE} (MS) (min)	105.01±32.57	110.89±47.45	132.96±50.39	129.01±53.91

Table 3.6 Bland and Altman method (20).

	Elashoff (E)		**Siegel (S)**		**Difference E-S**	
	Mean	**2SD**	**Mean**	**2SD**	**Mean**	**2SD**
$T_{1/2}$	97.98	58.43	96.59	59.35	1.29	2.21
Tlag (MS)	31.87	38.26	32.60	35.36	-0.70	5.30
T_{RE} (MS)	130.01	95.97	124.22	97.85	6.00	13.00

Couturier et al (20) conclude that the Elashoff and Siegel functions are equivalent and that the maximum slope tangent method allows a reliable description of the two independent phases of gastric emptying.

3.3.4 Characterization of antral motility using scintigraphy

Gastric emptying is regulated in part by gastric myoelectric and contractile activity. The normal gastric electric slow wave, originating from a "pacemaker" region located along the greater curvature, occurs at a frequency of approximately 3 cycles per minute and serves to coordinate peristaltic contractions of the body and antrum by electromechanical coupling. The force of gastric contractions can be measured clinically by intraluminal antral manometry (ADM). Several noninvasive techniques are available to record antral contractility. Cutaneous electrogastrography (EGG) entails the noninvasive measurement of the underlying gastric myoelectric activity and can be performed in either the fasting or the postprandial states. Dynamic antral scintigraphy (DAS) assesses the movements of antral contents induced by antral contractions in the postprandial state using a rapid scintigraphic imaging technique (22).

Urbain et al. (23) evaluated food distribution in stomach and gastric antral motor activity in patients with longstanding diabetes. Antral contractions were characterized by using a standard gastric emptying test with an acquisition protocol and a refined Fourier algorithm to analyze the data. Gastric motility parameters were correlated to gastric retention in 20 diabetic patients with or without gastroparesis and in 10 healthy subjects.

They (23) studied 10 diabetic patients with retarded gastric emptying (6 females, 4 males; mean age 36.7±11 yr) and compared their results to 10 diabetics with normal gastric emptying tests (5 females, 5 males; mean age 40±18 yr) and 10 healthy subjects (5 females, 5 males; mean age 43±12 yr). All controls and patients were studied after an overnight fast of at least 12 hr. The scintigraphic test procedure was performed as follows: after ingestion of a standardized test meal consisting of 50 g of scrambled egg label with 2 mCi of ^{99m}Tc-sulfur colloid, two slices of regular white bread and 150 ml of water, each subject and patient were imaged on dual headed gamma camera. Simultaneous 1 min anterior and posterior images (128×128 pixels) of the stomach were acquired on the 140 keV ^{99m}Tc peak with a symmetric window of 20%. Images were taken every 10 min for 1 hr and every 15 min for the second hour and if needed until 50% of the meal had emptied from stomach. Anterior dynamic (64×64 pixels) frames of 1 sec also were acquired for 4 min at 1, 11, 21, 31, 41, 51, 61,

76, 91, 106, 121 min and until 150 min for 4 patients after meal completion until 50% emptying had occurred. Total gastric emptying data of static images were analyzed using the modified power exponential function of Siegel et al. (21) to estimate the lag phase time and the half emptying time. For analysis of dynamic images, the 1 sec dynamic images were first reframed in a single 4 min image. A ROI was drawn around the horizontal portion of the stomach between the incisura angularis and the pylorus on each reframed image. A 240-point curve was then generated for each dynamic set of images to generate antral time-activity curves. These curves were first normalized to their respective mean count. The autocorrelation function

$$A(T) = \int C(t).C(t+T)dt, \qquad (14)$$

Where t is time and T the lag time of the correlation, was then applied to each set of normalized data. This function eliminates background noise and nonperiodical events in the defined time interval. Furthermore, Normalized data can be filtered by using Butterworth filter to eliminate noise and patient motion artifacts as suggested by Linda et al, 1997. To obtain the frequency (in contractions/min) and amplitude in the time domain (in absolute value) of the cyclical phenomena, the Fourier Transform

$$F(\omega) = \Delta t \int A(T).\cos.(\omega T)dT, \qquad (15)$$

Where ω is the pulsation frequency, was calculated for each dynamic acquisition set (Figure 3.10D, left and right). The application of these functions to a normal and to a diabetic antral time-activity curve is shown Figure 3.10.

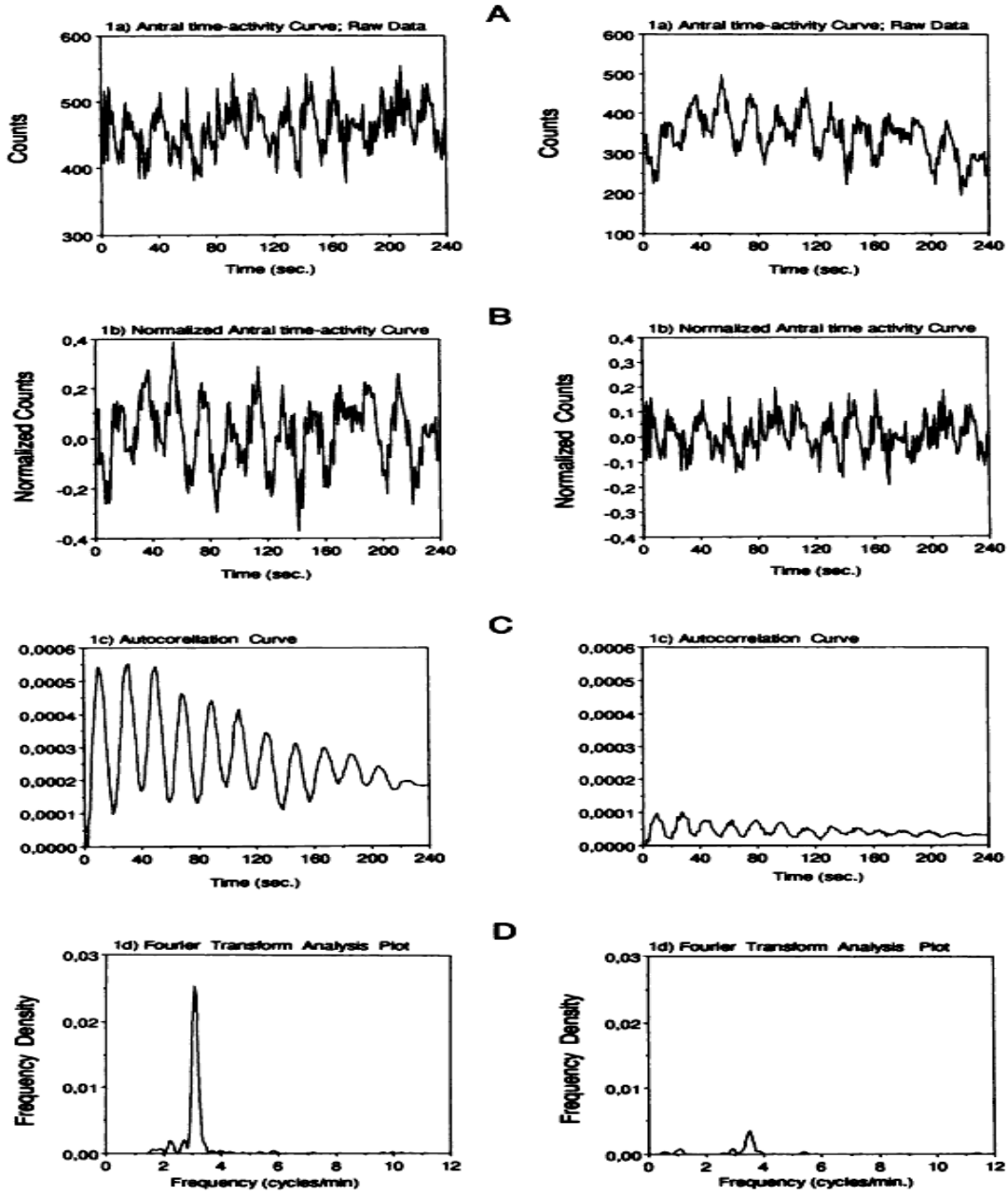

Figure 3.10 A 4-min raw antral time-activity curve (61-65 min) is figured at the top (A) for a healthy control (left column) and a diabetic patient with gastric emptying delay (right column). Data are normalized to their respective mean count (B). The autocorrelation function (C) and the Fourier transform (D) are then applied. Variations of antral counts are lower in the diabetic patient compared to the healthy control (A and B). Frequency of the contractions in the healthy control is about 3 cycles per min; in the diabetic, the frequency is around 3.5 cycles per min. (D). The differences in amplitudes between the antral time-activity curves are highlighted by the Fourier plot (23).

The results of gastric emptying parameters show that, half-emptying time was almost double in diabetics with delayed emptying (132±17 min; $p < 0.0001$) when compared to controls and diabetics with normal emptying as shown in Figure 3.11. Although no statistically significant difference was observed between half-emptying times for controls and normal diabetics (62±11 min versus 65±15 min), the lag phase was significantly prolonged in normal diabetics in comparison to controls (44±12 min versus 25±11 min; $p < 0.001$).

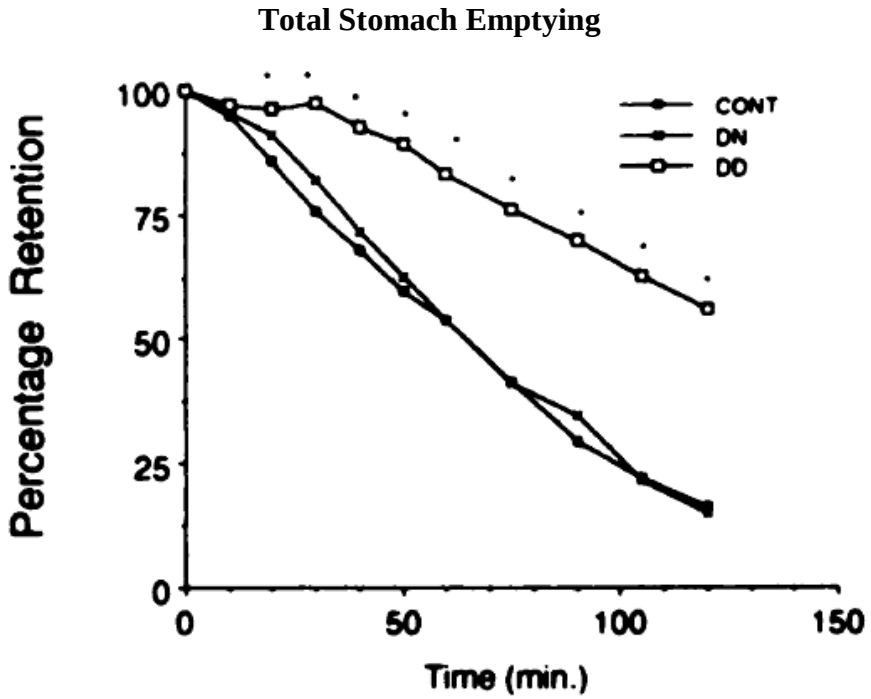

Figure 3.11 Meal retention of the total stomach in controls (CONT), diabetics with normal gastric emptying (DN) and diabetics with delayed gastric emptying (DD). Half-emptying time is doubled in DD compared to DN and CONT (23).

Food distribution in the stomach was different between normal controls and diabetics immediately following meal ingestion. Sixty-four percent of the test meal was retained in the proximal stomach in healthy controls versus 82% in diabetics with normal gastric emptying and 80% in diabetics with gastric retardation. Inversely, after meal ingestion, the filling of the antral stomach was greater in the control group when compared to the diabetics groups as shown in Figure 3.12.

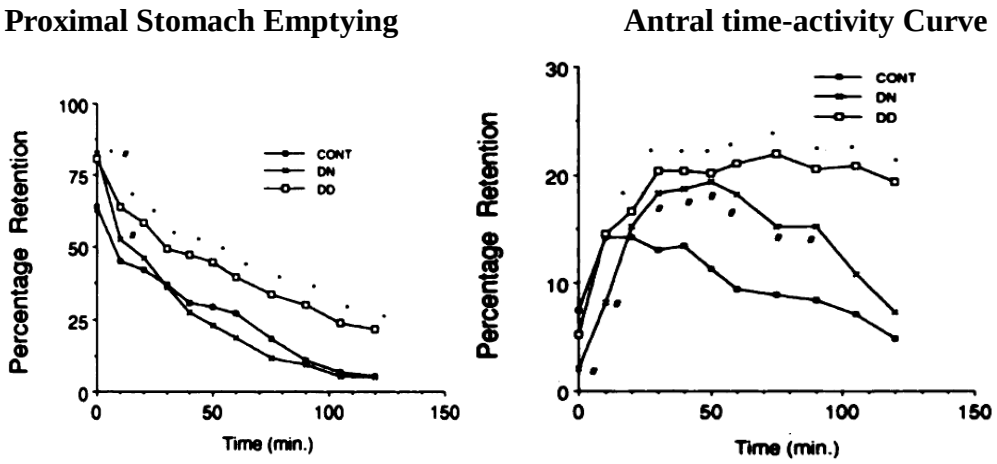

Figure 3.12 Meal retention of the proximal and antral stomach in controls (CONT), diabetics with normal gastric emptying (DN) and diabetics with delayed gastric emptying (DD) (23).

The results of antral motor activity show that, antral contractions frequencies were remarkably stable during emptying for the three groups, with a mean of 2.9±0.5, 3.0±0.3 and 3.2±0.3 contractions per minute in controls, normal diabetics and diabetics with delayed emptying as shown in Figure 3.13(A). A striking decrease in the amplitude of antral contractions in diabetics with delayed gastric emptying was seen during the entire gastric emptying course when compared to controls and after the 50^{th} min when compared to diabetics with normal emptying as shown in Figure 3.13(B). Despite the higher contraction frequency, the motility index in diabetics with delayed emptying was significantly lower than that in controls at all imaging times. It was also lower than that in diabetics with normal emptying after 20 min as shown in Figure 3.13(C).

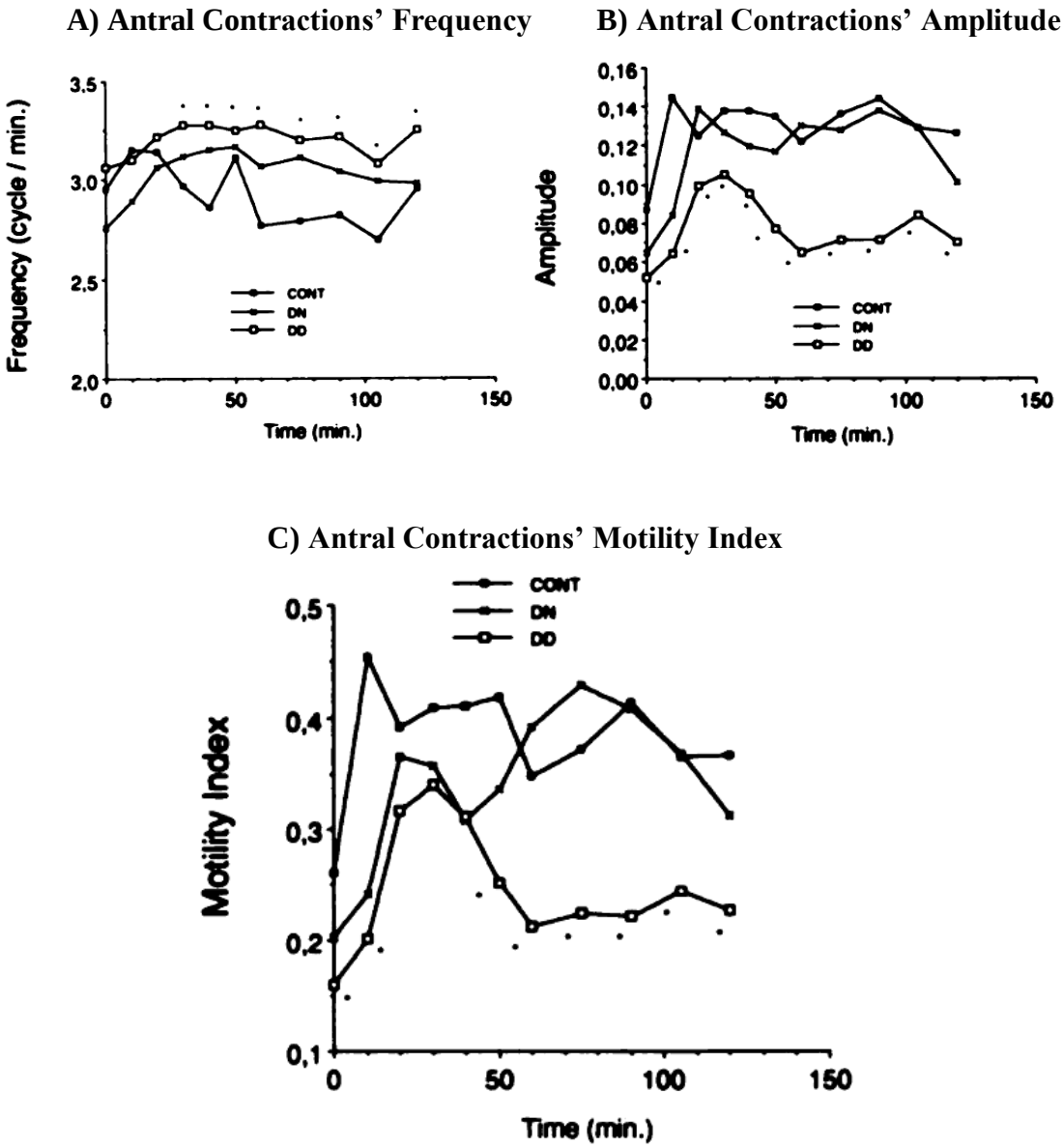

Figure 3.13 Average antral contractions' frequency (A), amplitude (B) and motility indices (C) during the gastric emptying course for controls (CONT), diabetics with a normal gastric emptying (DN) and diabetics with delayed gastric emptying (DD) (23).

Urbain et al. (23) conclude that, in longstanding diabetes, gastric emptying retardation is accounted for by a retention of food in the proximal stomach, which is reflected by a prolonged lag phase as well as by a reduction in antral motor activity that is determined by a decrease in the amplitude of the antral contractions. This study demonstrates that scintigraphy can noninvasively characterize abnormalities of food distribution in the stomach and provides information similar to that obtained from manometry.

CHAPTER IV
MATERIALS AND METHODS

4.1 MATERIALS

4.1.1 Subjects

Make a public announcement in Ramathibodi hospital by distributing leaflets to solicit volunteers interested in the scintigraphic study to evaluate gastric functions through nuclear medicine. Target samples were 20 Thais at the age of 18 or older, strong and healthy. Interested people who wanted to become volunteers would be given with a document with explanation and advice for them to read and make decision. However, before making decision to join the research project, they had to read the document in details in order to learn the reasons and procedures of the research. If they had questions, they might ask a doctor in the research team, who would clarify any issues raised. As soon as they agreed to participate in the research, they would be asked to fill a questionnaire to evaluate their gastric functions. If they had proper qualifications and agreed to participate in the research, they would be asked to see a doctor for nuclear medicine on the scheduled date and time.

Twenty healthy volunteers were recruited for this study and divided into ten groups according to gender and age. The study of these volunteers was approved by Ethical Clearance Committee on Human Rights Related to Researches Involving Human Subjects Faculty of Medicine, Ramathibodi Hospital, Mahidol University. Written informed consent was obtained from each volunteer before enrolling. To obtain a representative of the entire adult population, we distributed recruitment evenly as shown in Table 4.1.

Table 4.1 Distribution of healthy volunteers among age and gender

Age group (years)	Male	Female
18-29	2	2
30-39	2	2
40-49	2	2
50-59	2	2
≥ 60	2	2
Total	10	10

Exclusion criteria were as follows:

- Prior abdominal surgery (except appendectomy and tubal ligament)
- Presence of gastrointestinal symptom during the past 3 months.
- Use of any gastrointestinal or other medications that might affect gastrointestinal motility
- Pregnant women
- Breast feeding women

All volunteers underwent a medical history interview. Female were studied only during the first 10 days of the menstrual cycle.

4.1.2 The imaging system

The imaging system used was the Genesys single detector gamma camera with low energy general purpose and interfaced to an ADAC Atlas imaging system.

4.1.3 Test meal

A test meal included ^{99m}Tc-Phytate labeled egg, 100 g of steamed rice, a glass of water (100 cc). To label the egg, 1 mCi of ^{99m}Tc-Phytate was added to a mixture of 1 beaten raw egg (size 1), 5 cc of oil and 10 cc of water. After stirring to ensure good blending of the mixture, it was cooked in the microwave oven at high heat for 3 minutes.

4.1.4 Image J software

Image J is a public domain Java image processing program inspired by NIH Image for the Macintosh. It runs, either as an online applet or as a downloadable application, on any computer with a Java 1.4 or later virtual machine. Downloadable distributions are available for Windows, Mac OS, Mac OS X and Linux.

It can display, edit, analyze, process, save and print 8-bit, 16-bit and 32-bit images. It can read many image formats including TIFF, GIF, JPEG, BMP, DICOM, FITS and "raw". It can calculate area and pixel value statistics of user-defined selections. It can measure distances and angles. It can create density histograms and line profile plots. It supports standard image processing functions such as contrast manipulation, sharpening, smoothing, edge detection and median filtering.

ImageJ was designed with an open architecture that provides extensibility via Java plugins. Custom acquisition, analysis and processing plugins can be developed using ImageJ's built in editor and Java compiler. User-written plugins make it possible to solve almost any image processing or analysis problem.

ImageJ is being developed on Mac OS X using its built in editor and Java compiler, plus the BBEdit editor and the Ant build tool. The source code is freely available. The author, Wayne Rasband mailto:wayne@codon.nih.gov, is at the Research Services Branch, National Institute of Mental Health, Bethesda, Maryland, USA.

In this study, Image J software was used to read DICOM files of the stomach images and calculate gastric counts.

4.1.5 STATGRAPHICS Plus software

STATGRAPHICS Plus software was used to analyze the gastric emptying data. The version of software is STATGRAPHICS plus 5.1, operated on Windows XP operating system.

4.1.6 MATLAB software

MATLAB software was used to analyze the antral motility data. The version of software is 7.04, operated on Windows XP operating system.

4.2 Methods

4.2.1 Data acquisition

4.2.1.1 Gastric scintigraphy

After an overnight fast, each volunteer was encouraged to complete the test meal within 10 minutes. The start and completion times of ingestion were recorded. Immediately after ingestion of the meal, the volunteers were imaged standing upright with a single head gamma camera. Left anterior oblique 45˚ dynamic (128×128 pixels) frames of 2 sec were acquired for 5 min at 1, 31 min and dynamic frames of 60 sec also were acquired for 25 min at 6 min. Left anterior oblique 45˚ static 60 sec per frame were acquired at 61, 91, 121,181 and 241 min as shown in Table 4.2.

Table 4.2 Acquisition protocol of gastric scintigraphy

Image acquisition		
Phase 1 1st-5th min	LAO 45˚ dynamic	2 sec/frame for 5 minutes
Phase 2 6th-30th min	LAO 45˚ dynamic	60 sec/frame for 25 minutes
Phase 3 31st-35th min	LAO 45˚ dynamic	2 sec/frame for 5 minutes
Phase 4 61st	LAO 45˚ static	60 sec/frame for 1 minute
Phase 6 91st	LAO 45˚ static	60 sec/frame for 1 minute
Phase 8 121st	LAO 45˚ static	60 sec/frame for 1 minute
Phase 10 181st	LAO 45˚ static	60 sec/frame for 1 minute
Phase 11 241st	LAO 45˚ static	60 sec/frame for 1 minute
Acquisition parameter		
Matrix size: 128×128		
Magnification: 1.46		
Collimator type: Low energy general purpose		
^{99m}Tc photopeak energy channel: window ± 20%		

4.2.1.2 Dynamic antral scintigraphy

Anterior dynamic (128×128 pixels) frames of 2 sec were acquired for 5 min at 62, 92, 122 min, shown in Table 4.3. The volunteers were standing still, with the support of the gamma camera detector, and were instructed not to talk or move during image acquisition.

Table 4.3 Acquisition protocol of dynamic antral scintigraphy

Image acquisition		
Phase 5 62^{nd}-66^{th} min	Anterior dynamic	2 sec/frame for 5 minutes
Phase 7 92^{nd}-96^{th} min	Anterior dynamic	2 sec/frame for 5 minutes
Phase 9 122^{nd}-126^{th} min	Anterior dynamic	2 sec/frame for 5 minutes
Acquisition parameter		
Matrix size: 128×128		
Magnification: 1.46		
Collimator type: Low energy general purpose		
^{99m}Tc photopeak energy channel: window ± 20%		

4.2.2 Data Analysis

Gastric emptying data were analyzed using the Elashoff and Siegel equation. When the data were fitted by the Elashoff equation, R^2 values were higher than 0.9. The gastric emptying curve from the Elashoff equation and data from examination, the shapes were heavily different as shown in Figure 4.1.

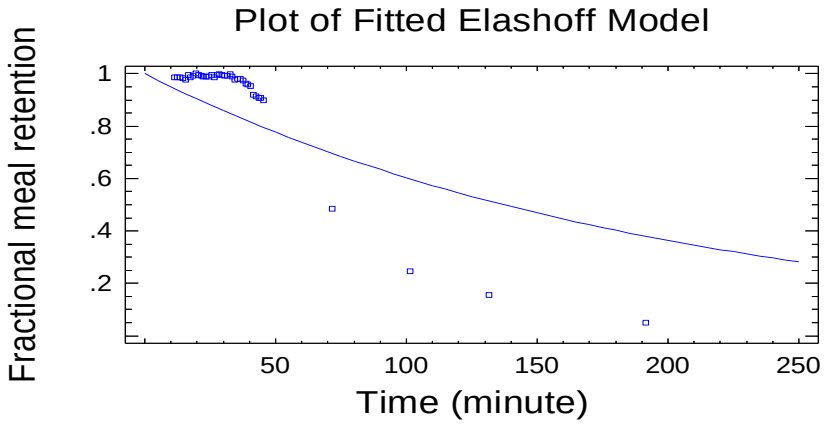

Figure 4.1 Time activity curve is described by power exponential function of Elashoff et al (19). (R^2 =0.911)

But fitted the data in the Siegel equation, R^2 values were higher than 0.9 and the gastric emptying curve from the Siegel equation and data from examination, the shapes were slightly different as shown in Figure 4.2. Thus, the Siegel equation was chosen to fit the gastric emptying data.

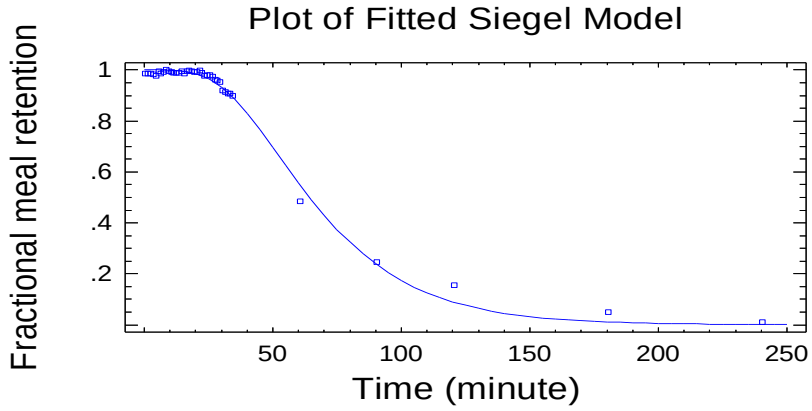

Figure 4.2 Time activity curve is described by modified power exponential function of Siegel et al (21). (R^2 =0.998)

4.2.2.1 Gastric emptying analysis

1. Images of a stomach derived from dynamic (2 sec/frame for 5 minutes) sets at phases 1 and 3 were summed in one minute per image from Pegasys.

2. Save images of the stomach in phase1 and 3 summed in one minute per image, and save images of the stomach derived from a dynamic (60 sec/frame for 25 minutes) set at phase 2 and images of the stomach derived from a static (60 sec/frame for one minute) set of phases 4, 6, 8, 10 and 11, which were dicom files from Pegasys. Then export the dicom files to a personal computer.

3. Find gastric counts using the Image J program featuring the following procedures:

3.1 Use the Image J program to open images of volunteers' stomachs and use the Tool Bar in the Image J to draw ROI around the stomach as shown in Figure 4.3.

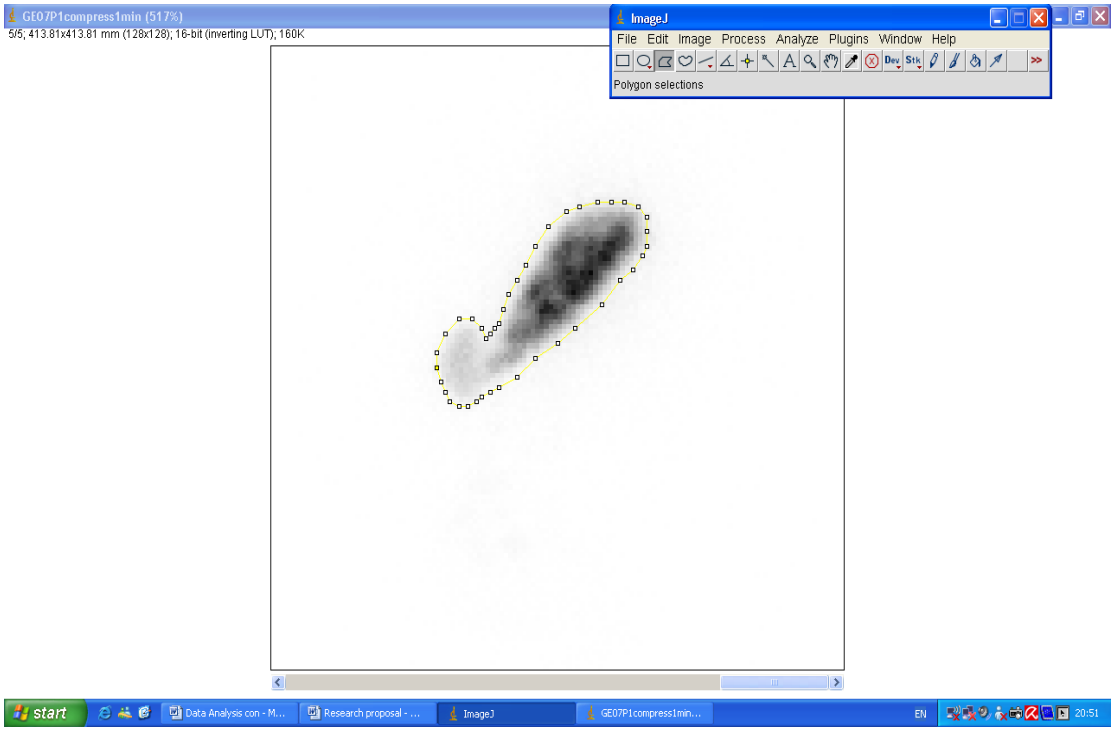

Figure 4.3 Stomach images were analyzed by manually defining the outline of the entire stomach on left anterior oblique images.

3.2 To proceed with a measurement, use the following commands:

Analyze ⇨ Set Measurements and the screen will be as shown in Figure 4.4. Then click Area, Integrated Density and Mean Gray Value and then click OK.

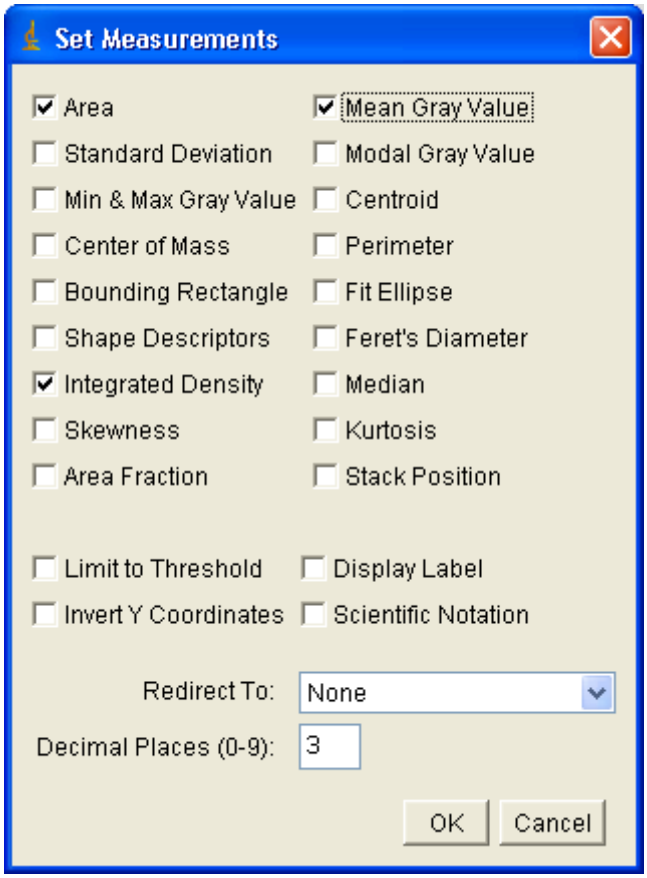

Figure 4.4 Set measurements

3.3 Set the scale of the stomach image in pixel unit using the following commands:

Analyze ⇨ Set Scale and the screen will be as shown in Figure 4.5(A). The scale of the stomach image will be in mm unit. Then click Remove Scale to change the scale in pixel unit, shown in Figure 4.5(B).

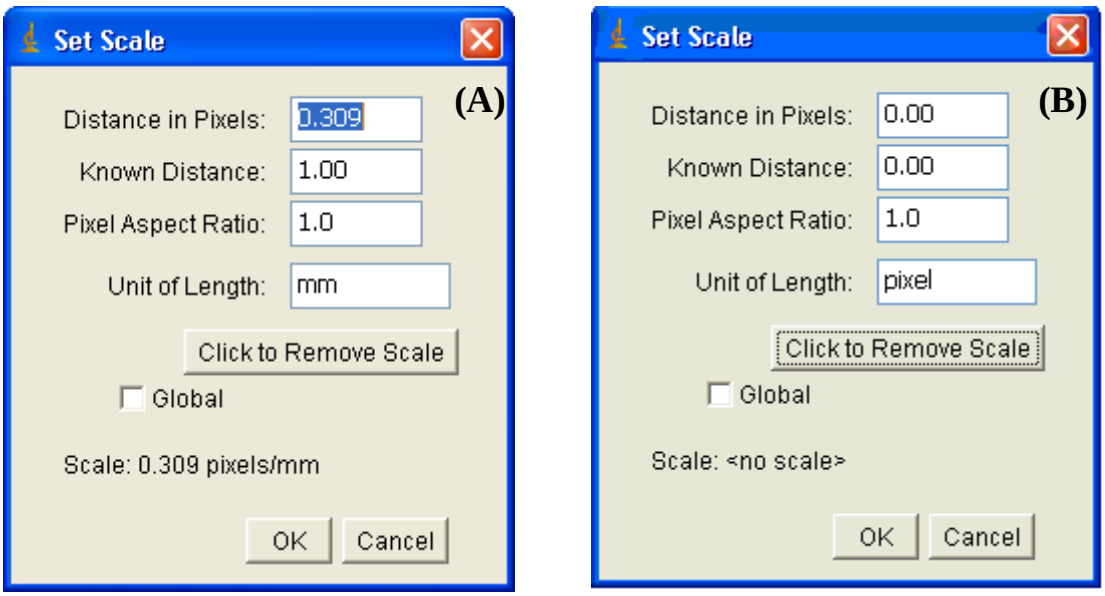

Figure 4.5 (A) Displays the scale of the stomach image in mm unit and (B) the scale in pixel unit.

3.4 Measure gastric counts in ROI using the following commands:

Analyze ⇨ Tools ⇨ ROI Manager and the screen will be as shown in Figure 4.6(A). Then click Add [t] to add ROI of the stomach, drawn shown in Figure 4.3 to calculate gastric counts in ROI, show in Figure 4.6(B). From this example, we name ROI as gastric.

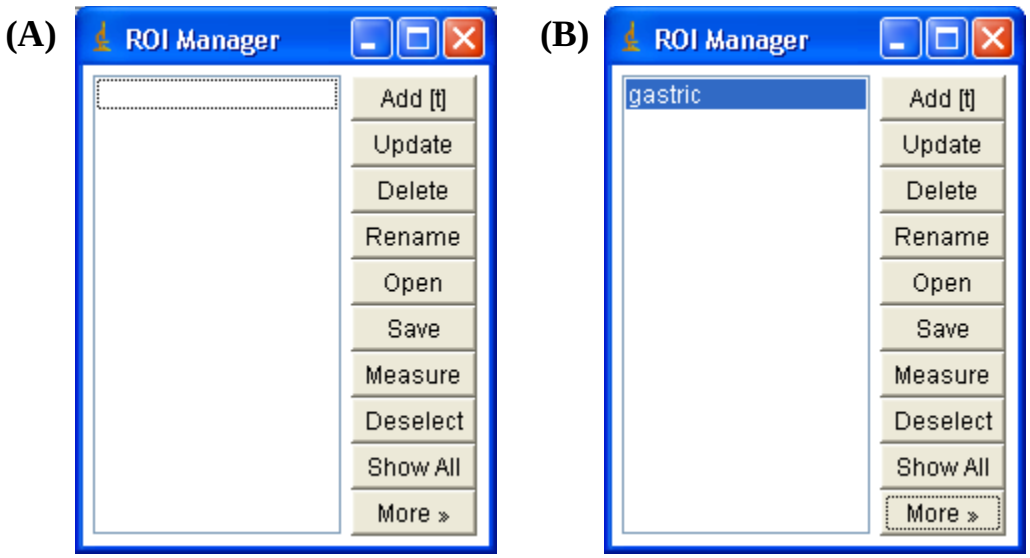

Figure 4.6 ROI Manager

3.5 Click More » on the screen of ROI manager as in Figure 4.6 and click Multi Measure and you will see the screen as in Figure 4.7. Then click Measure All 5 Slices and One Row Per slice, and then click OK and you will see the screen as shown in Figure 4.8.

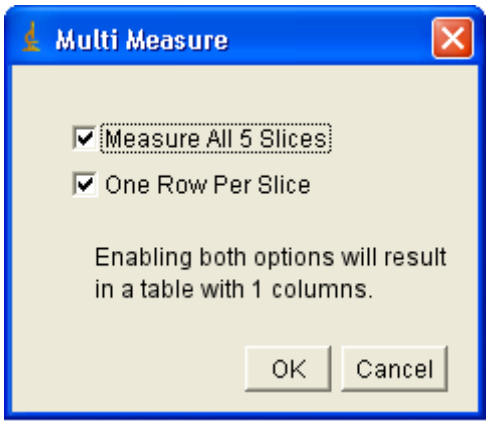

Figure 4.7 Multi Measure

Results

File Edit Font

	Area(gastric)	Mean(gastric)	IntDen(gastric)
1	811	246.847	200193
2	811	247.293	200555
3	811	244.700	198452
4	811	245.501	199101
5	811	246.007	199512

Figure 4.8 Column1 shows ranking of the stomach images; column 2 shows area of ROI of the stomach in pixel^2; column 3 shows mean counts in ROI of the stomach from each image, calculated from the sum of the gastric counts of all the pixels in ROI divided by the number of pixels; column 4 Integrated Density shows the sum of the gastric counts in ROI of the stomach, calculated from the area of ROI multiplied by mean counts in ROI of each image.

4. Gastric counts in ROI from each image from the Image J program will be exported to the Excel program to correct the decay and change into fractional meal retention. Normalize the peak count to one. However, it's not necessary that the normalized peak count must be 1 at the start of scanning.

5. Time 0 shall be set at the start of scanning.

6. Data of fractional meal retention at each period shall be exported to the Statgraphics program to fit using the Siegel's equation and find parameters k and β using the nonlinear least-squares fitting algorithm featuring the following procedures:

6.1 Export the fractional meal retention at each period to the Statgraphics program and the screen will be as shown in Figure 4.9.

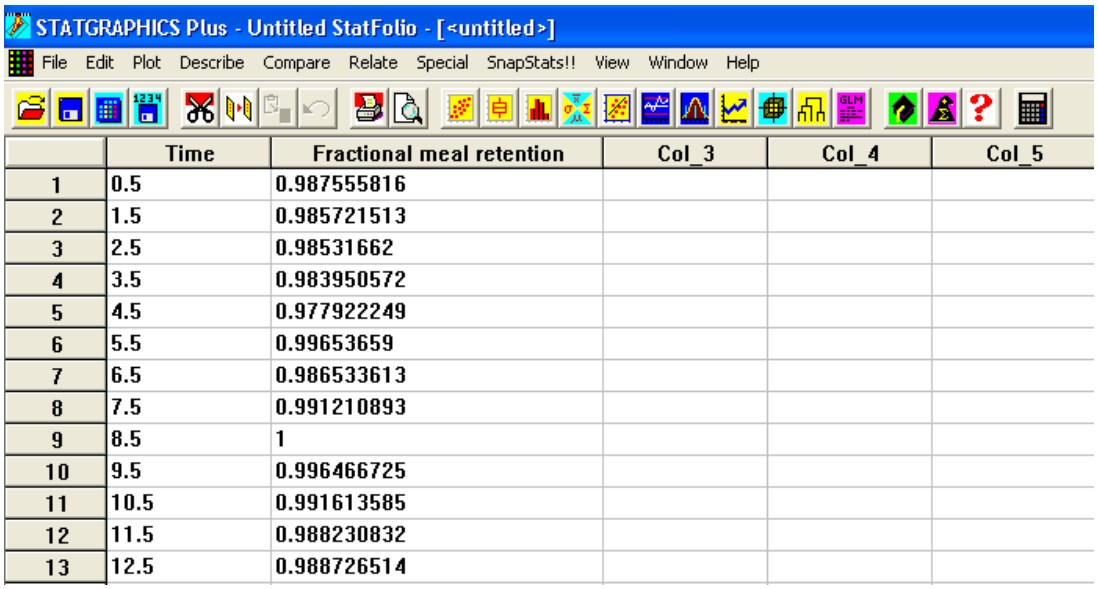

	Time	Fractional meal retention	Col_3	Col_4	Col_5
1	0.5	0.987555816			
2	1.5	0.985721513			
3	2.5	0.98531662			
4	3.5	0.983950572			
5	4.5	0.977922249			
6	5.5	0.99653659			
7	6.5	0.986533613			
8	7.5	0.991210893			
9	8.5	1			
10	9.5	0.996466725			
11	10.5	0.991613585			
12	11.5	0.988230832			
13	12.5	0.988726514			

Figure 4.9 displays fractional meal retention at each period exported to the Statgraphics program.

6.2 Fit the fractional meal retention at each period using the Siegel's equation as shown in equation (5).

Find parameters k and β using the nonlinear least-squared fitting algorithm, using the following commands:

Special ⇨ Advanced Regression ⇨ Nonlinear Regression. The Screen will look like Figure 4.10.

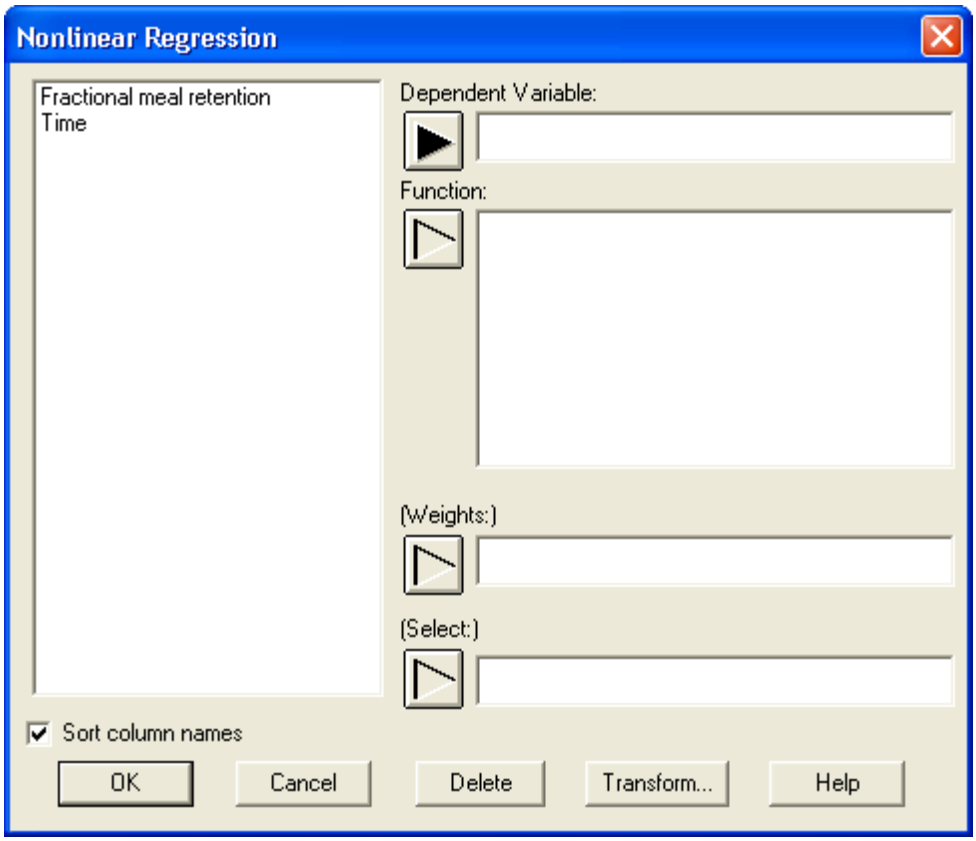

Figure 4.10 Nonlinear Regression

6.3 The user shall choose a dependent variable, namely, fractional meal retention into the Dependent Variable block and Click Transform. You will see the screen as shown in Figure 4.10. Then type the Siegel's equation in the Expression block and click OK and the screen in Figure 4.11 will be shown.

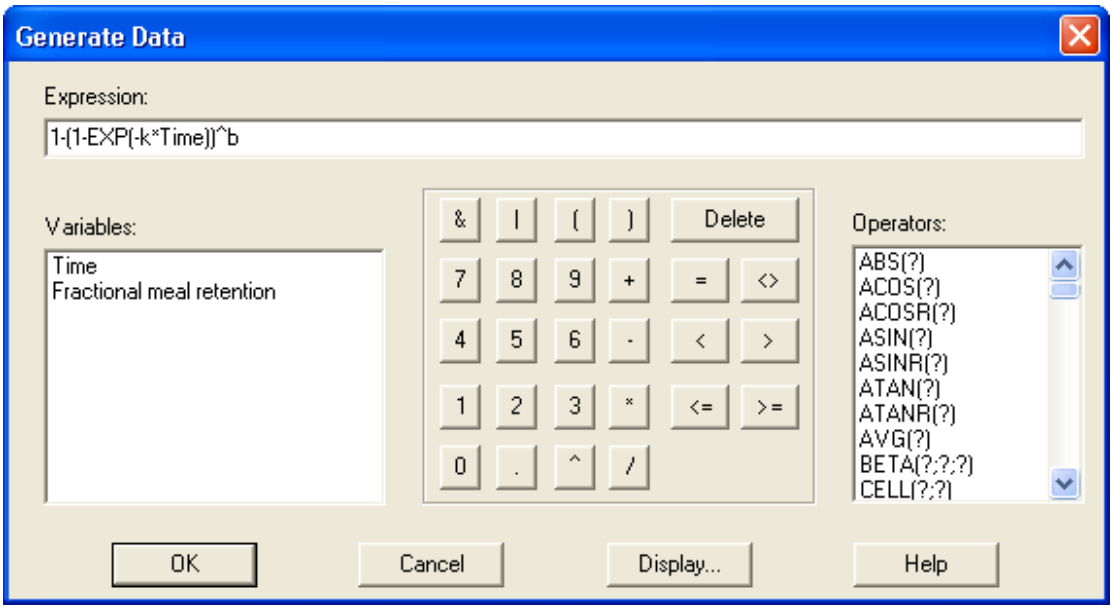

Figure 4.11 Generate Data

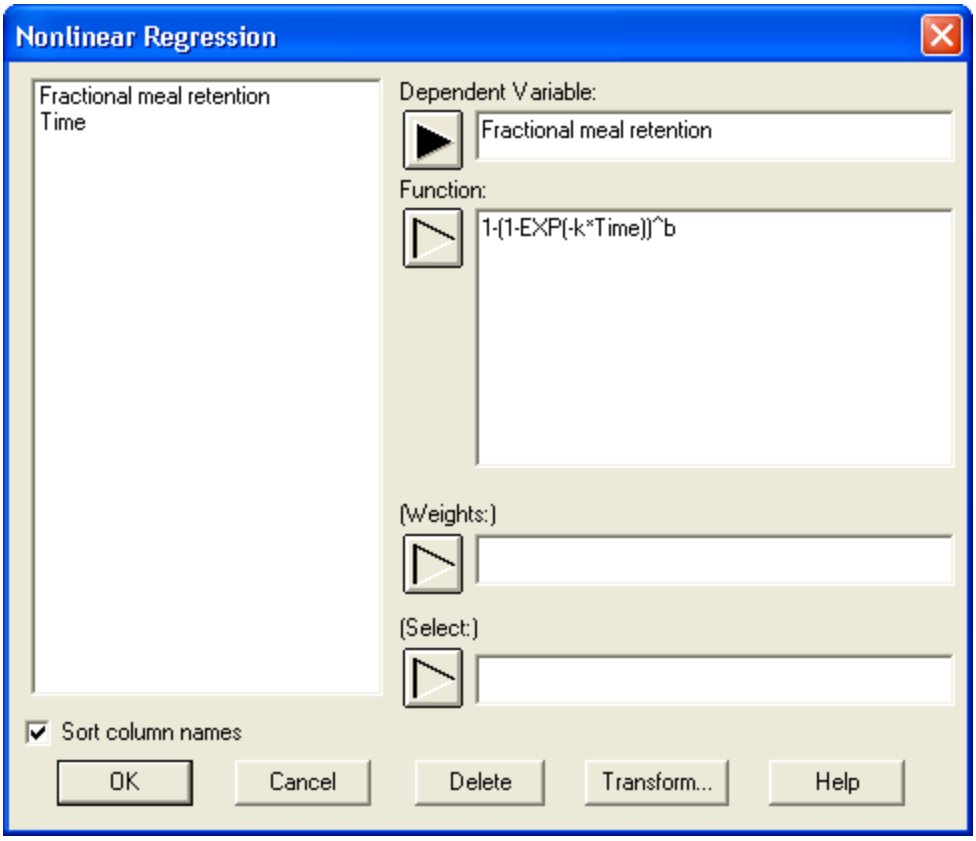

Figure 4.12 Nonlinear Regression

6.4 As you click OK for the Nonlinear Regression on the screen as in Figure 4.12, the Initial Parameter Estimates will be displayed, as in Figure 4.13. Then assign the starting value of parameters k and β. From a literature review, the starting value is k = 0.01 and β =1. And then click OK. You will see the screen as in Figure 4.14.

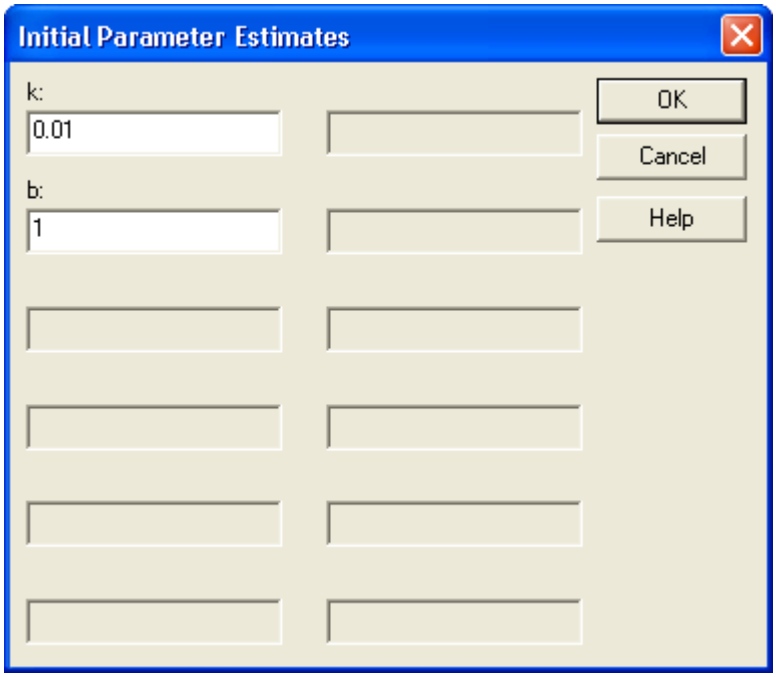

Figure 4.13 Initial Parameter Estimates

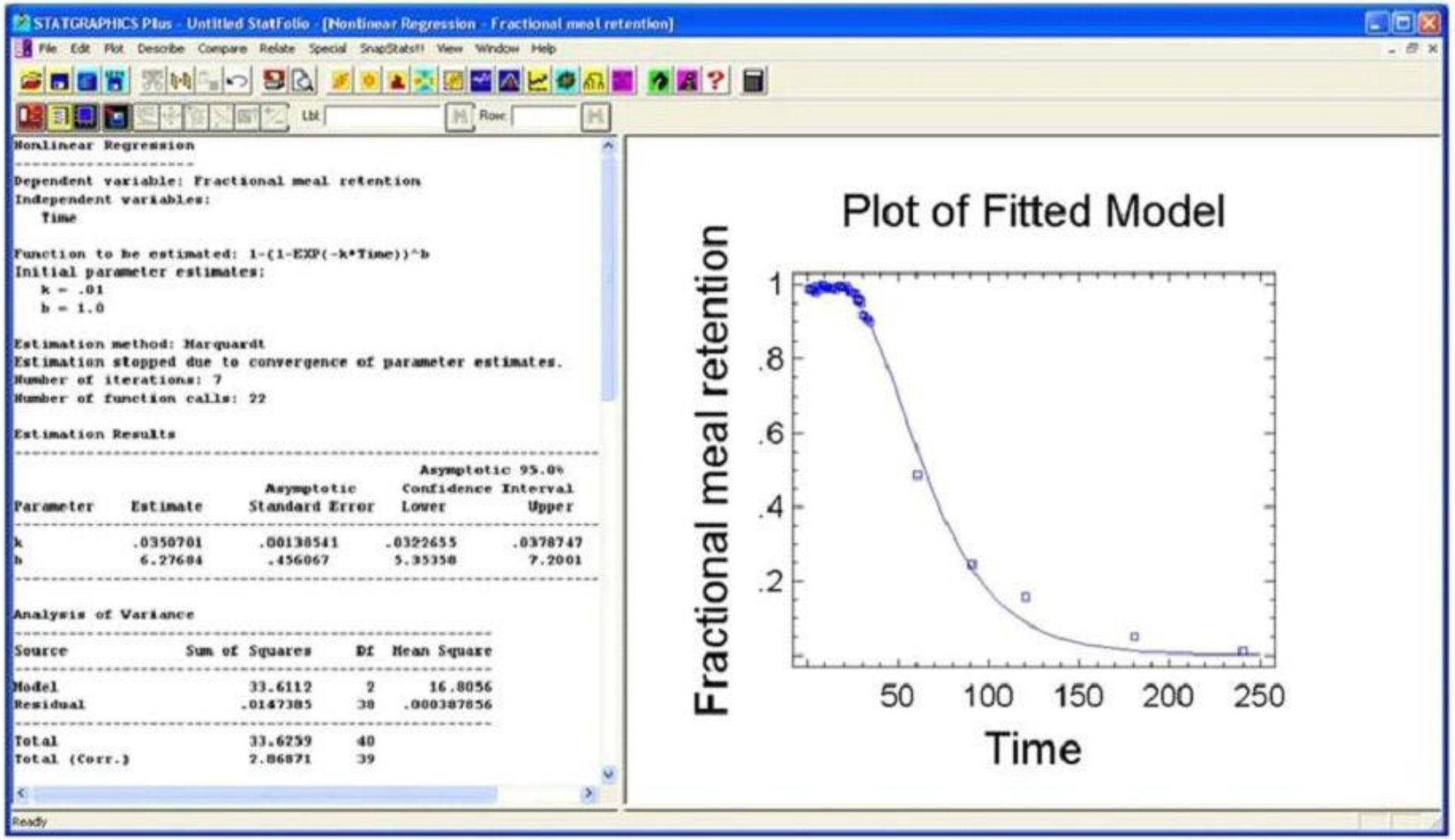

Figure 4.14 Fit the fractional meal retention at each period using the modified power exponential function of Siegel and display parameters k and β which derived from nonlinear least-squared fitting algorithm.

6.5 From the screen in Figure 4.14, fit gastric emptying data using the Siegel's equation and you will obtain the values of parameters k and β, from which you can calculate the emptying half time (T1/2), lag phase time and constant emptying time based the equation from Maximum slope tangent method of Couturier. The method of Couturier consisted in describing the modified power exponential function of Siegel et al by two straight lines. The first line is the line of 100% retention rate and the second line is tangent to the maximum slope of the modified power exponential function (see theoretical curve in Figure 4.15). The time at the intercept of these two lines defined the lag phase time. The intersection of the tangent and the abscissa defined the end of the constant emptying phase. The formulae are given below:

Maximum slope tangent (MS)

Couturier Siegel's model

The half emptying time $T_{(1/2)S} = -\mathrm{Ln}\left(1-2^{\left(-1/\beta\right)}\right)\Big/k$ (11)

The lag phase time is $T_{lag(MS)\,(S)} = \frac{Ln\beta}{k} - \left(\frac{\beta-1}{k\beta}\right)$ (12)

The real emptying time is $T_{RE}(MS)_{(S)} = \frac{1}{k}\left(\frac{\beta-1}{\beta}\right)^{1-\beta}$ (13)

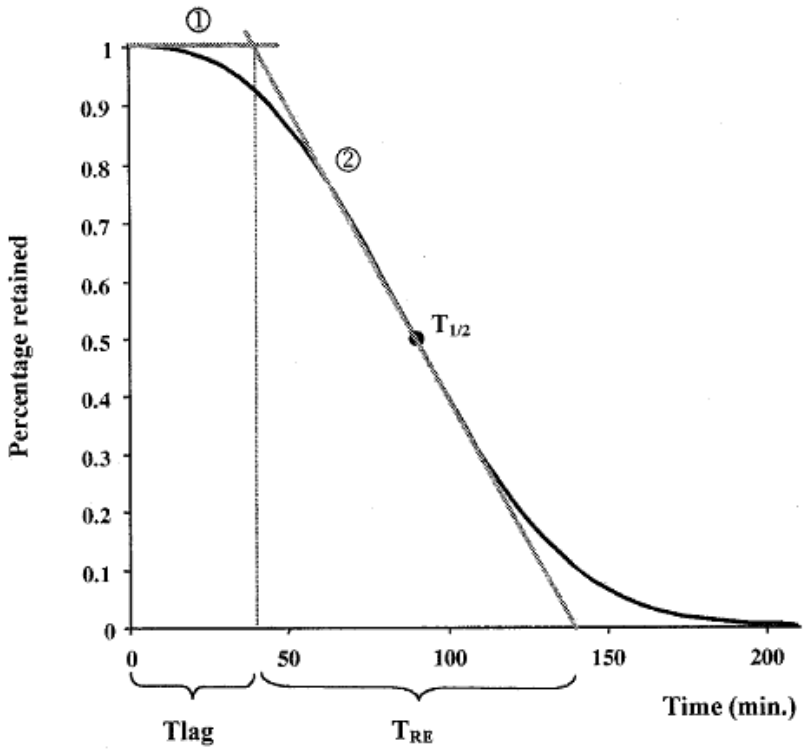

Figure 4.15 Power exponential function described by two straight lines. The first line is horizontal and represents the lag phase. The second line is a tangent and represents constant gastric emptying. The time at the intercept of these two lines marks the end of the lag phase and the start of the constant emptying phase. The intercept of the tangent with the abscissa defines the end of the real emptying time T_{RE} (20).

4.2.2.2 Dynamic antral scintigraphy analysis

1. Save images of a stomach from dynamic (2 sec/frame for 5 minutes) sets of phases 5, 7 and 9 which are in dicom files from Pegasys and then export the dicom files to the personal computer. Then use the Image J program to open images of volunteers' stomachs. Use the Tool Bar in the Image J program to draw a rectangular ROI at antrum between incisura angularis and pylorus, shown in Figure 4.16. ROI of the antrum will be drawn vertically at not more than 20 pixels and horizontally not more than 15 pixels.

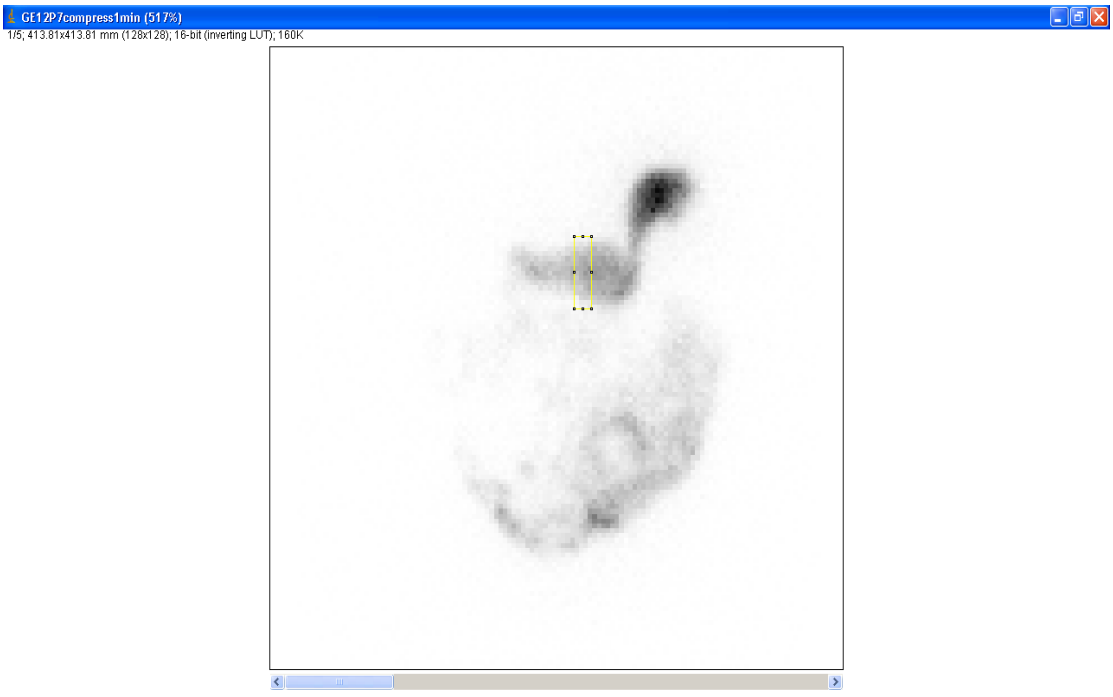

Figure 4.16 Rectangular ROI was drawn around antrum between incisura angularis and pylorus on each reframed image by Image J.

2. Counts in the rectangular ROI in each dynamic set from Image J program will be exported to MATLAB program to find frequency of antral contraction with the following procedures:

2.1 Counts in the rectangular ROI will be exported to the MATLAB program in a Matrix format, as shown below.

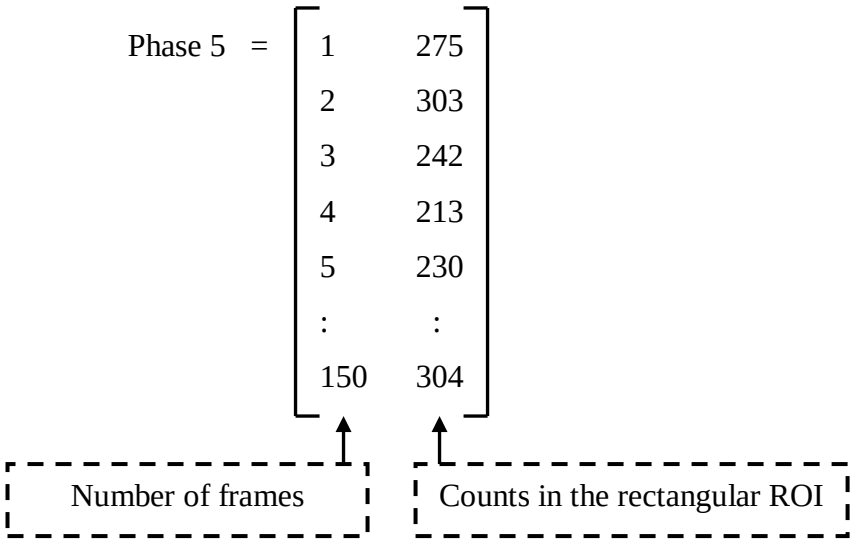

2.2 Counts derived from the rectangular ROI in each dynamic set will be used to build a graph: Antral time-activity curve, using the following commands.

```
» plot(phase5(:,2))
» title('Antral time-activity Curve; Raw data')
» xlabel('Frames')
» ylabel('Counts')
```

The outcome will be as shown in Figure 4.17.

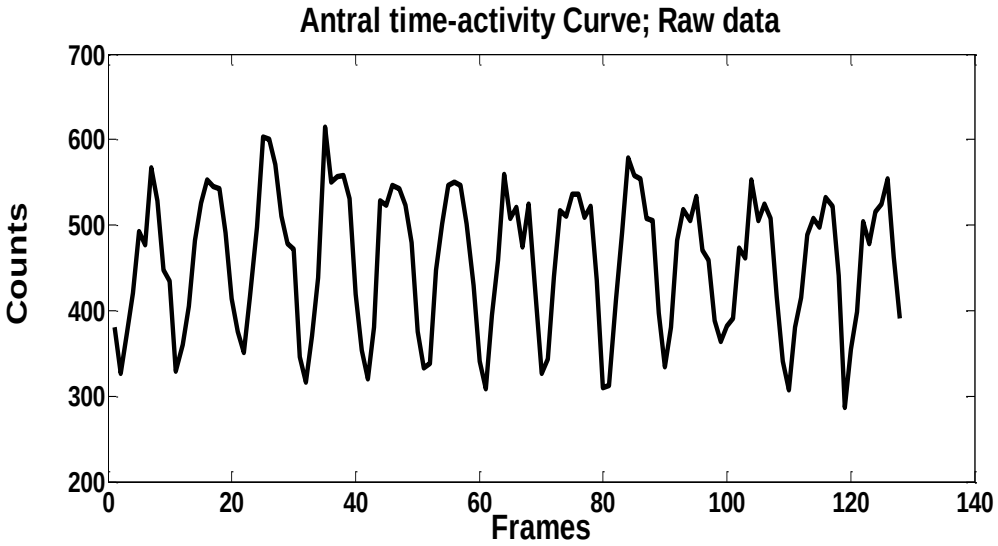

Figure 4.17 Antral time activity curve

2.3 Counts derived from the rectangular ROI in each dynamic set will be normalized, namely, normalized data = (raw data – mean counts)/mean counts, and then build a graph of Normalized antral time-activity curve, using the following commands.

» normdata=(data-mean(data))/mean(data)

» plot(normdata)

» title('Normalized Antral time-activity curve')

» xlabel('Frames')

» ylabel('Normalized Counts')

The outcome will be as shown in Figure 4.18.

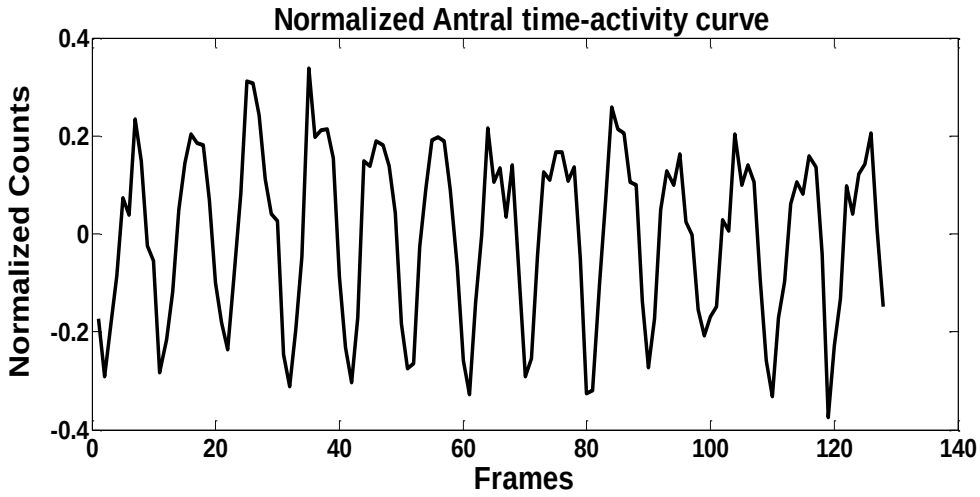

Figure 4.18 Normalized Antral time activity curve

2.4 Data normalized will be analyzed using Fourier algorithm to find the frequency of antral contraction using the following commands.

» Y=fft(normdata,128)

» Pyy=Y.*conj(Y)/128

» f=30/128*(0:63)

» plot(f(1:64),Pyy(1:64))

» title('Fourier Transform Analysis Plot')

» xlabel('Frequency (cycles/min)')

» ylabel('Amplitude')

The outcome will be as shown in Figure 4.19.

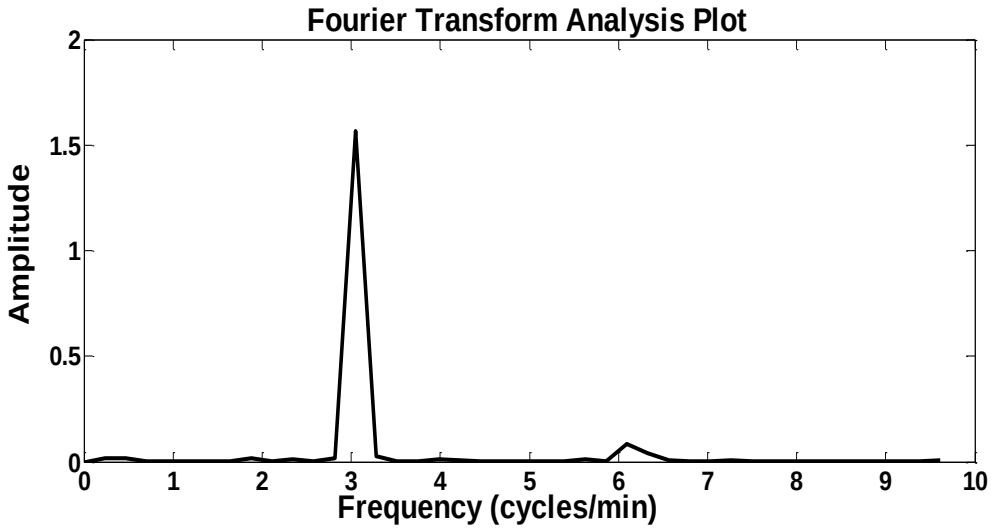

Figure 4.19 Fourier Transform Analysis Plot

4.3 Statistical Analysis

Descriptive statistics are applied to explain gastric emptying parameters, frequency and amplitude of antral contraction. The statistics used in the calculation include Median, Maximum, Minimum and Standard Deviation.

Mann-Whitney U Test, which is a non-parametric statistics, is used to test the difference of gastric emptying parameters (k, β, lag phase time, constant emptying time, half emptying time), frequency and amplitude of antral contraction among female and male volunteers. If $p<0.05$, that difference is significant.

An example of the Mann-Whitney U Test for this study:

To test whether the lag phase time between female and male volunteers is different or not:

1) Hypotheses used in the test,

Hypotheses are as follows:

H_o: Female volunteers' lag phase time = male volunteers,

H_a: Female volunteers' lag phase time ≠ male volunteers,

or

H_o: $M_1=M_2$
H_a: $M_1\neq M_2$ } two-tailed test

(M_1 is Median lag phase time for female volunteers and M_2 is Median lag phase time for male volunteers.)

2) Combine data of female and male volunteers' lag phase time, put them in order from less to more and then rank them. In case of tied observations, the Mean will be used.

3) To find the sum of ranks of female and male volunteers' lag phase time:

W_1 = the sum of ranks of female volunteers' lag phase time,

W_2 = the sum of ranks of male volunteers' lag phase time,

The following will be derived:

$$W_1+W_2 = \frac{n(n+1)}{2} \quad (16)$$

(n_1 = the number of female volunteers and n_2 = the number of male volunteers: $n=n_1+n_2$)

4) Statistical test of U and U'

$$U = n_1 n_2 + \frac{n_1(n_1+1)}{2} - W1 \quad (17)$$

$$U' = n_1 n_2 + \frac{n_2(n_2+1)}{2} - W2 \quad (18)$$

Whereas

$$U' = n_1 n_2 - U \quad (19)$$

5) Conclusion from the test:

(1) Compare the Probability $P(U \leq U_0)$ if $U_0 = \min(U, U')$ and the set significant level (α). The test can be concluded as follows:

Two-tailed test:

- Main hypothesis H_o will be denied if $P(U \leq U_0) < \alpha/2$

(2) Compare the $U_0 = \max(U, U')$ with the critical value of Mann Whitney U (U_α) with the main hypothesis. H_o will be denied if

- $U_0 = \max(U, U') > U_{\alpha(2),n1,n2}$ if applied in the two-tailed test.

U and U' are the value of test statistics for Mann-Whitney U. U_0 is the value of the Mann-Whitney U statistics. The probability $P(U \leq U_0)$ and critical values for Mann Whitney U test (U_α) are shown in Table C-1 and C-2 in Appendix C respectively (24).

CHAPTER V
RESULTS

5.1 Goodness of fits

Curve fitting of gastric emptying experimental data derived from 20 Thai volunteers by the mathematical function of Siegel et al. R^2 values were reported as an index of whether or not a curve provides a good fit to the data. R^2 should be high (say above 0.9). Furthermore, the estimated curve was plotted with the observed points to check differences between the shapes of the estimated curve and observed points.

The results of assessing the goodness of modified power exponential fit showed that, in all volunteers, R^2 values were higher than 0.9 as shown in Table 5.1 and there were little differences between the shapes of the estimated curve and observed points as shown in appendix A. Therefore, the goodness of fit with modified power exponential function was good.

Table 5.1 Coefficient of determination (R^2)

No.	gender	Age (years)	R^2
1		25	0.9947
2		29	0.9952
3		33	0.9769
4		34	0.9900
5	Male	40	0.9972
6		48	0.9944
7		52	0.9944
8		59	0.9901
9		60	0.9883
10		64	0.9934
11		27	0.9955
12		28	0.9932
13		31	0.9797
14		42	0.9973
15	Female	46	0.9963
16		50	0.9970
17		51	0.9692
18		60	0.9966
19		64	0.9726

5.2 Comparison of gastric emptying parameters between the female and male volunteers.

Table 5.2 shows gastric emptying parameters of all the 19 volunteers. Gastric emptying parameters from the analysis of the time the stomach empties food to small intestine until the stomach is emptied:

- k refers to the emptying rate in one minutes (1/minute).
- β is the extrapolated y-intercept from the terminal portion of the modified power exponential curve.
- Lag phase time is the time the stomach consumes to digest food until it can pass through the pylorus.
- Constant emptying time is the emptying rate which is being constant.
- Emptying half time is the time the stomach has emptied half of the food in the stomach.

The descriptive statistics of gastric emptying parameters in male and female volunteers, which explain the gastric emptying parameters in terms of median, maximum, minimum, and standard deviation, were shown in Table 5.3. The test whether the gastric emptying parameters of male volunteers are different from those of female volunteers, using the Mann-Whitney U Test, which is non-parametric statistics to test the hypotheses, was shown in Table 5.4. If $p<0.05$, that difference is significant. The findings from the test show that gastric emptying parameters, namely, k, β, lag phase time, constant emptying time, half emptying time between female and male volunteers are not different as $p>0.05$. Table 5.5 shows normal range of gastric emptying parameters, derived from an analysis of solid gastric emptying of the 19 volunteers at the percentage cut-off points of 2.5 and 97.5. The study on the lag phase time, constant emptying time, half emptying time among normal people at the percentage cut-off points of 2.5 and 97.5, features the values derived 5.56-38.37, 69.64-134.94 and 50.49-87.48 minutes, respectively.

Table 5.2 Gastric emptying parameters

No.	gender	Age (years)	Gastric emptying rate (k, 1/min)	β	Lag phase time (min)	Constant emptying time (min)	Half emptying time (min)
1	Male	25	0.035	6.28	28.4	71.23	64.39
2		29	0.031	7.17	36.27	82.58	77.95
3		33	0.016	2.3	17.28	134.94	86.60
4		34	0.028	5.32	30.11	86.13	73.66
5		40	0.031	6.1	30.96	79.4	71.07
6		48	0.027	4.02	23.68	87.63	68.11
7		52	0.033	3.3	15.07	69.64	50.49
8		59	0.022	3.8	27.1	106.44	81.11
9		60	0.025	4.9	31.61	97.1	80.73
10		64	0.023	4.12	28.98	104.85	82.12
11	Female	27	0.031	6.7	34.12	81.56	75.3
12		28	0.021	4.11	30.86	111.7	87.48
13		31	0.021	1.69	5.56	87.93	51.65
14		42	0.018	2.36	15.82	118.39	76.58
15		46	0.029	3.55	18.79	79.5	59.17
16		50	0.026	5.66	34.93	94.95	82.92
17		51	0.027	3.82	23.4	91.53	69.84
18		60	0.031	4.82	24.78	77.21	63.85
19		64	0.026	6.28	38.37	96.22	86.96

One woman volunteer in age range 30-39 years with $T_{1/2}$ = 192.94 min was excluded from the summary.

Table 5.3 Comparison of the gastric emptying parameters in terms of median, maximum, minimum and standard deviation between the male and female volunteers

Gastric emptying rate (k, 1/min)	**Male (n=10)**	**Female (n=9)**
Median	0.0275	0.0260
SD	0.0058	0.0046
Min, Max	0.02, 0.04	0.02, 0.03

β	**Male (n=10)**	**Female (n=9)**
Median	4.51	4.11
SD	1.50	1.70
Min, Max	2.30, 7.17	1.69, 6.70

Lag phase time (min)	**Male (n=10)**	**Female (n=9)**
Median	28.69	24.78
SD	6.55	10.59
Min, Max	15.07, 36.27	5.56, 38.37

Constant emptying time (min)	**Male (n=10)**	**Female (n=9)**
Median	86.88	91.53
SD	19.65	14.13
Min, Max	69.64, 134.94	77.21, 118.39

Half emptying time (min)	Male (n=10)	Female (n=9)
Median	75.80	75.30
SD	10.66	12.55
Min, Max	50.49, 86.60	51.65, 87.48

Table 5.4 Comparison of gastric emptying parameters between female and male volunteers

	Gastric emptying rate (k, 1/min)	β	Lag phase time (min)	Constant emptying time (min)	Half emptying time (min)
Female (n=9)	0.0260	4.11	24.78	91.53	75.30
Male (n=10)	0.0275	4.51	28.69	86.88	75.80
F vs. M	p = 0.447	p = 0.661	p = 0.905	p = 0.720	p = 1.000

Data are represented as median. Statistical analysis was performed by Mann Whitney U test.

Table 5.5 Normal range of gastric emptying parameters among the 19 volunteers at the percentage cut-off points of 2.5 and 97.5.

Percentiles	Gastric emptying rate (k, 1/min)	β	Lag phase time (min)	Constant emptying time (min)	Half emptying time (min)
2.5	0.016	1.69	5.56	69.64	50.49
97.5	0.035	7.17	38.37	134.94	87.48

5.3 Comparison of antral frequency between the female and male volunteers.

A study on gastric antral contraction using the dynamic antral scintigraphy jointly with the Fourier Algorithm was used to evaluate frequency of antral contraction. Table 5.6 shows the frequency of antral contraction. Data collected at the 62^{nd}, 92^{nd} and 122^{nd} minute of all the 19 volunteers. Descriptive statistics of the frequency of antral contraction, collected at the 62^{nd}, 92^{nd} and 122^{nd} minute of the male and female volunteers, which explain the frequency of antral contraction in terms of median, maximum, minimum and standard deviation, were shown in Table 5.7. The test whether the frequency of antral contraction at the 62^{nd}, 92^{nd} and 122^{nd} minute between female and male volunteers is different from each other using the Mann-Whitney U Test, which is non-parametric statistics to test the hypotheses was shown in Table 5.8. If $p<0.05$, that difference is significant. The findings from the test show that the frequency of antral contraction at the 62^{nd}, 92^{nd} and 122^{nd} minute of the female and male volunteers is not different as $p>0.05$.

The gastric antral contraction analysis using dynamic antral scintigraphy jointly with the Fourier Algorithm is apparent that the approach can show clear antral contraction frequency in all volunteers as shown in appexdix B.

Table 5.6 Frequency of antral contraction at the 62nd, 92nd and 122nd minute of all the 19 volunteers.

No.	gender	Age (years)	Frequency of antral contraction (cycles/min)		
			62 min after the start of scanning	92 min after the start of scanning	122 min after the start of scanning
1		25	3.52	3.52	3.52
2		29	3.28	3.28	3.28
3		33	3.75	3.05	3.28
4		34	3.28	3.28	3.28
5	Male	40	3.28	3.28	3.28
6		48	3.28	3.05	3.28
7		52	3.05	3.05	3.28
8		59	2.81	2.81	2.81
9		60	3.05	3.28	3.05
10		64	3.05	3.05	3.05
11		27	3.28	3.28	3.28
12		28	3.05	3.05	2.81
13		31	3.28	3.05	3.28
14		42	3.28	2.58	3.28
15	Female	46	3.28	3.05	3.05
16		50	3.05	3.05	2.81
17		51	3.05	3.05	3.05
18		60	3.05	3.05	2.81
19		64	3.52	3.52	3.28

One woman volunteer in age range 30-39 years with $T_{1/2}$ = 192.94 min was excluded from the summary.

Table 5.7 Comparison of the frequency of antral contraction, collected at the 62nd, 92nd and 122nd minute in terms of median, maximum, minimum and standard deviation between the male and female volunteers

Frequency of antral contraction at 62 min after the start of scanning (cycles/min)	**Male (n=10)**	**Female (n=9)**
Median	3.28	3.28
SD	0.27	0.16
Min, Max	2.81, 3.75	3.05, 3.52

Frequency of antral contraction at 92 min after the start of scanning (cycles/min)	**Male (n=10)**	**Female (n=9)**
Median	3.16	3.05
SD	0.20	0.25
Min, Max	2.81, 3.52	2.58, 3.52

Frequency of antral contraction at 122 min after the start of scanning (cycles/min)	**Male (n=10)**	**Female (n=9)**
Median	3.28	3.05
SD	0.19	0.22
Min, Max	2.81, 3.52	2.81, 3.28

Table 5.8 Comparison of the frequency of antral contraction at the 62nd, 92nd and 122nd minute between female and male volunteers

	Frequency of antral contraction (cycles/min)		
	62 min after the start of scanning	**92 min after the start of scanning**	**122 min after the start of scanning**
Female (n=9)	3.28	3.05	3.05
Male (n=10)	3.28	3.16	3.28
F vs. M	p = 0.842	p = 0.400	p = 0.211

Data are represented as median. Statistical analysis was performed by Mann Whitney U test.

5.4 Comparison of amplitude of antral contraction between the female and male volunteers.

Table 5.9 shows the amplitude of antral contraction. Data collected at the 62nd, 92nd and 122nd minute of all the 19 volunteers. Descriptive statistics of the amplitude of antral contraction, collected at the 62nd, 92nd and 122nd minute of the male and female volunteers, which explain the amplitude of antral contraction in terms of median, maximum, minimum and standard deviation, were shown in Table 5.10. The test whether the amplitude of antral contraction at the 62nd, 92nd and 122nd minute between female and male volunteers is different from each other using the Mann-Whitney U Test, which is non-parametric statistics to test the hypotheses was shown in Table 5.11. If $p<0.05$, that difference is significant. The findings from the test show that the amplitude of antral contraction at the 62nd, 92nd and 122nd minute of the female and male volunteers is not different as $p>0.05$.

Table 5.12 shows range of the amplitude of antral contraction. Finding from the study of the amplitude, collected at the 62nd, 92nd and 122nd minute in normal persons are in the range of 0.16–2.62, 0.17-3.51 and 0.35-1.99, respectively.

Table 5.9 The amplitude of antral contraction at the 62nd, 92nd and 122nd minute of all the 19 volunteers.

No.	gender	Age (years)	Amplitude of antral contraction		
			62 min after the start of scanning	92 min after the start of scanning	122 min after the start of scanning
1		25	1.40	1.00	0.58
2		29	1.18	0.64	0.59
3		33	0.22	1.58	0.78
4		34	0.23	1.08	1.70
5	Male	40	0.20	0.45	0.45
6		48	1.18	2.30	0.42
7		52	0.61	0.81	0.43
8		59	2.62	1.37	1.90
9		60	1.22	0.92	1.99
10		64	0.49	0.27	0.88
11		27	0.45	1.19	1.60
12		28	1.90	1.10	0.67
13		31	0.86	0.17	0.35
14		42	0.37	1.17	0.99
15	Female	46	0.16	1.37	0.77
16		50	0.99	3.51	1.10
17		51	1.18	0.82	1.40
18		60	1.59	0.77	0.97
19		64	0.93	0.43	0.48

One woman volunteer in age range 30-39 years with T1/2 =192.94 min was excluded from the summary.

Table 5.10 Comparison of the amplitude of antral contraction, collected at the 62nd, 92nd and 122nd minute in terms of median, maximum, minimum and standard deviation between the male and female volunteers.

Amplitude of antral contraction at 62 min after the start of scanning	Male (n=10)	Female (n=9)
Median	0.89	0.93
SD	0.75	0.57
Min, Max	0.20, 2.62	0.16, 1.90

Amplitude of antral contraction at 92 min after the start of scanning	Male (n=10)	Female (n=9)
Median	0.96	1.10
SD	0.59	0.96
Min, Max	0.27, 2.30	0.17, 3.51

Amplitude of antral contraction at 122 min after the start of scanning	Male (n=10)	Female (n=9)
Median	0.68	0.97
SD	0.64	0.41
Min, Max	0.42, 1.99	0.35, 1.60

Table 5.11 Comparison of the amplitude of antral contraction at the 62nd, 92nd and 122nd minute between female and male volunteers

	Amplitude of antral contraction		
	62 min after the start of scanning	92 min after the start of scanning	122 min after the start of scanning
Female (n=9)	0.93	1.10	0.97
Male (n=10)	0.89	0.96	0.68
F vs. M	p = 1.000	p = 0.902	p = 0.806

Data are represented as median. Statistical analysis was performed by Mann Whitney U test.

Table 5.12 Range of the amplitude of antral contraction among the 19 volunteers at the 62nd, 92nd and 122nd minute after the start of scanning

Time	Range of the amplitude of antral contraction
62 min after the start of scanning	0.16–2.62
92 min after the start of scanning	0.17-3.51
122 min after the start of scanning	0.35-1.99

CHAPTER VI
DISCUSSION AND CONCLUSION

6.1 DISCUSSION

Gastric emptying data were analyzed using the Elashoff and Siegel equation. When the data were fitted by the Elashoff equation, R^2 values were higher than 0.9. The gastric emptying curve from the Elashoff equation and data from examination, the shapes were heavily different as shown in Figure 6.1.

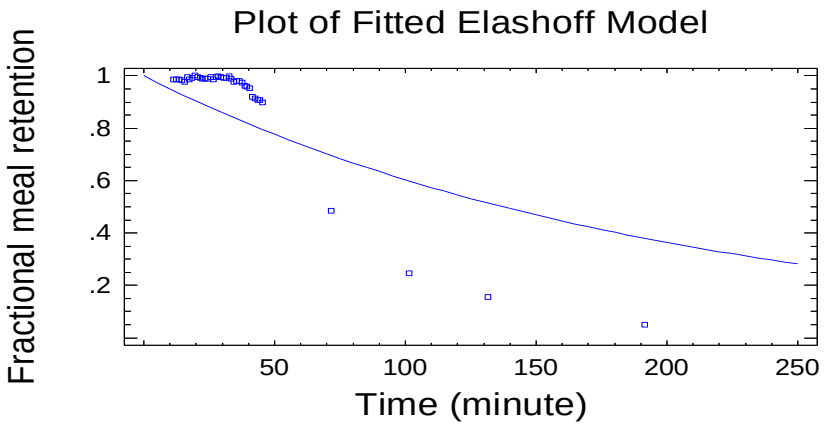

Figure 6.1 Time activity curve is described by power exponential function of Elashoff et al (19). (R^2 =0.911)

But fitted the data in the Siegel equation, R^2 values were higher than 0.9 and the gastric emptying curve from the Siegel equation and data from examination, the shapes were slightly different as shown in Figure 6.2. Thus, the Siegel equation was chosen to fit the gastric emptying data.

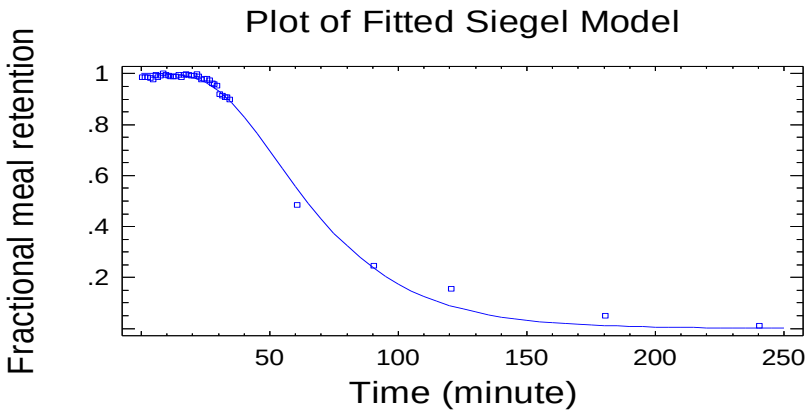

Figure 6.2 Time activity curve is described by modified power exponential function of Siegel et al (21). (R^2 =0.998)

From the gastric function study of 20 male and female Thai volunteers through the gastric emptying scintigraphy, gastric emptying data derived from all the volunteers through the modified power exponential function of Siegel has shown that the time activity curve offers good fits to the gastric emptying data of all volunteers and has explained 2 gastric emptying phases – lag phase time or time of gastric emptying until food is small enough to pass through pylorus and constant emptying time. In addition, parameters derived from the modified power exponential function of Siegel will be calculated to find emptying half-time ($T_{1/2}$), lag phase time and constant emptying time through the maximum slope tangent method of Couturier. From the gastric emptying scintigraphy, the researcher manages to obtain normal values of emptying half-time ($T_{1/2}$), lag phase time and constant emptying time of solid food tested with Thai volunteers. Comparing the value of parameters k and β derived from Siegel's equation between Thai volunteers and healthy volunteers studied by Couturier, results are similar, shown in Table 6.1. Comparing the emptying half-time ($T_{1/2}$), lag phase time and constant emptying time derived from putting parameters k and β in the equation from the maximum slope tangent method of Couturier, the values from Thai volunteers and healthy volunteers studied by Couturier are similar, shown in Table 6.1.

Table 6.1 Comparison of gastric emptying parameters between Thai volunteers and healthy volunteers studied by Couturier et al (20).

Gastric emptying parameter	Thai volunteers (n=19)	Healthy volunteers studied by Couturier et al. (n=15)
β	4.54±1.57	4.48±2.40
k (1/min)	0.0264±0.005	0.0242±0.010
emptying half-time ($T_{1/2}$)	73.16±11.27	81.29±19.95
Lag phase time (min)	26.11±8.49	24.02±11.53
Constant emptying time (min)	92.57±16.80	110.89±47.45

Furthermore, the researcher has performed an additional study on gastric antral contraction using the dynamic antral scintigraphy jointly with the Fourier algorithm to evaluate Thai volunteers' gastric functionality. The study can clearly identify the frequency of antral contraction during each period of data collection as shown in appendix B.

Though the sample size in this research is not sufficient to offer significant statistical explanation, data from the gastric emptying scintigraphy using the modified power exponential function of Siegel to check gastric emptying data among Thai volunteers and normal values of emptying half-time ($T_{1/2}$), lag phase time and constant emptying time using the maximum slope tangent method of Couturier, the researcher believes, based on Siegel and Couturier's approaches, are quite reliable and credible to apply in the gastric emptying analysis and explain the gastric emptying pattern of the Thai volunteers. In addition, the gastric antral contraction analysis using the dynamic antral scintigraphy that can study the movement of antral contents from antral contraction using rapid scintigraphic imaging technique jointly with the Fourier algorithm is apparent that the approach can show clear antral contraction frequency. Therefore, the researcher believes this approach will best serve as an alternative to evaluate the antral contraction frequency and the data from which will be useful for a further study on the antral contraction strength.

6.2 CONCLUSION

The normal values of lag phase time, half emptying-time ($T_{1/2}$) and constant emptying time of Thai volunteers found in this research using the cut-off value at percentile 2.5 and 97.5 are in the range of 5.56-38.37, 50.49-87.48 and 69.64-134.94 minutes respectively. The average frequency of gastric antral contraction in Thai volunteers at the 62^{nd}, 92^{nd} and 122^{nd} minute is 3.2 ± 0.2, 3.1 ± 0.2 and 3.1 ± 0.2 cycles / min, respectively. In addition, finding from the study of the amplitude of antral contraction, collected at the 62^{nd}, 92^{nd} and 122^{nd} minute in normal persons are in the range of 0.16–2.62, 0.17-3.51 and 0.35-1.99, respectively.

REFERENCES

1. Lin HC, Prather C, Fisher RS, Meyer JH, Summers RW, Pimentel M, et al. Measurement of gastrointestinal transit. Dig Dis Sci. 2005 Jun; 50(6):989-1004.
2. Mariani G, Boni G, Barreca M, Bellini M, Fattori B, AlSharif A, et al. Radionuclide gastroesophageal motor studies. J Nucl Med. 2004 Jun; 45(6):1004-28.
3. Doran S, Jones KL, Andrews JM, Horowitz M. Effects of meal volume and posture on gastric emptying of solids and appetite. Am J Phsiol. 1998 Nov; 275(5 Pt 2):R1712-8.
4. Moore JG, Datz FL, Christian PE, Greenberg E, Alazraki N. Effect of body posture on radionuclide measurements of gastric emptying. Dig Dis Sci. 1988 Dec; 33(12):1592-5.
5. Scott AM, Kellow JE, Shuter B, Nolan JM, Hoschl R, Jones MP. Effects of cigarette smoking on solid and liquid intragastric distribution and gastric emptying. Gastroenterology. 1993 Feb; 104(2):410-6.
6. Bennink R, Peeters M, Van den Maegdenbergh V, Geypens B, Rutgeerts P, De roo M, et al. Comparison of total and compartmental gastric emptying and antral motility between healthy men and women. Eur Nucl Med. 1998 Sep; 25(9):1293-9.
7. Carrio I, Notivol R, Estorch M, Berna L, Vilardell F. Gender-related differences in gastric emptying. J Nucl Med. 1988 Apr; 29(4):573-5.
8. Datz FL, Christian PE, Moore J. Gender-related differences in gastric emptying. J Nucl Med. 1987 Jul; 28(7):1204-7.
9. Degen LP, Phillips SF. Variability of gastrointestinal transit in healthy women and men. Gut. 1996 Aug; 39(2):299-305.
10. Hermansson G, Sivertsson R. Gender-related differences in gastric emptying rate of solid meals. Dig Dis Sci. 1996 Oct; 41(10):1994-8.

11. Hutson WR, Roehrkasse RL, Wald A. Influence of gender and menopause on gastric emptying and motility. Gastroenterology. 1989 Jan; 96(1):11-7.
12. Knight LC, Parkman HP, Brown KL, Miller MA, Trate DM, Maurer AH, et al. Delayed gastric emptying and decreased antral contractility in normal premenopausal women compared with men. Am J Gastroenterol. 1997 Jun; 92(6):968-75.
13. Jonderko K. Effect of the menstrual cycle on gastric emptying. Acta Physiol Pol. 1989 Sep-Dec; 40(5-6):504-10.
14. Gill RC, Murphy PD, Hooper HR, Bowes KL, Kingma YJ. Effect of the menstrual cycle on gastric emptying. Digestion. 1987; 36(3):168-74.
15. Maurer AH, Parkman HP. Update on gastrointestinal scintigraphy. Semin Nucl Med. 2006 Apr; 36(2):110-8.
16. Stanghellini V, Tosetti C, Corinaldesi R. Standards for non-invasive methods for gastrointestinal motility: scintigraphy. A position statement from the Gruppo Italian di Studio Motilita Apparato Digerente (GISMAD). Dig Liver Dis. 2000 Jun-Jul; 32(5):447-52.
17. Tougas G, Eaker EY, Abell TL, Abrahamsson H, Boivin M, Chen J, et al. Assessment of gastric emptying using a low fat meal: establishment of international control values. Am J Gastroenterol. 2000 Jun; 95(6):1456-62.
18. Jean-Luc C, Urbain and N, David Charkes. Recent advances in gastric emptying scintigraphy. Semin Nucl Med. 1995 Oct; 25(4):318-325.
19. Elashoff JD, Reedy TJ, Meyer JH. Analysis of gastric emptying data. Gastroenterology. 1982 Dec; 83:1306-1312.
20. Couturier O, Le Rest C, Gournay J, Pourdehnad M, Bridji B, Turzo A, et al. Gastric emptying of solids: Estimates of lag phase and constant emptying times. Nucl Med Commun. 2000; 21:665-675.
21. Siegel J, Urbain J, Adler L, Charkes N, Maurer A, Krevsky B, et al. Biphasic nature of gastric emptying. Gut 1988; 29: 85-89.
22. Bland JM, Altman DG. Statistical methods for assessing agreement between two methods of clinical measurements. Lancet. 1986; 8:307-310.

23. Urbain J-LC, Vekemans MC, Bouillon R, Cauteren Van J, Bex M, Mayeur MS, et al. Characterization of gastric antral motility disturbances in diabetes using the scintigraphic technique. J Nucl Med. 1993 Apr; 34:576-581.

24. กัลยา วานิชย์บัญชา . การวิเคราะห์สถิติ : สถิติสำหรับการบริหารและวิจัย . พิมพ์ครั้งที่ 11. กรุงเทพมหานคร : ภาควิชาสถิติ คณะพาณิชยศาสตร์และการบัญชี จุฬาลงกรณ์มหาวิทยาลัย; 2551.

APPENDICES

APPENDIX A

Goodness of fits

The results of assessing the goodness of modified power exponential fit showed that, in 19 volunteers, R^2 values were higher than 0.9 and there were little differences between the shapes of the estimated curve and observed points as shown in appendix A-1 to A-5**.**

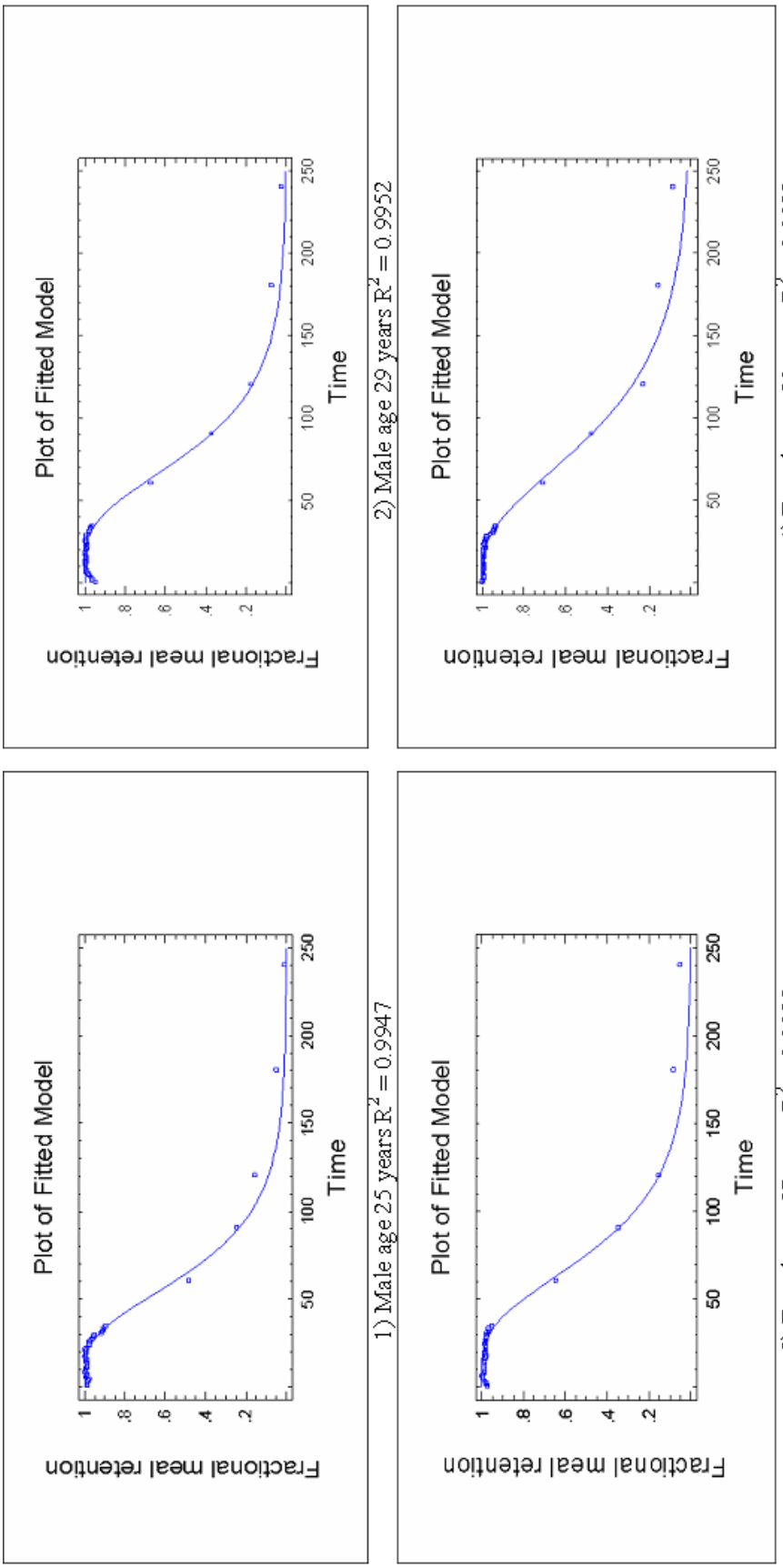

Figure A-1 Time activity curves are described by the modified power exponential function for males versus females in the age range 18-29 years.

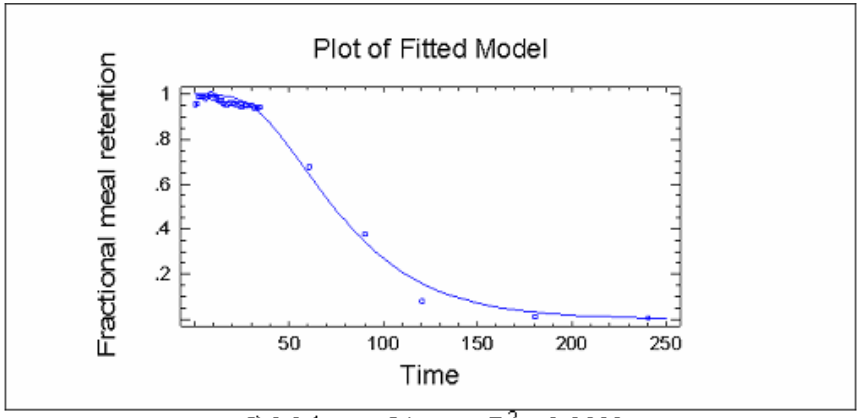

5) Male age 34 years $R^2 = 0.9900$

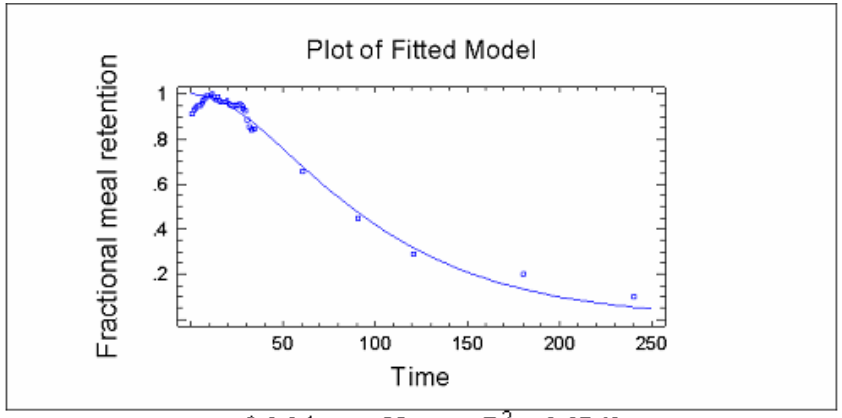

6) Male age 33 years $R^2 = 0.9769$

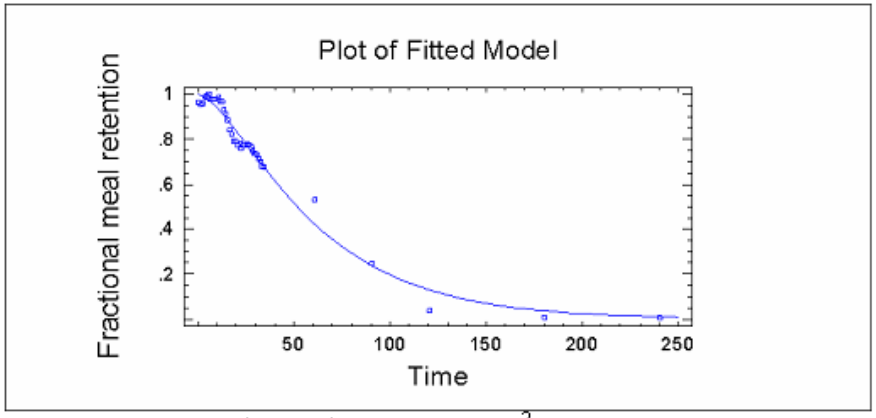

7) Female age 31 years $R^2 = 0.9797$

Figure A-2 Time activity curves are described by the modified power exponential function for males versus female in the age range 30-39 years. One woman volunteer in age range 30-39 years with $T_{1/2} = 192.94$ min was excluded from the summary.

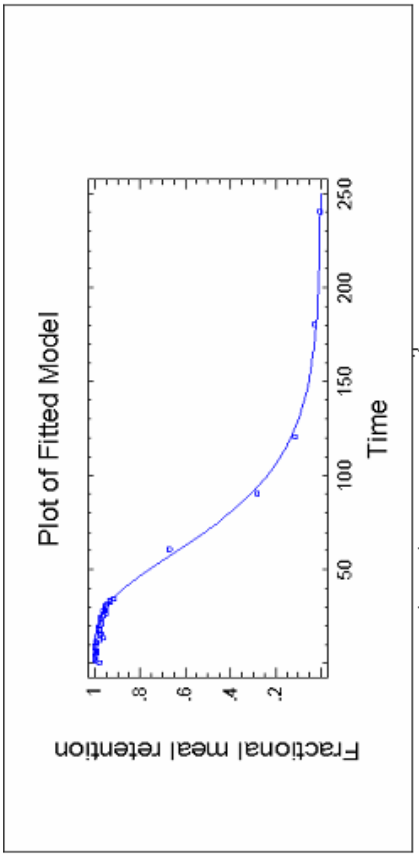

9) Male age 40 years $R^2 = 0.9972$

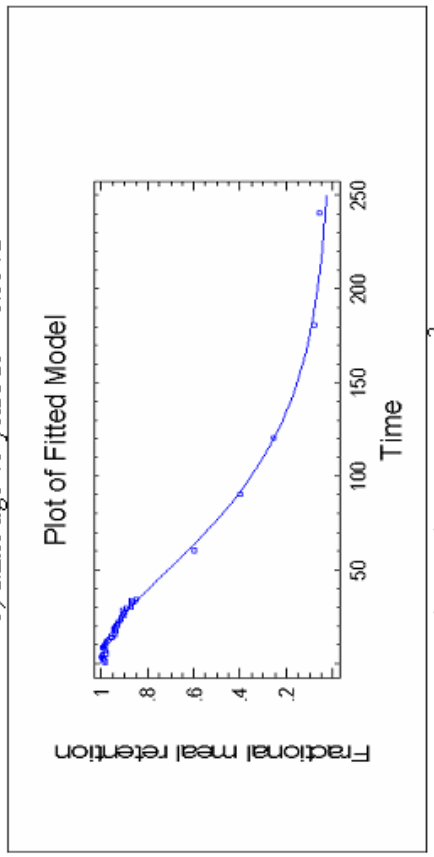

11) Female age 42 years $R^2 = 0.9973$

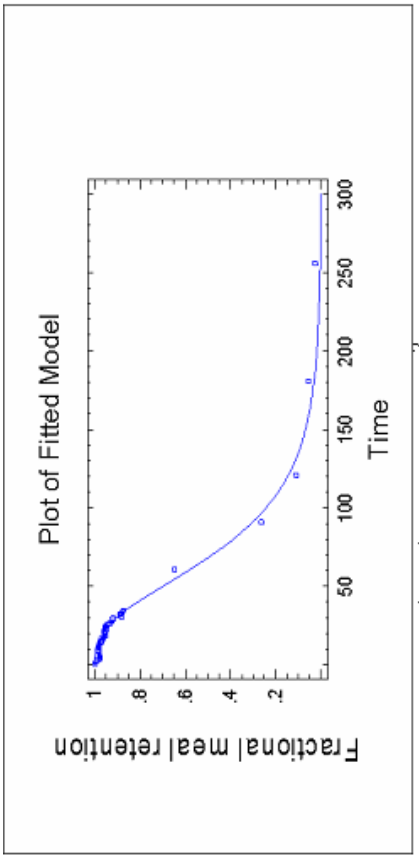

8) Male age 48 years $R^2 = 0.9944$

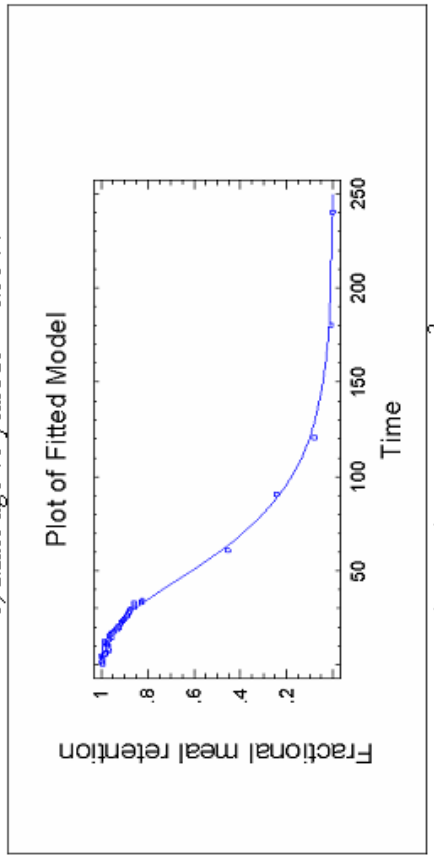

10) Female age 46 years $R^2 = 0.9963$

Figure A-3 Time activity curves are described by the modified power exponential function for males versus females in the age range 40-49 years.

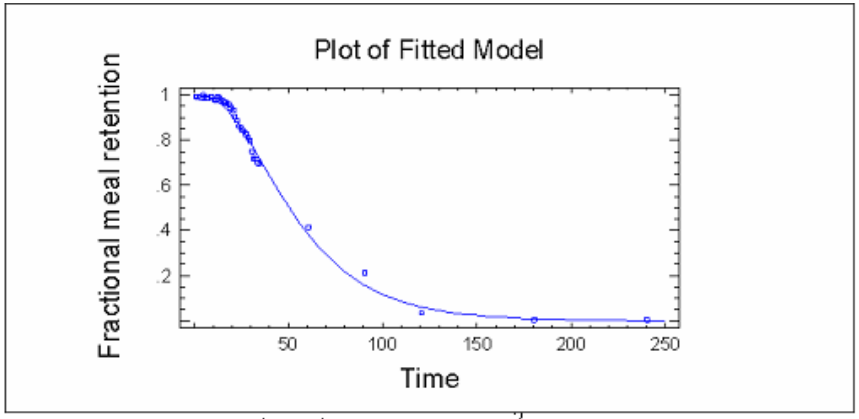

12) Male age 52 years $R^2 = 0.9944$

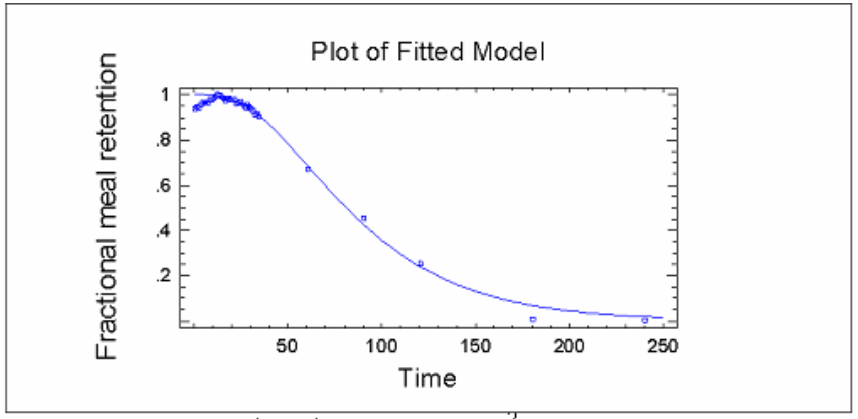

13) Male age 59 years $R^2 = 0.9901$

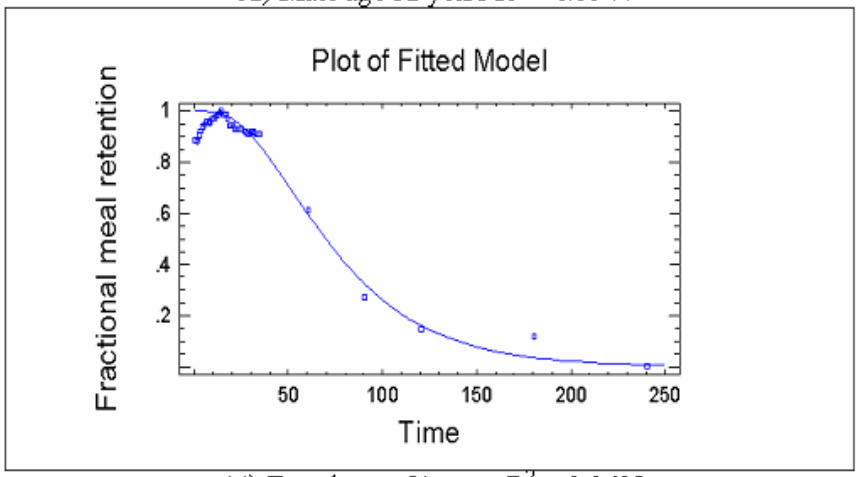

14) Female age 51 years $R^2 = 0.9692$

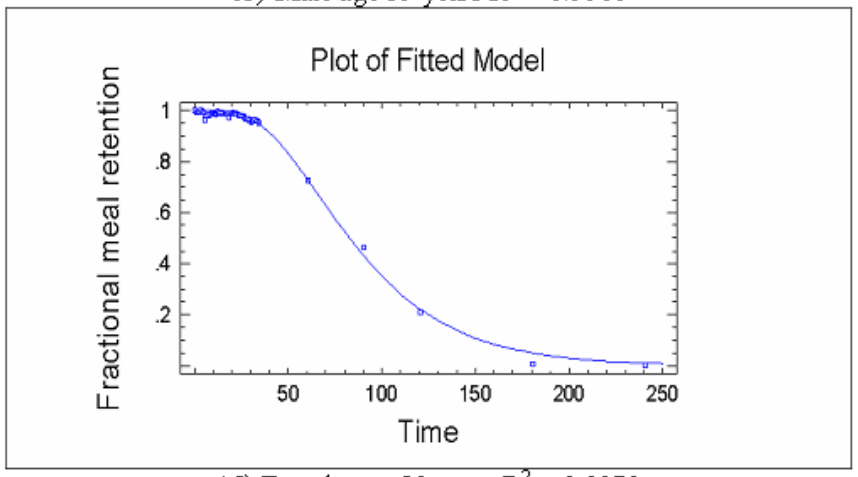

15) Female age 50 years $R^2 = 0.9970$

Figure A-4 Time activity curves are described by the modified power exponential function for males versus females in the age range 50-59 years.

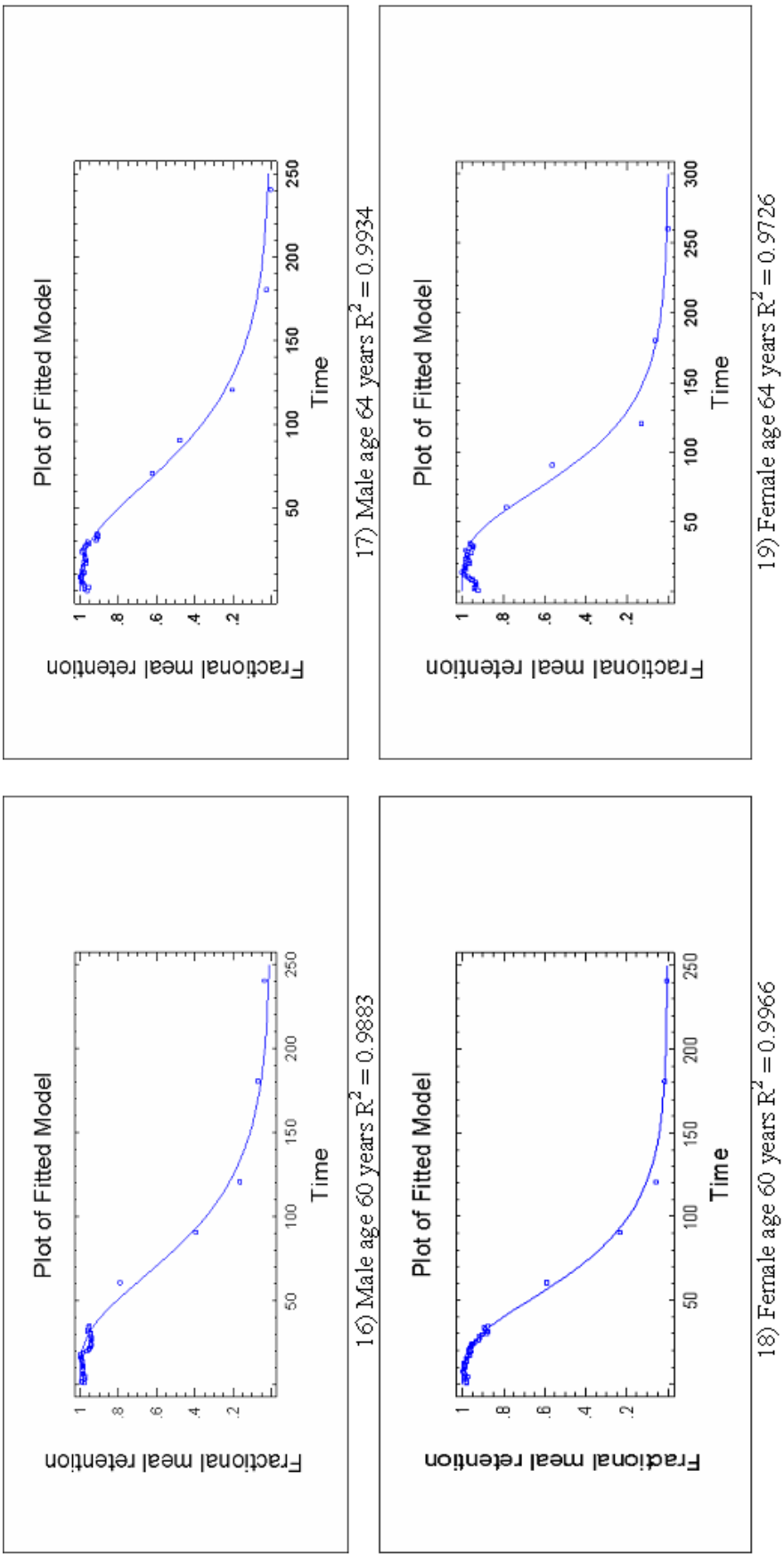

Figure A-5 Time activity curves are described by the modified power exponential function for males versus females in the age range ≥ 60 years.

APPENDIX B

The frequency of antral contraction in 19 Thai healthy volunteer

A study on gastric antral contraction using the dynamic antral scintigraphy jointly with the Fourier Algorithm was used to evaluate frequency of antral contraction. Figure B-1 to B-19 show the frequency of antral contraction. Data collected at the 62^{nd}, 92^{nd} and 122^{nd} minute of all the 19 volunteers. The gastric antral contraction analysis using dynamic antral scintigraphy that can study the movement of antral contents from antral contraction using rapid scintigraphic imaging technique jointly with the Fourier Algorithm is apparent that the approach can show clear antral contraction frequency.

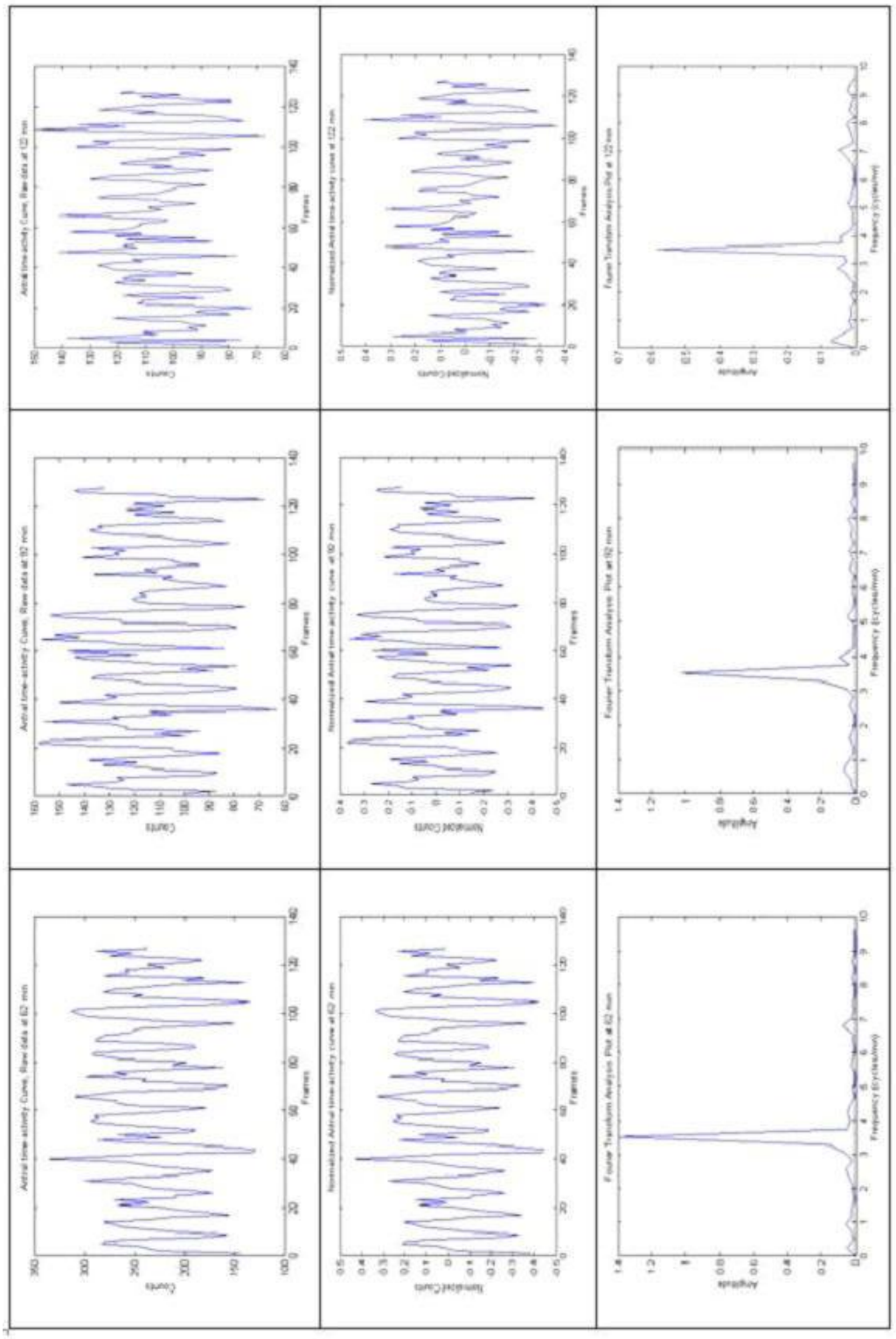

Figure B-1 The frequency of antral contraction at the 62nd, 92nd and 122nd minute in male volunteer at 25 years of age.

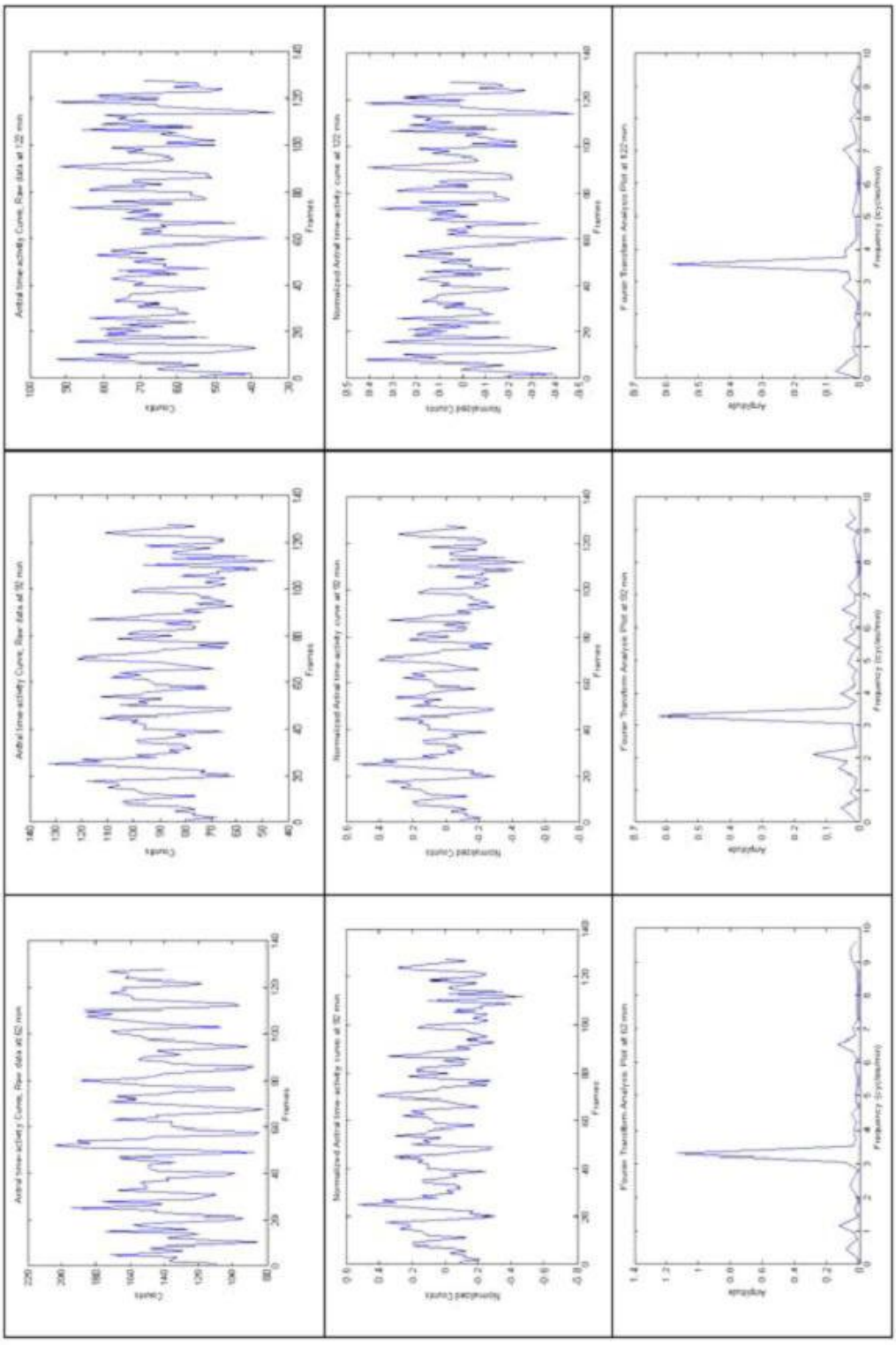

Figure B-2 The frequency of antral contraction at the 62nd, 92nd and 122nd minute in male volunteer at 29 years of age.

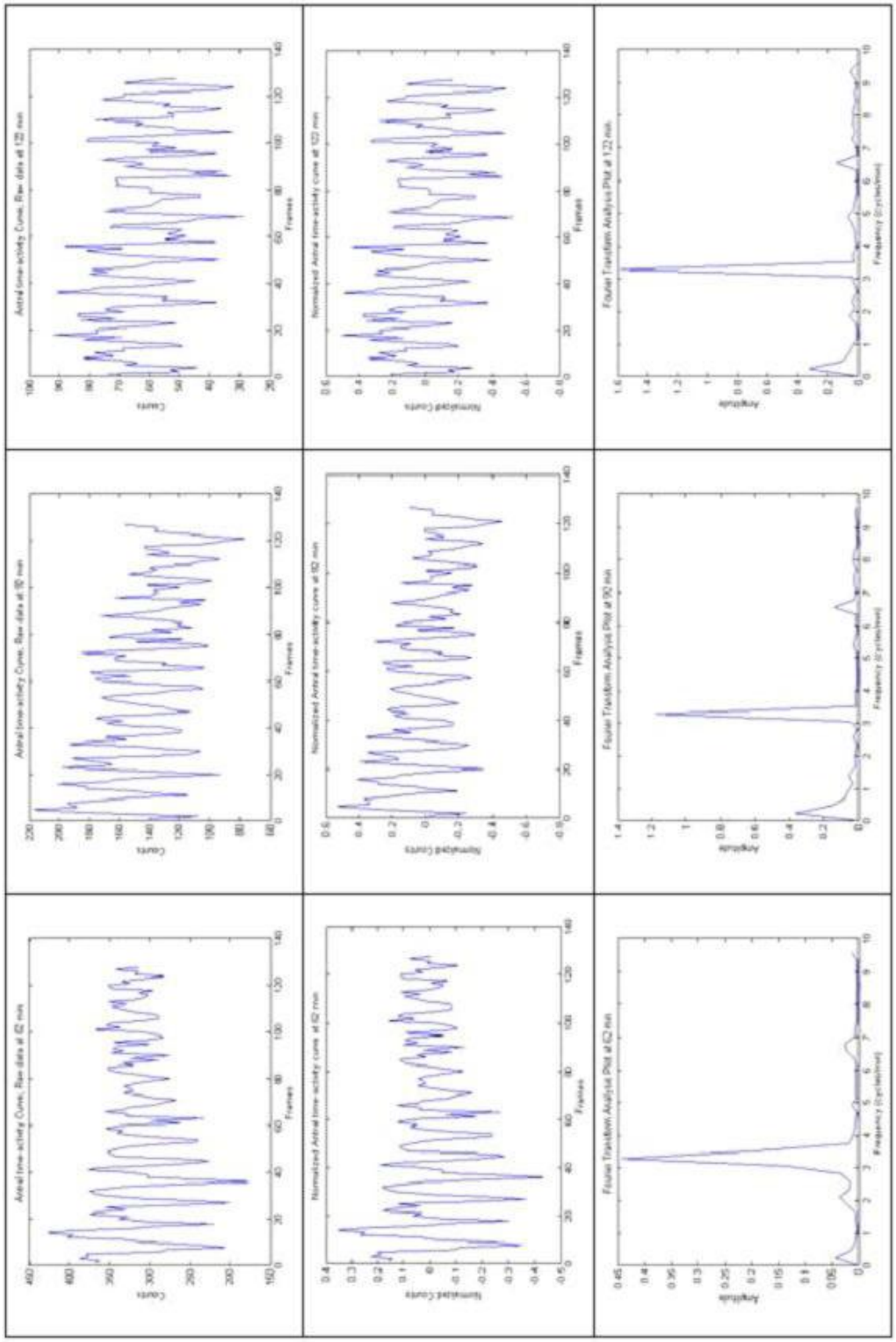

Figure B-3 The frequency of antral contraction at the 62nd, 92nd and 122nd minute in female volunteer at 27 years of age.

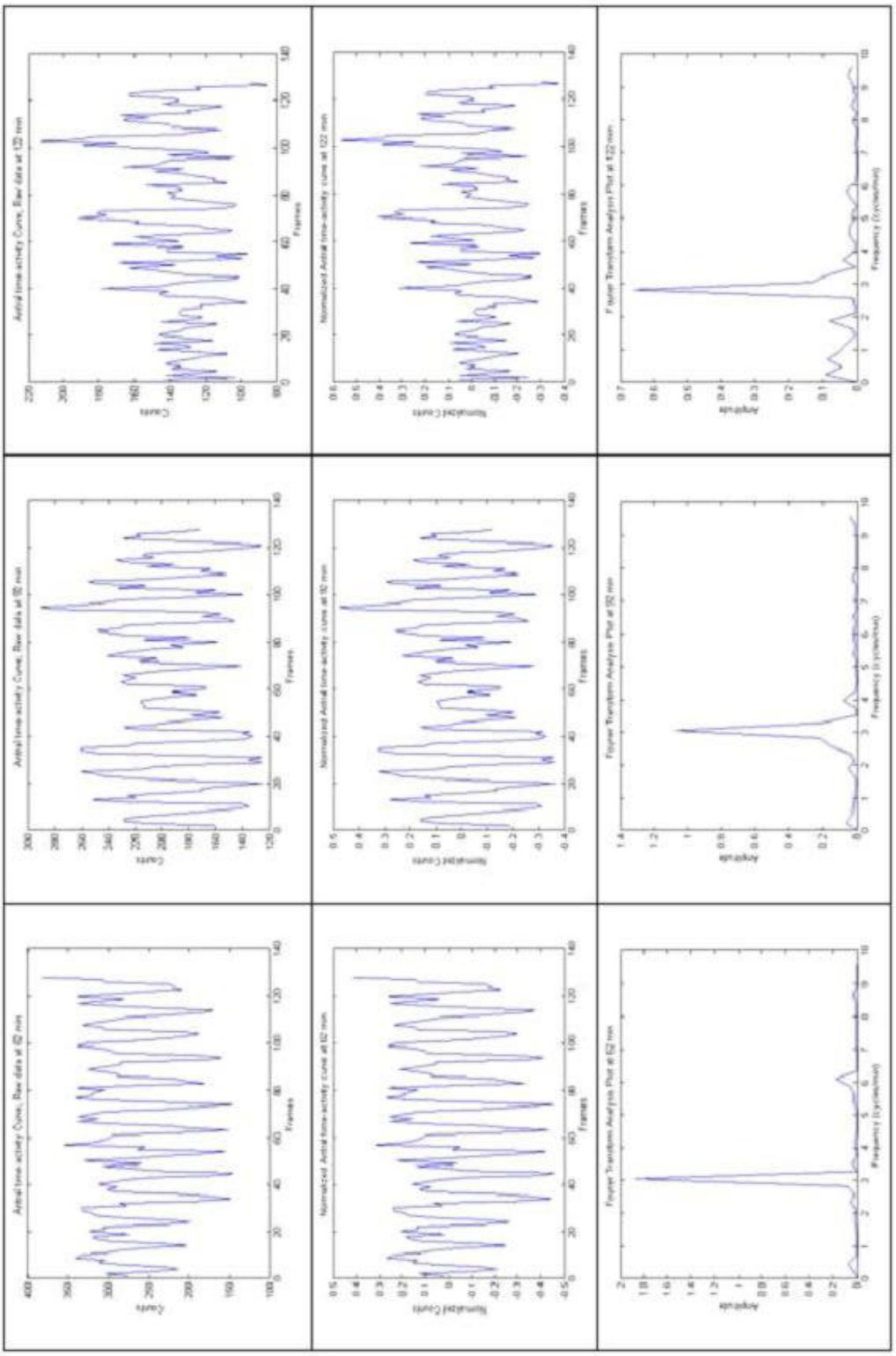

Figure B-4 The frequency of antral contraction at the 62nd, 92nd and 122nd minute in female volunteer at 28 years of age.

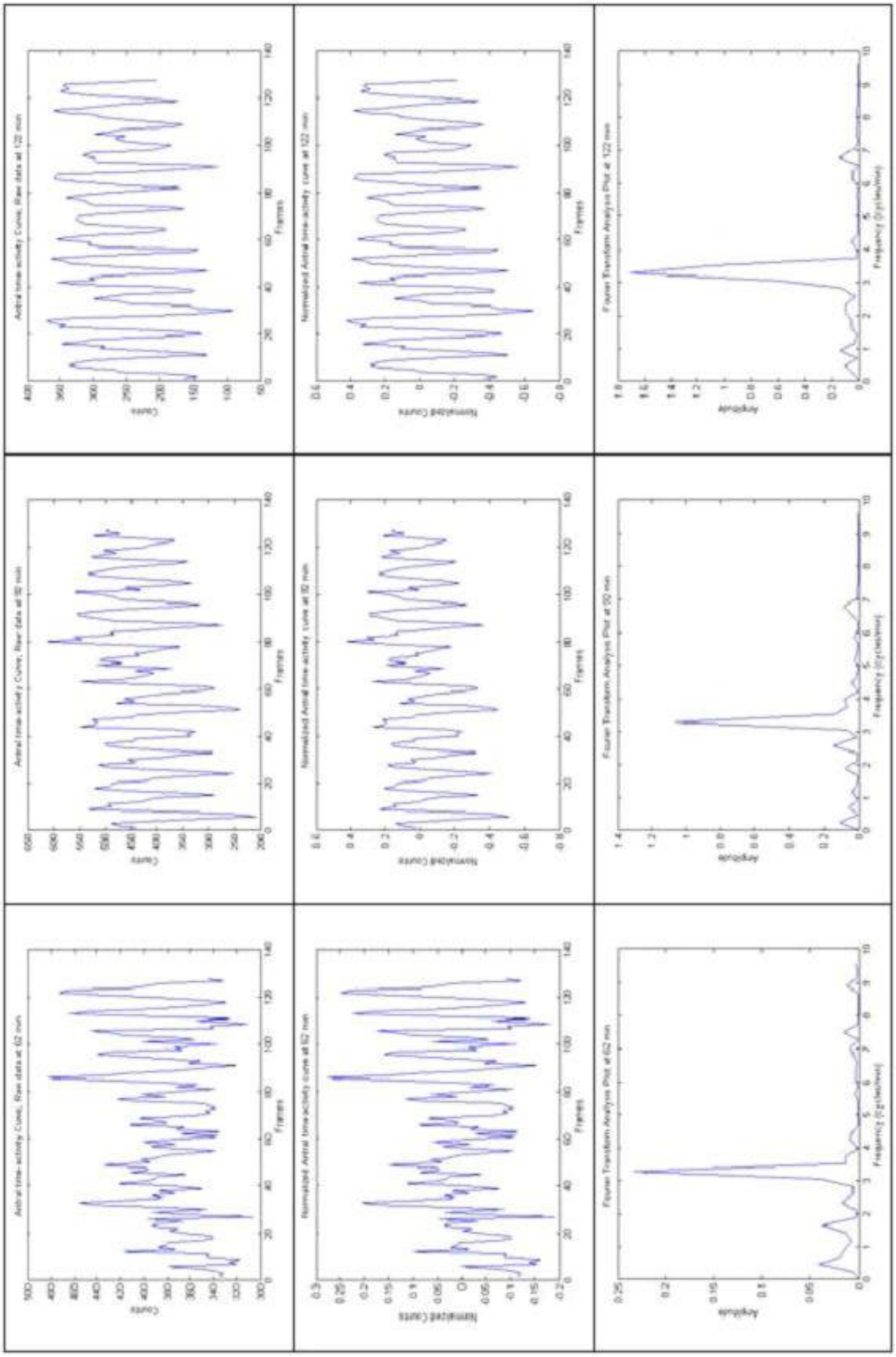

Figure B-5 The frequency of antral contraction at the 62nd, 92nd and 122nd minute in male volunteer at 34 years of age.

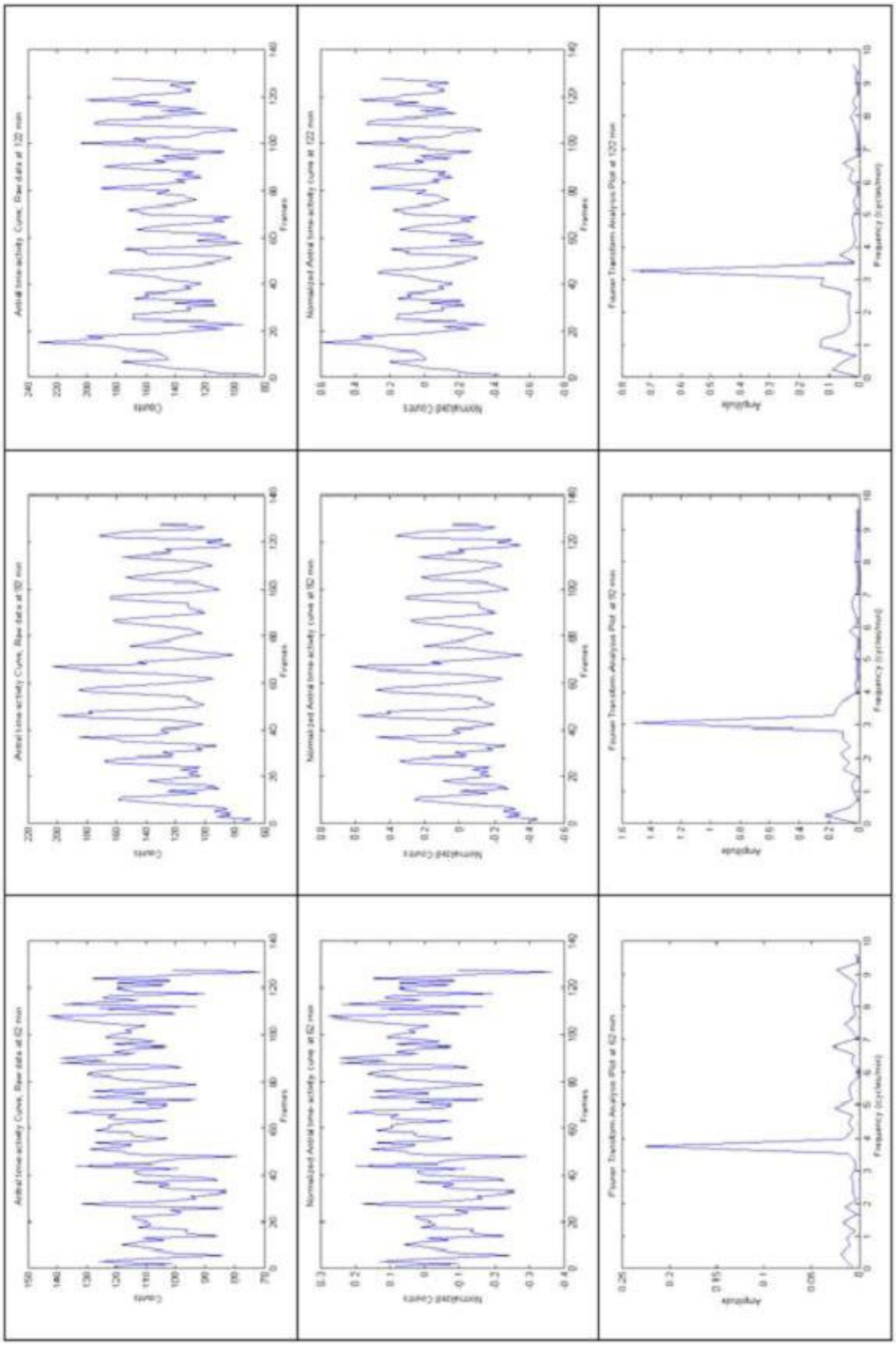

Figure B-6 The frequency of antral contraction at the 62nd, 92nd and 122nd minute in male volunteer at 33 years of age.

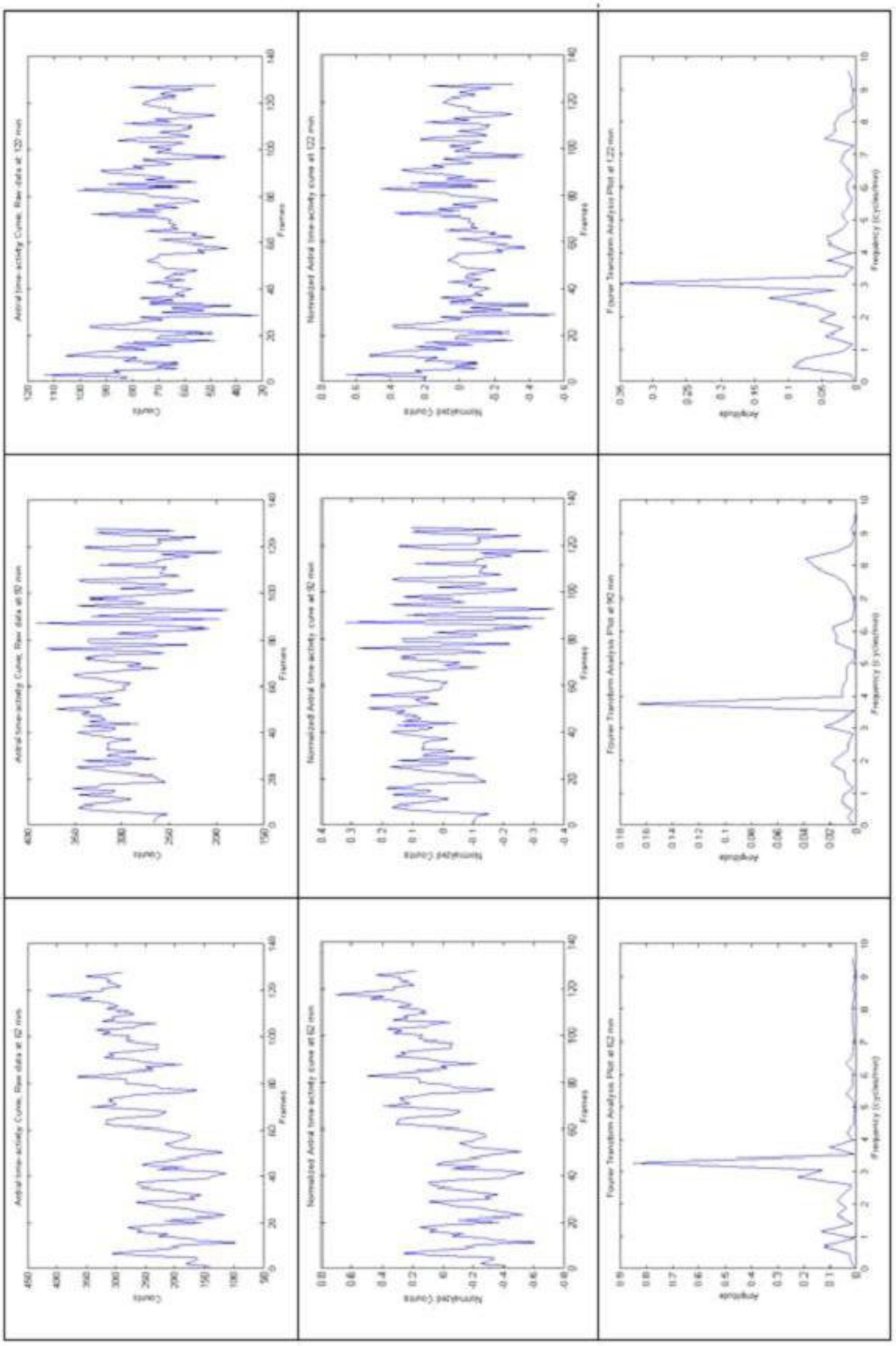

Figure B-7 The frequency of antral contraction at the 62nd, 92nd and 122nd minute in female volunteer at 31 years of age.

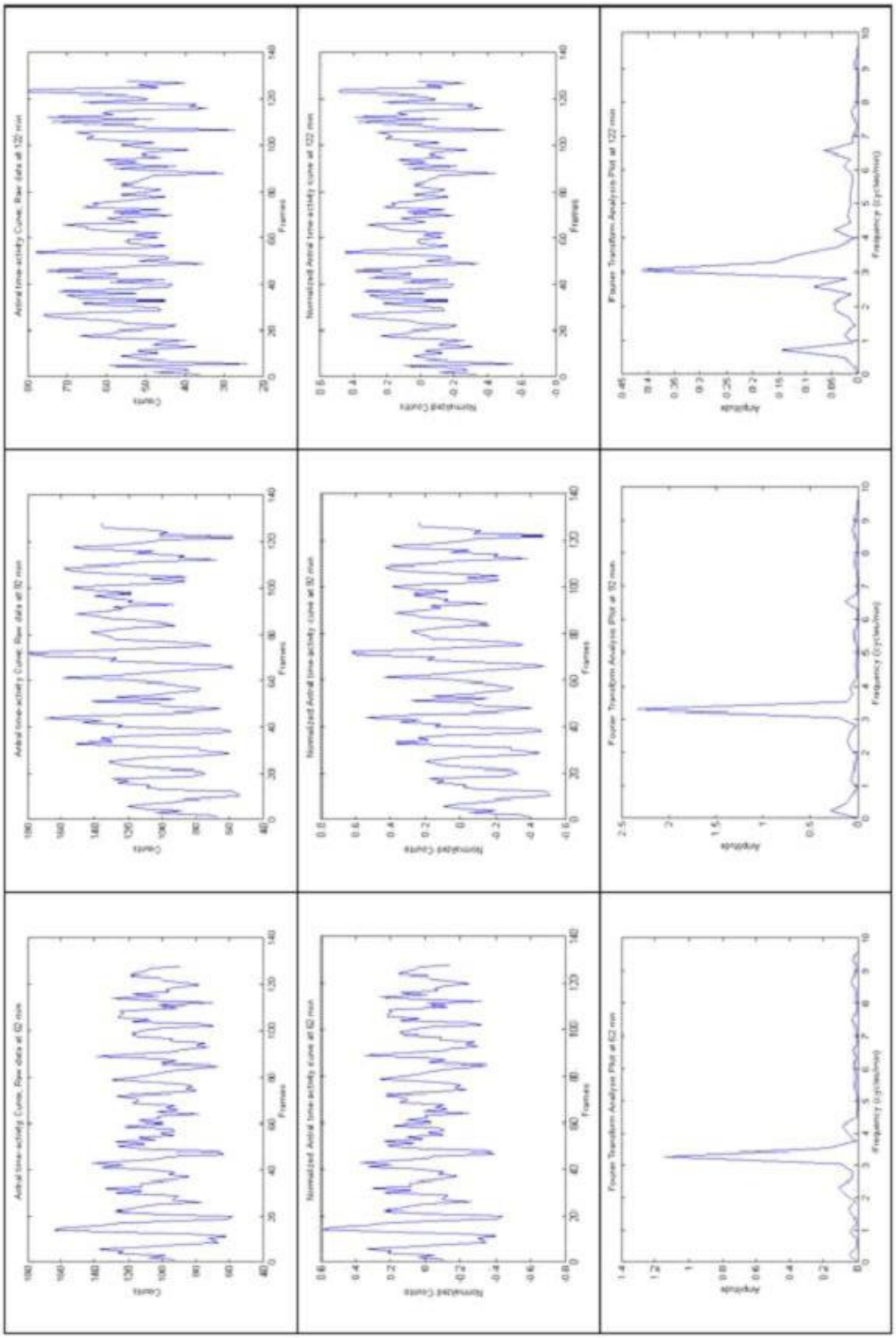

Figure B-8 The frequency of antral contraction at the 62nd, 92nd and 122nd minute in male volunteer at 48 years of age.

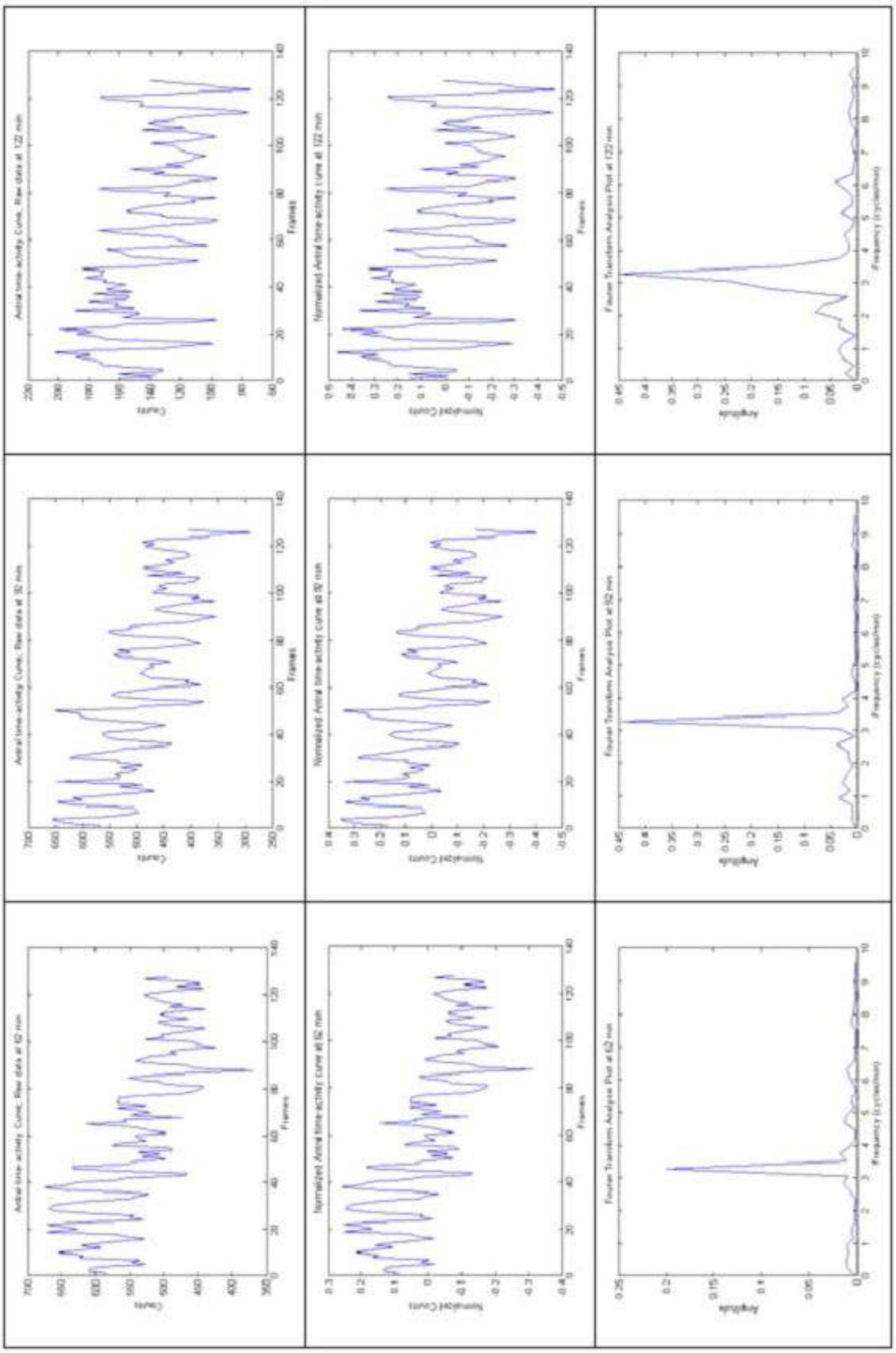

Figure B-9 The frequency of antral contraction at the 62nd, 92nd and 122nd minute in male volunteer at 40 years of age.

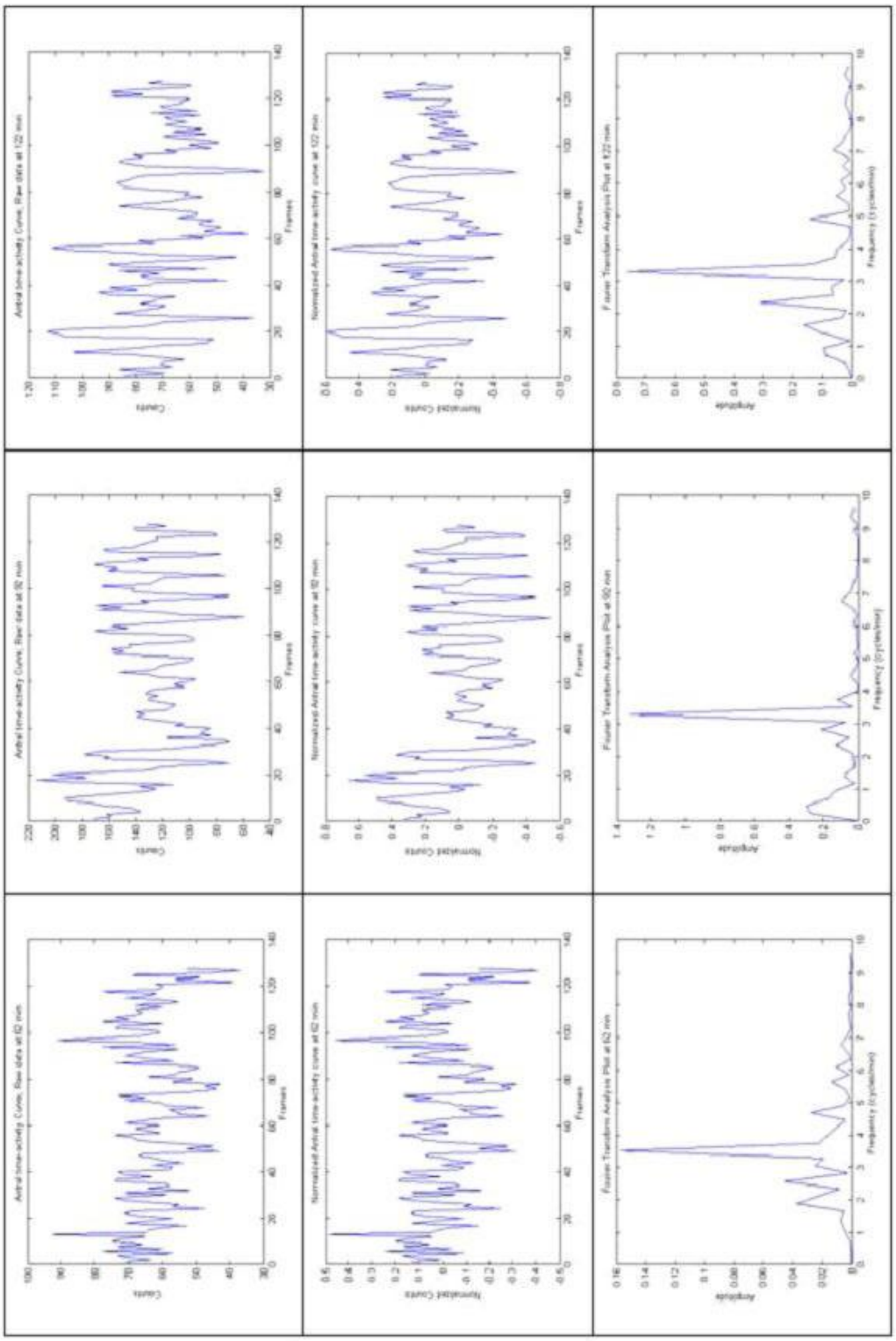

Figure B-10 The frequency of antral contraction at the 62nd, 92nd and 122nd minute in female volunteer at 46 years of age.

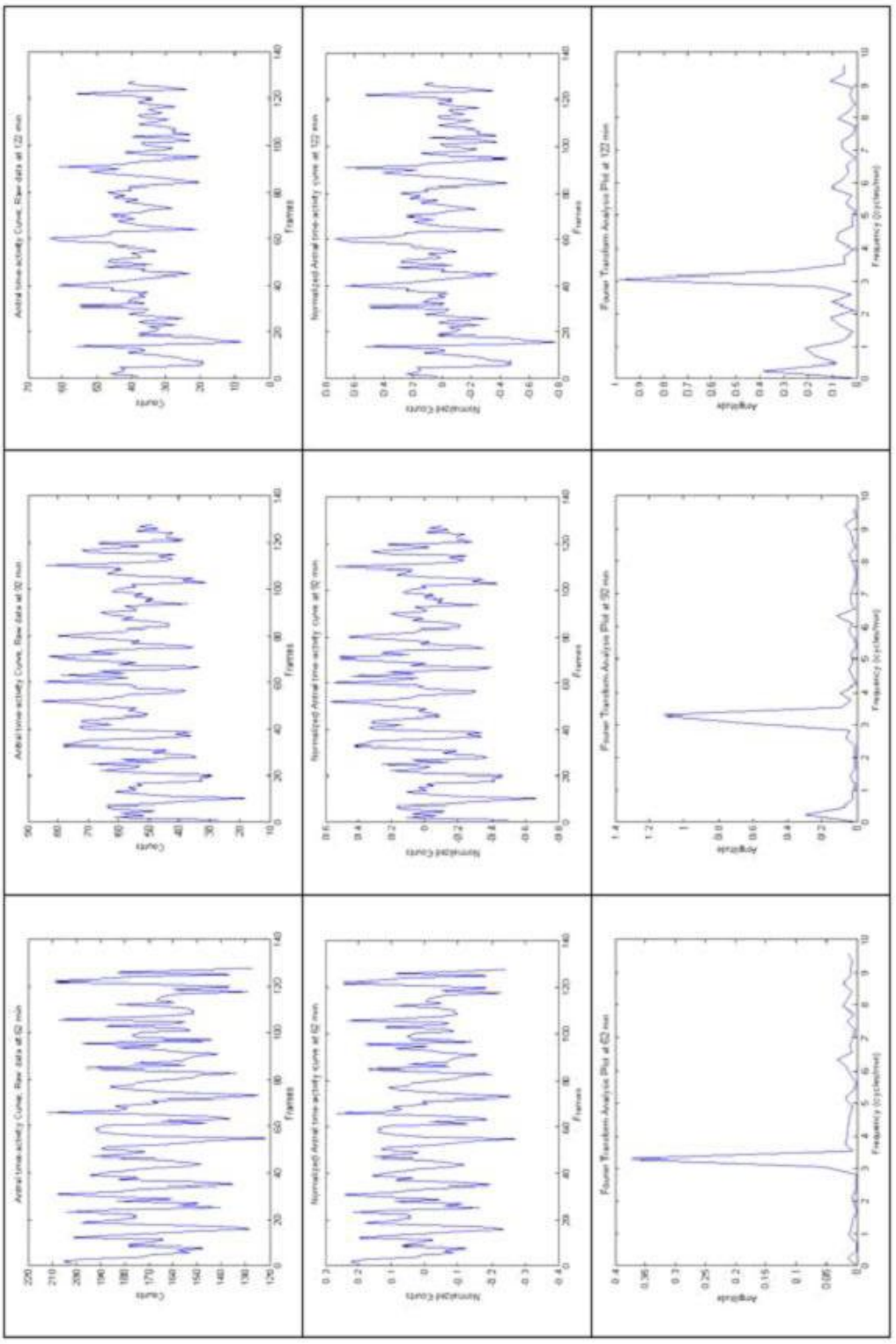

Figure B-11 The frequency of antral contraction at the 62nd, 92nd and 122nd minute in female volunteer at 42 years of age.

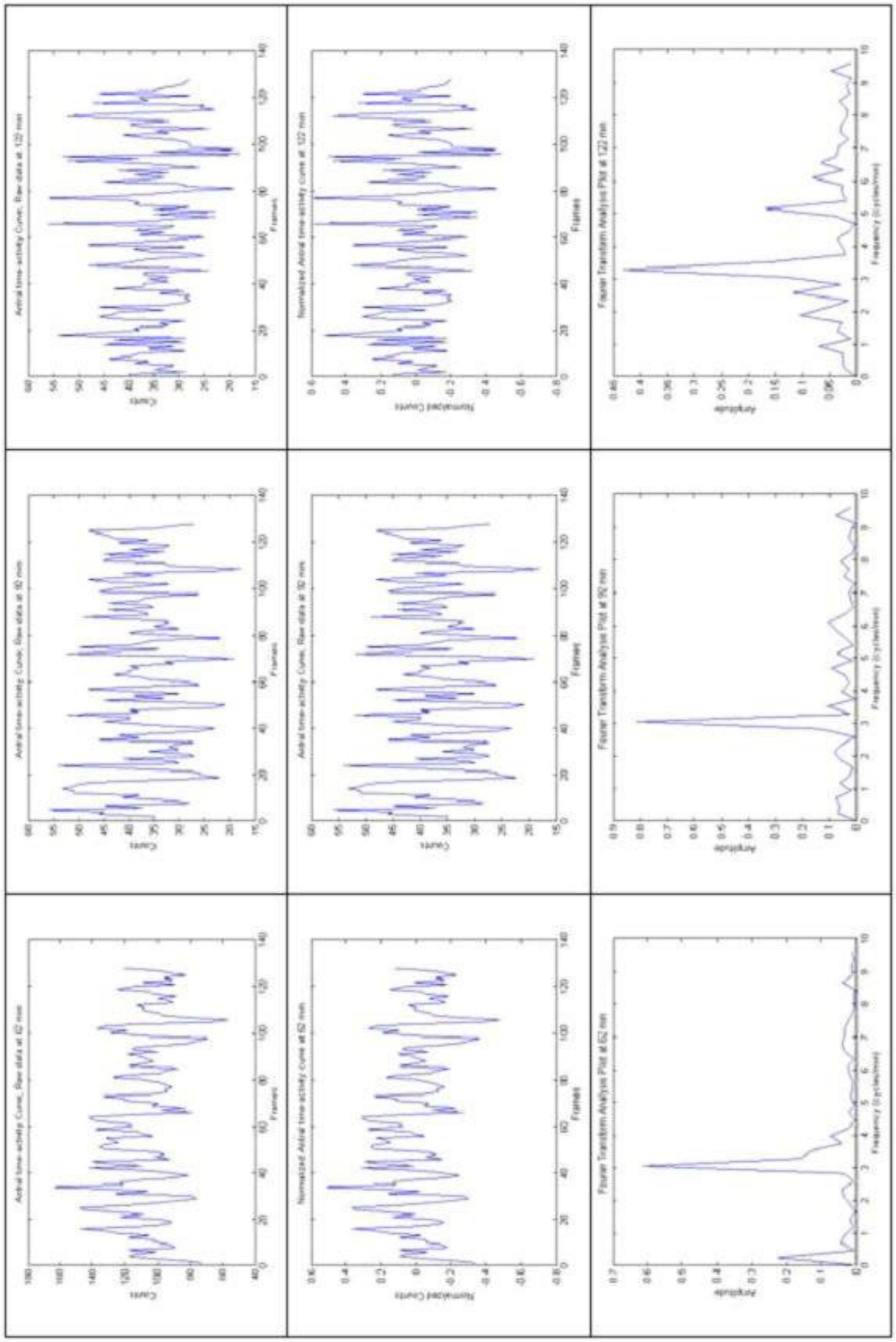

Figure B-12 The frequency of antral contraction at the 62nd, 92nd and 122nd minute in male volunteer at 52 years of age.

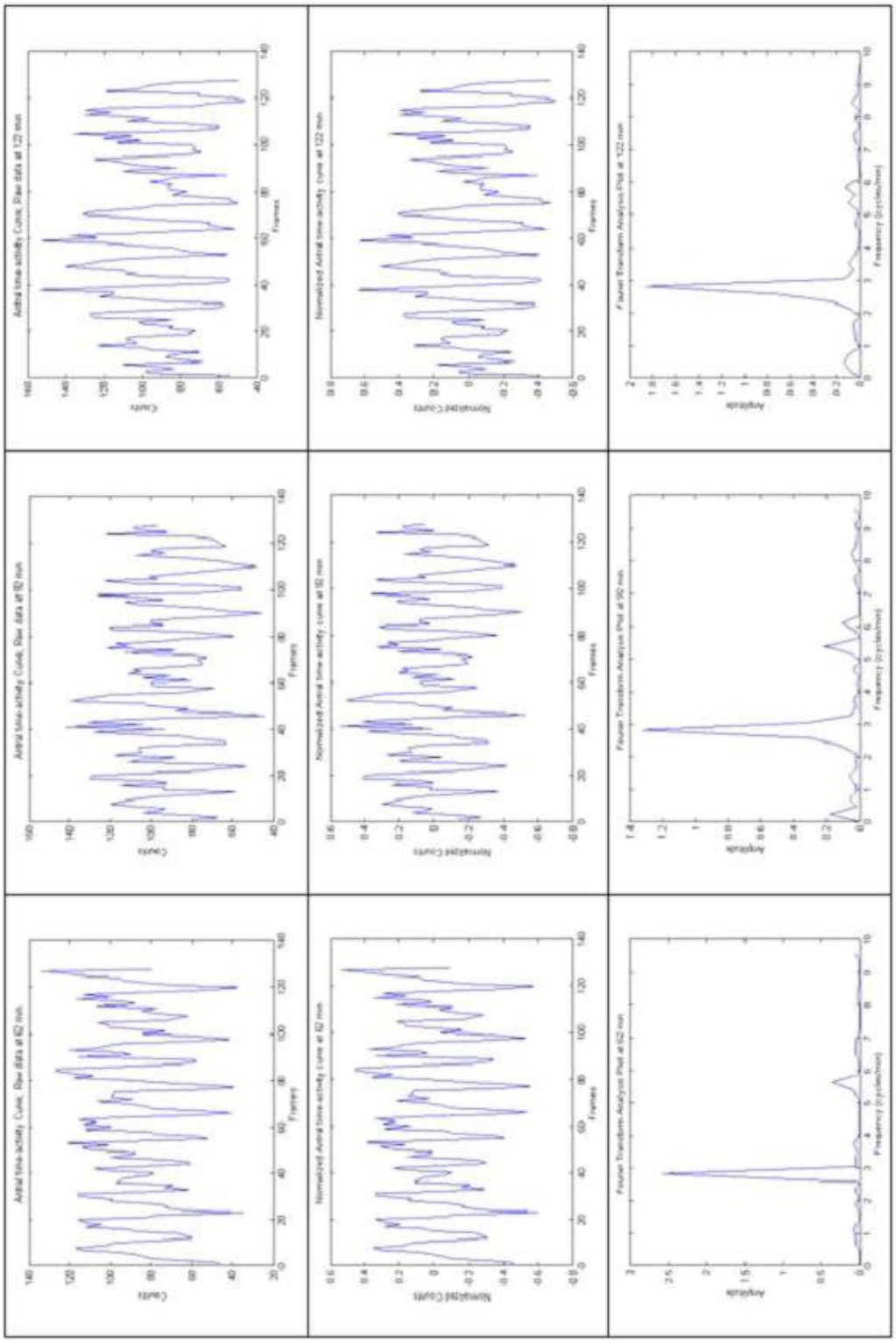

Figure B-13 The frequency of antral contraction at the 62nd, 92nd and 122nd minute in male volunteer at 59 years of age.

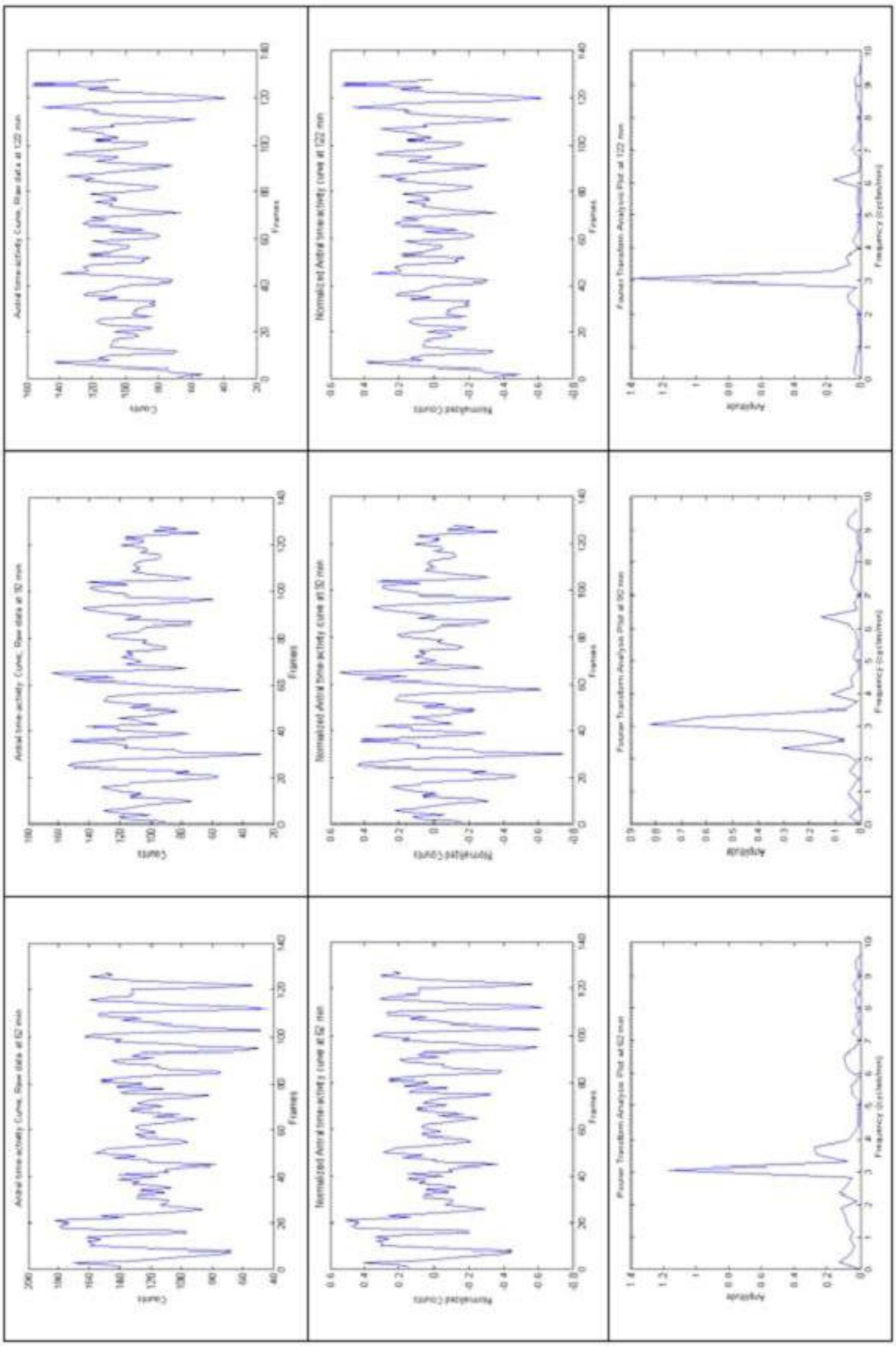

Figure B-14 The frequency of antral contraction at the 62nd, 92nd and 122nd minute in female volunteer at 51 years of age.

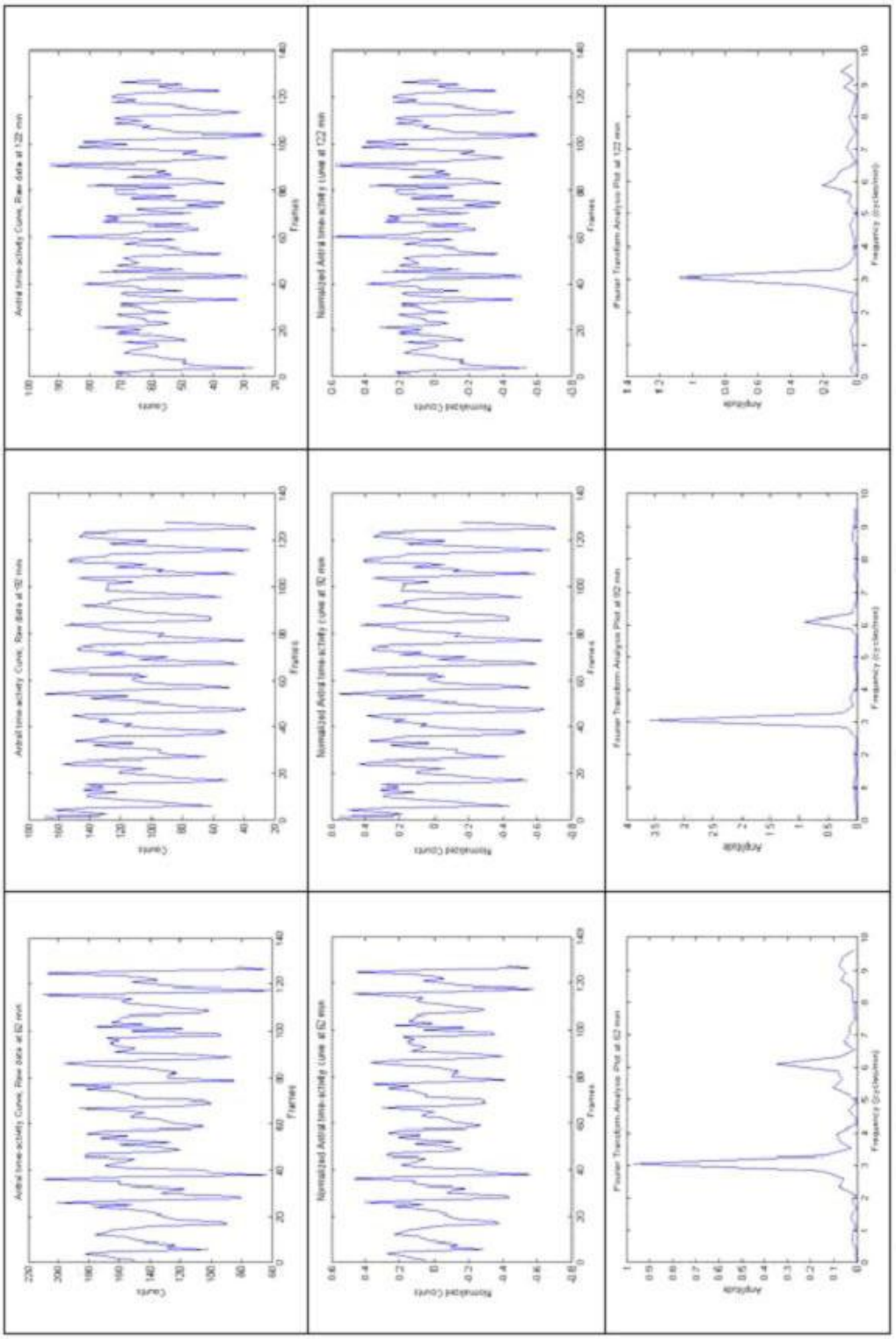

Figure B-15 The frequency of antral contraction at the 62nd, 92nd and 122nd minute in female volunteer at 50 years of age.

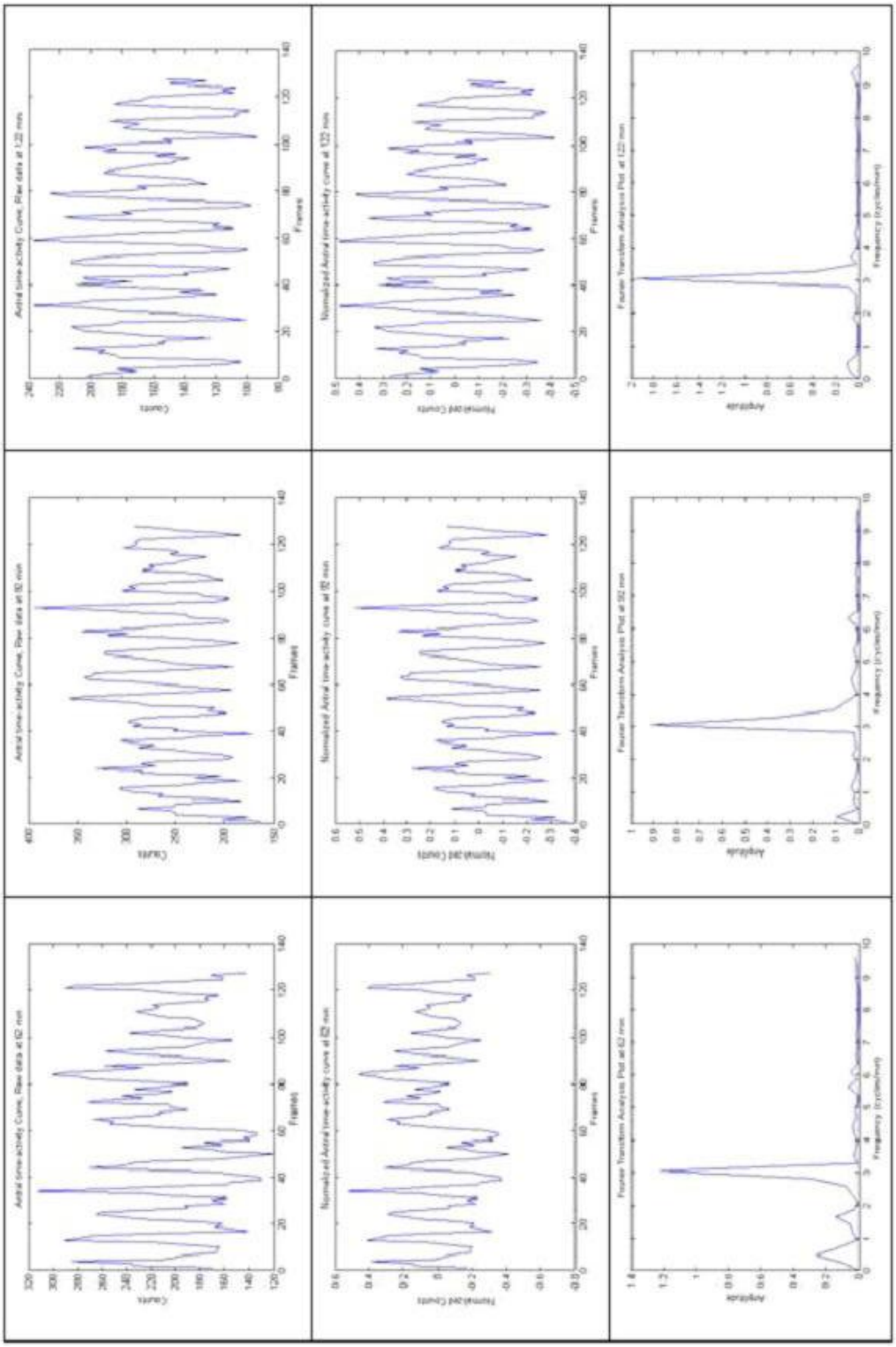

Figure B-16 The frequency of antral contraction at the 62nd, 92nd and 122nd minute in male volunteer at 60 years of age.

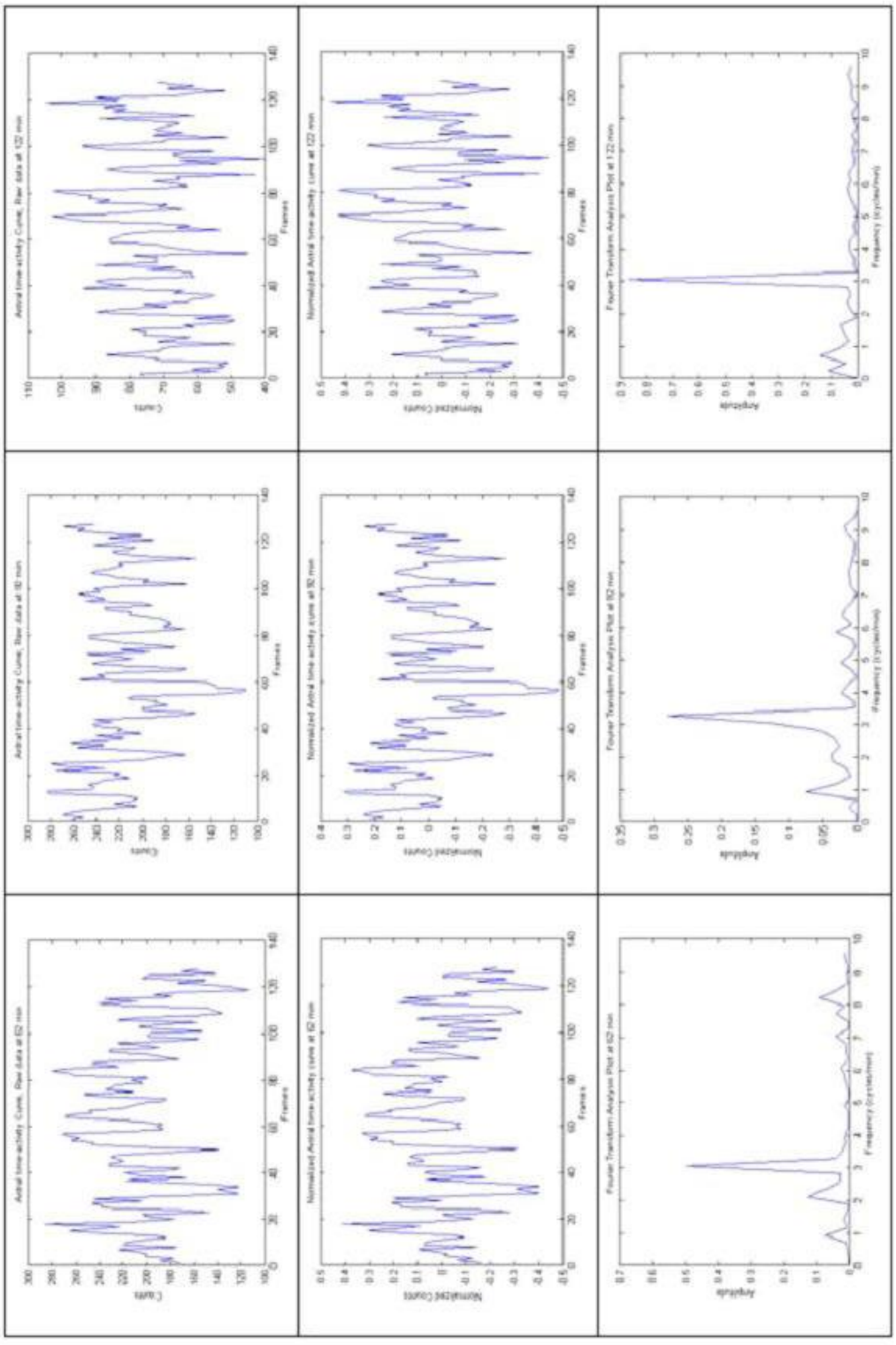

Figure B-17 The frequency of antral contraction at the 62nd, 92nd and 122nd minute in male volunteer at 64 years of age.

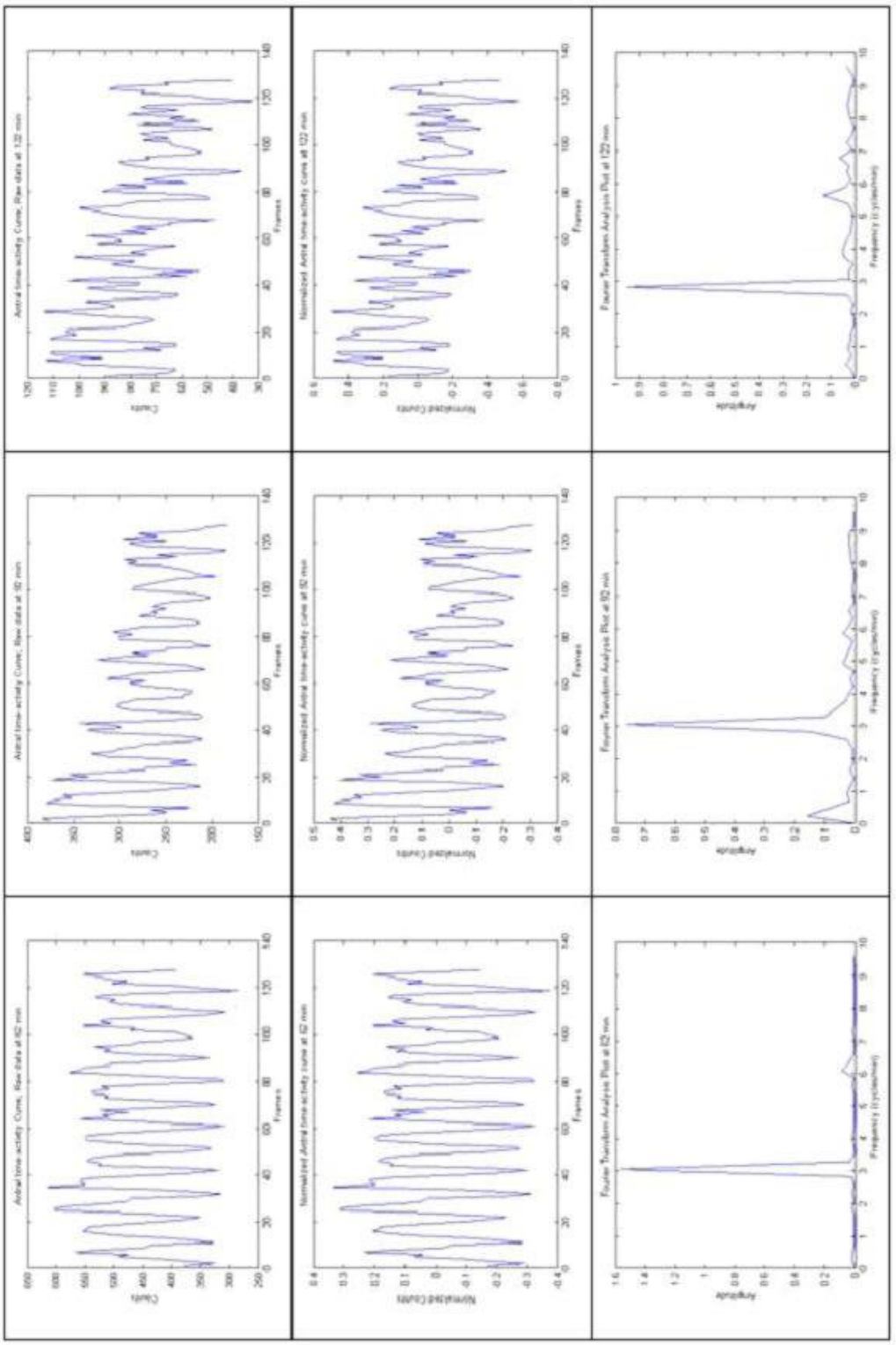

Figure B-18 The frequency of antral contraction at the 62nd, 92nd and 122nd minute in female volunteer at 60 years of age.

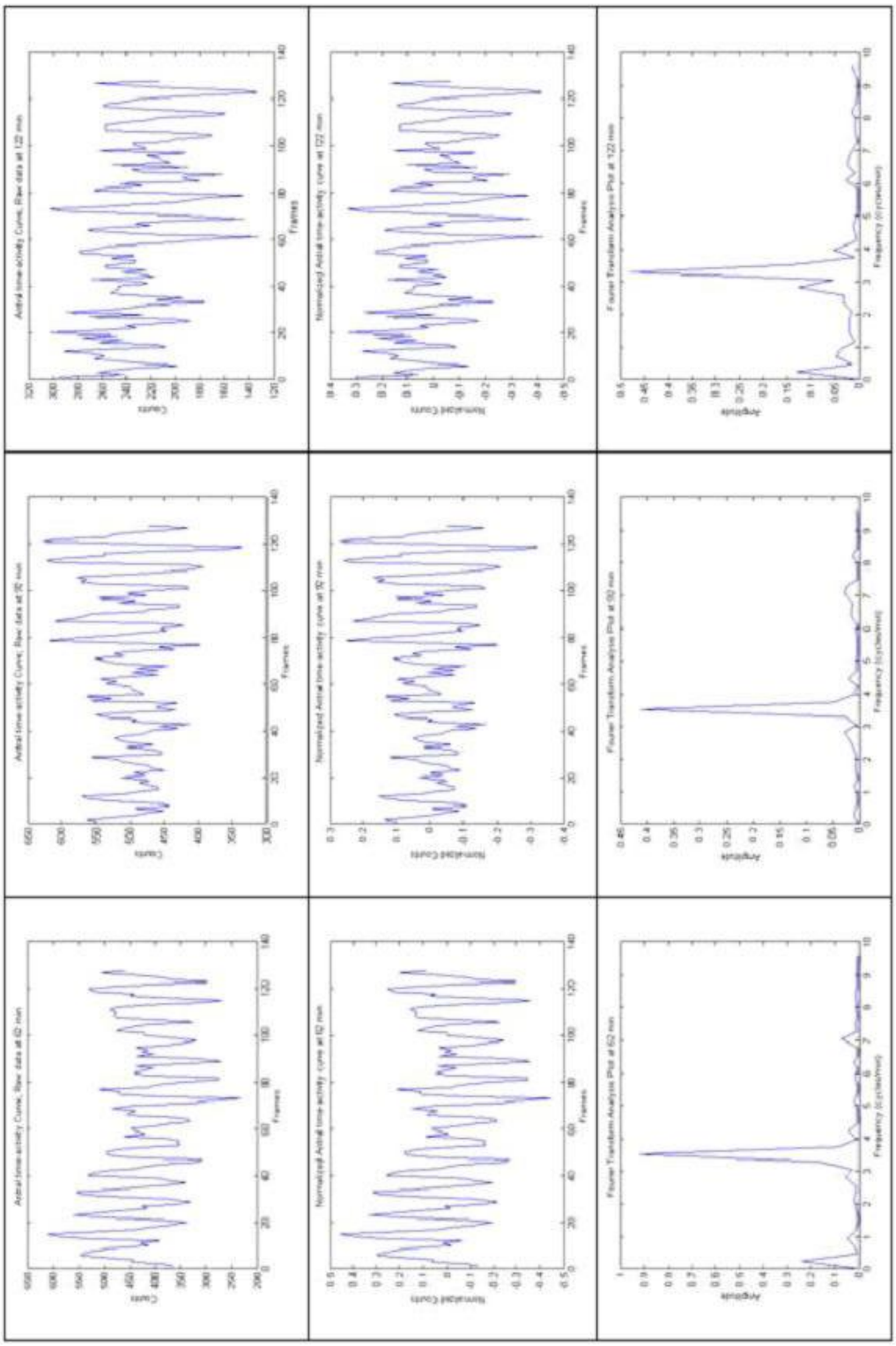

Figure B-19 The frequency of antral contraction at the 62nd, 92nd and 122nd minute in female volunteer at 64 years of age.

APPENDIX C

Table C-1 Probability of $P(U \leq U_0)$ (24).

$n_2=3$

	n_1	1	2	3
	0	.25	.10	.05
	1	.50	.20	.10
U_0	2		.40	.20
	3		.60	.35
	4			.50

$n_2=4$

	n_1	1	2	3	4
	0	0.2000	0.0667	0.0286	0.0143
	1	0.4000	0.1333	0.0571	0.0286
	2	0.6000	0.2667	0.1143	0.0571
	3		0.4000	0.2000	0.1000
U_0	4		0.6000	0.3143	0.1714
	5			0.4286	0.2429
	6			0.5714	0.3429
	7				0.4429
	8				0.5571

$n_2=5$

	n_1	1	2	3	4	5
	0	.1667	.0476	.0179	.0079	.0040
	1	.3333	.0952	.0357	.0159	.0079
	2	.5000	.1905	.1250	.0317	.0159
	3		.2857	.1964	.0556	.0278
	4		.4286	.2857	.0952	.0476
	5		.5714	.3929	.1429	.0754
U_0	6			.5000	.2063	.1111
	7				.2778	.1548
	8				.3651	.2103
	9				.4524	.2738
	10				.5476	.3452
	11					.4206
	12					.5000

Table C-1 Probability of $P(U \leq U_0)$ (24). (cont.)

n_2=6

	n_1	1	2	3	4	5	6
	0	.1429	.0357	.0119	.0048	.0022	.0011
	1	.2857	.0714	.0238	.0095	.0043	.0022
	2	.4286	.1429	.0476	.0190	.0087	.0043
	3	.5714	.2143	.0833	.0333	.0152	.0076
	4		.3214	.1310	.0571	.0260	.0130
	5		.4286	.1905	.0857	.0411	.0206
	6		.5714	.2738	.1286	.0628	.0325
	7			.3571	.1762	.0887	.0465
	8			.4524	.2381	.1234	.0660
U_0	9			.5476	.3048	.1645	.0898
	10				.3810	.2143	.1201
	11				.4571	.2684	.1548
	12				.5429	.3312	.1970
	13					.3961	.2424
	14					.4654	.2944
	15					.5346	.3496
	16						.4091
	17						.4686
	18						.5314

n_2=7

	n_1	1	2	3	4	5	6	7
	0	.1250	.0278	.0083	.0030	.0013	.0006	.0003
	1	.2500	.0556	.0167	.0061	.0025	.0012	.0006
	2	.3750	.1111	.0333	.0121	.0051	.0023	.0012
	3	.5000	.1667	.0583	.0212	.0088	.0041	.0020
	4		.2500	.0917	.0364	.0152	.0070	.0035
	5		.3333	.1333	.0545	.0240	.0111	.0055
	6		.4444	.1917	.0818	.0366	.0175	.0087
	7		.5556	.2583	.1152	.0530	.0256	.0131
	8			.3333	.1576	.0745	.0367	.0189
	9			.4167	.2061	.1010	.0507	.0265
	10			.5000	.2636	.1338	.0688	.0364
	11				.3242	.1717	.0903	.0487
U_0	12				.3939	.2159	.1171	.0641
	13				.4636	.2652	.1474	.0825
	14				.5364	.3194	.1830	.1043
	15					.3775	.2226	.1297
	16					.4381	.2669	.1588
	17					.5000	.3141	.1914
	18						.3654	.2279
	19						.4178	.2675
	20						.4726	.3100
	21						.5274	.3552
	22							.4024
	23							.4508
	24							.5000

Table C-1 Probability of $P(U \leq U_0)$ (24). (cont.)

		n_2=8							
	n_1	1	2	3	4	5	6	7	8
	0	.1111	.0222	.0061	.0020	.0008	.0003	.0002	.0001
	1	.2222	.0444	.0121	.0040	.0016	.0007	.0003	.0002
	2	.3333	.0889	.0242	.0081	.0031	.0013	.0006	.0003
	3	.4444	.1333	.0424	.0141	.0054	.0023	.0011	.0005
	4	.5556	.2000	.0667	.0242	.0093	.0040	.0019	.0009
	5		.2667	.0970	.0384	.0148	.0063	.0030	.0015
	6		.3556	.1394	.0545	.0225	.0100	.0047	.0023
	7		.4444	.1879	.0768	.0326	.0147	.0070	.0035
	8		.5556	.2485	.1071	.0466	.0213	.0103	.0052
	9			.3152	.1414	.0637	.0296	.0145	.0074
	10			.3879	.1838	.0855	.0406	.0200	.0103
	11			.4606	.2303	.1111	.0539	.0270	.0141
	12			.5394	.2818	.1422	.0709	.0361	.0190
	13				.3414	.1772	.0906	.0469	.0249
	14				.4040	.2176	.1142	.0603	.0325
	15				.4667	.2618	.1412	.0760	.0415
U_0	16				.5333	.3108	.1725	.0946	.0524
	17					.3621	.2068	.1159	.0652
	18					.4165	.2454	.1405	.0803
	19					.4716	.2864	.1678	.0974
	20					.5284	.3310	.1984	.1172
	21						.3773	.2317	.1393
	22						.4259	.2679	.1641
	23						.4749	.3063	.1911
	24						.5251	.3472	.2209
	25							.3894	.2527
	26							.4333	.2869
	27							.4775	.3227
	28							.5225	.3605
	29								.3992
	30								.4392
	31								.4796
	32								.5204

Table C-1 Probability of $P(U \leq U_0)$ (24). (cont.)

	n_2=9								
	n_1	1	2	3	4	5	6	7	8	9
	0	.1000	.0182	.0045	.0014	.0005	.0002	.0001	.0000	.0000
	1	.2000	.0364	.0091	.0028	.0010	.0004	.0002	.0001	.0000
	2	.3000	.0727	.0182	.0056	.0020	.0008	.0003	.0002	.0001
	3	.4000	.1091	.0318	.0098	.0035	.0014	.0006	.0003	.0001
	4	.5000	.1636	.0500	.0168	.0060	.0024	.0010	.0005	.0002
	5		.2182	.0727	.0252	.0091	.0038	.0017	.0008	.0004
	6		.2909	.1045	.0378	.0145	.0060	.0026	.0012	.0006
	7		.3636	.1409	.0531	.0210	.0088	.0039	.0019	.0009
	8		.4545	.1884	.0410	.0300	.0128	.0058	.0028	.0014
	9		.5455	.2409	.0993	.0415	.0180	.0082	.0039	.0020
	10			.3000	.1301	.0559	.0248	.0115	.0056	.0028
	11			.3636	.1650	.0734	.0332	.0156	.0076	.0039
	12			.4318	.2070	.0949	.0440	.0209	.0103	.0053
	13			.5000	.2517	.1199	.0567	.0274	.0137	.0071
	14				.3021	.1489	.0723	.0356	.0180	.0094
	15				.3552	.1818	.0905	.0454	.0232	.0122
	16				.4126	.2188	.1119	.0571	.0296	.0157
	17				.4699	.2592	.1361	.0708	.0372	.0200
	18				.5301	.3032	.1638	.0869	.0464	.0252
	19					.3497	.1942	.1052	.0570	.0313
U_0	20					.3986	.2280	.1261	.0694	.0365
	21					.4491	.2643	.1496	.0836	.0470
	22					.5000	.3035	.1755	.0998	.0567
	23						.3445	.2039	.1179	.0680
	24						.3878	.2349	.1383	.0807
	25						.4320	.2680	.1606	.0951
	26						.4773	.3032	.1852	.1112
	27						.5227	.3403	.2117	.1290
	28							.3788	.2404	.1487
	29							.4185	.2707	.1701
	30							.4591	.3029	.1933
	31							.5000	.3365	.2181
	32								.3715	.2447
	33								.4074	.2729
	34								.4442	.3024
	35								.4813	.3332
	36								.5187	.3652
	37									.3981
	38									.4317
	39									.4657
	40									.5000

Table C-1 Probability of $P(U \leq U_0)$ (24). (cont.)

		n_2=10									
	n_1	1	2	3	4	5	6	7	8	9	10
	0	.0909	.0152	.0035	.0010	.0003	.0001	.0001	.0000	.0000	.0000
	1	.1818	.0303	.0070	.0020	.0007	.0002	.0001	.0000	.0000	.0000
	2	.2727	.0606	.0140	.0040	.0013	.0005	.0002	.0001	.0000	.0000
	3	.3636	.0909	.0245	.0070	.0023	.0009	.0004	.0002	.0001	.0000
	4	.4545	.1364	.0385	.0120	.0040	.0015	.0006	.0003	.0001	.0001
	5	.5455	.1818	.0559	.0180	.0063	.0024	.0010	.0004	.0002	.0001
	6		.2424	.0804	.0270	.0097	.0037	.0015	.0007	.0003	.0002
	7		.3030	.1084	.0380	.0140	.0055	.0023	.0010	.0005	.0002
	8		.3788	.1434	.0529	.0200	.0080	.0034	.0015	.0007	.0004
	9		.4545	.1853	.0709	.0276	.0112	.0048	.0022	.0011	.0005
	10		.5455	.2343	.0939	.0376	.0156	.0068	.0031	.0015	.0008
	11			.2867	.1199	.0496	.0210	.0093	.0043	.0021	.0010
	12			.3462	.1518	.0646	.0280	.0125	.0058	.0028	.0014
	13			.4056	.1868	.0823	.0363	.0165	.0078	.0038	.0019
	14			.4685	.2268	.1032	.0467	.0215	.0103	.0051	.0025
	15			.5315	.2697	.1272	.0589	.0277	.0133	.0066	.0034
	16				.3177	.1548	.0736	.0351	.0171	.0086	.0045
	17				.3666	.1855	.0903	.0439	.0217	.0110	.0057
	18				.4196	.2198	.1099	.0544	.0273	.0140	.0073
	19				.4725	.2567	.1317	.0665	.0338	.0175	.0093
	20				.5275	.2970	.1566	.0806	.0416	.0217	.0116
	21					.3393	.1838	.0966	.0506	.0267	.0144
	22					.3839	.2139	.1148	.0610	.0326	.0177
	23					.4296	.2461	.1349	.0729	.0394	.0216
	24					.4765	.2811	.1574	.0864	.0474	.0262
U_0	25					.5235	.3177	.1819	.1015	.0564	.0315
	26						.3564	.2087	.1185	.0667	.0376
	27						.3962	.2374	.1371	.0782	.0446
	28						.4374	.2681	.1577	.0912	.0526
	29						.4789	.3004	.1800	.1055	.0615
	30						.5211	.3345	.2041	.1214	.0716
	31							.3698	.2299	.1388	.0827
	32							.4063	.2574	.1577	.0952
	33							.4434	.2863	.1781	.1088
	34							.4811	.3167	.2001	.1237
	35							.5189	.3482	.2235	.1399
	36								.3809	.2483	.1575
	37								.4143	.2745	.1763
	38								.4484	.3019	.1965
	39								.4827	.3304	.2179
	40								.5173	.3598	.2406
	41									.3901	.2644
	42									.4211	.2894
	43									.4524	.3153
	44									.4841	.3421
	45									.5159	.3697
	46										.3980
	47										.4267
	48										.4559
	49										.4853
	50										.5147

Table C-2 Critical Values for Mann Whitney U Test (U_α)(24).

n_1	n_2	$\alpha(2)$: 0.20 / $\alpha(1)$: 0.10	0.10 / 0.05	0.05 / 0.025	0.02 / 0.01	0.01 / 0.005	0.005 / 0.0025	0.002 / 0.001	0.001 / 0.0005
1	1	—	—	—	—	—	—	—	—
	2	—	—	—	—	—	—	—	—
	3	—	—	—	—	—	—	—	—
	4	—	—	—	—	—	—	—	—
	5	—	—	—	—	—	—	—	—
	6	—	—	—	—	—	—	—	—
	7	—	—	—	—	—	—	—	—
	8	—	—	—	—	—	—	—	—
	9	9	—	—	—	—	—	—	—
	10	10	—	—	—	—	—	—	—
	11	11	—	—	—	—	—	—	—
	12	12	—	—	—	—	—	—	—
	13	13	—	—	—	—	—	—	—
	14	14	—	—	—	—	—	—	—
	15	15	—	—	—	—	—	—	—
	16	16	—	—	—	—	—	—	—
	17	17	—	—	—	—	—	—	—
	18	18	—	—	—	—	—	—	—
	19	18	19	—	—	—	—	—	—
	20	19	20	—	—	—	—	—	—
	21	20	21	—	—	—	—	—	—
	22	21	22	—	—	—	—	—	—
	23	22	23	—	—	—	—	—	—
	24	23	24	—	—	—	—	—	—
	25	24	25	—	—	—	—	—	—
	26	25	26	—	—	—	—	—	—
	27	26	27	—	—	—	—	—	—
	28	27	28	—	—	—	—	—	—
	29	27	29	—	—	—	—	—	—
	30	28	30	—	—	—	—	—	—
	31	29	31	—	—	—	—	—	—
	32	30	32	—	—	—	—	—	—
	33	31	33	—	—	—	—	—	—
	34	32	34	—	—	—	—	—	—
	35	33	35	—	—	—	—	—	—
	36	34	36	—	—	—	—	—	—
	37	35	37	—	—	—	—	—	—
	38	36	38	—	—	—	—	—	—
	39	36	38	39	—	—	—	—	—
1	40	37	39	40	—	—	—	—	—
2	2	—	—	—	—	—	—	—	—
	3	6	—	—	—	—	—	—	—
	4	8	—	—	—	—	—	—	—
	5	9	10	—	—	—	—	—	—
	6	11	12	—	—	—	—	—	—
	7	10	14	—	—	—	—	—	—
	8	14	15	16	—	—	—	—	—
	9	16	17	18	—	—	—	—	—
	10	17	19	20	—	—	—	—	—
	11	19	21	22	—	—	—	—	—
	12	20	22	23	—	—	—	—	—
	13	22	24	25	26	—	—	—	—
	14	23	25	27	28	—	—	—	—
2	15	25	27	29	30	—	—	—	—

Table C-2 Critical Values for Mann Whitney U Test (U_α) (24).(cont.)

n_1	n_2	$\alpha(2)$: 0.20	0.10	0.05	0.02	0.01	0.005	0.002	0.001
		$\alpha(1)$: 0.10	0.05	0.025	0.01	0.005	0.0025	0.001	0.0005
2	16	27	29	31	32	—	—	—	—
	17	28	31	32	34	—	—	—	—
	18	30	32	34	36	—	—	—	—
	19	31	34	36	37	38	—	—	—
	20	33	36	38	39	40	—	—	—
	21	34	37	39	41	42	—	—	—
	22	36	39	41	43	44	—	—	—
	23	37	41	43	45	46	—	—	—
	24	39	42	45	47	48	—	—	—
	25	41	44	47	49	50	—	—	—
	26	42	46	48	51	52	—	—	—
	27	44	47	50	52	53	54	—	—
	28	45	49	52	54	55	56	—	—
	29	47	51	54	56	57	58	—	—
	30	48	53	55	58	59	60	—	—
	31	50	54	57	60	61	62	—	—
	32	51	56	59	62	63	64	—	—
	33	53	58	61	64	65	66	—	—
	34	55	59	63	65	67	68	—	—
	35	56	61	64	67	69	70	—	—
	36	58	63	66	69	71	72	—	—
	37	59	64	68	71	73	74	—	—
	38	61	66	70	73	75	76	—	—
	39	62	68	71	75	76	77	—	—
2	40	64	69	73	77	78	79	—	—
3	3	8	9	—	—	—	—	—	—
	4	11	12	—	—	—	—	—	—
	5	13	14	15	—	—	—	—	—
	6	15	16	17	—	—	—	—	—
	7	15	19	20	21	—	—	—	—
	8	19	21	22	24	—	—	—	—
	9	22	23	25	26	27	—	—	—
	10	24	26	27	29	30	—	—	—
	11	26	28	30	32	33	—	—	—
	12	28	31	32	34	35	36	—	—
	13	30	33	35	37	38	39	—	—
	14	32	35	37	40	41	42	—	—
	15	35	38	40	42	43	44	—	—
	16	37	40	42	45	46	47	—	—
	17	39	42	45	47	49	50	51	—
	18	41	45	47	50	52	53	54	—
	19	43	47	50	53	54	56	57	—
	20	45	49	52	55	57	58	60	—
	21	48	52	55	58	60	61	62	63
	22	50	54	57	60	62	64	65	66
	23	52	56	60	63	65	67	68	69
	24	54	59	62	66	68	69	71	72
	25	56	61	65	68	70	72	74	75
	26	58	63	67	71	73	75	77	78
	27	60	66	70	74	76	78	79	80
	28	63	68	72	76	79	80	82	83
	29	65	70	74	79	81	83	85	86
3	30	67	73	77	81	84	86	88	89

Table C-2 Critical Values for Mann Whitney U Test (U_α) (24).(cont.)

n_1	n_2	$\alpha(2)$: 0.20	0.10	0.05	0.02	0.01	0.005	0.002	0.001
		$\alpha(1)$: 0.10	0.05	0.025	0.01	0.005	0.0025	0.001	0.0005
3	31	69	75	79	84	87	89	91	92
	32	71	77	82	87	89	91	94	95
	33	73	80	84	89	92	94	96	98
	34	76	82	87	92	95	97	99	101
	35	78	84	89	94	97	100	102	103
	36	80	87	92	97	100	103	105	106
	37	82	89	94	100	103	105	108	109
	38	84	91	97	102	105	108	111	112
	39	86	94	99	105	108	111	113	115
3	40	89	96	102	107	111	114	116	118
4	4	13	15	16	—	—	—	—	—
	5	16	18	19	20	—	—	—	—
	6	19	21	22	23	24	—	—	—
	7	20	24	25	27	28	—	—	—
	8	25	27	28	30	31	32	—	—
	9	27	30	32	33	35	36	—	—
	10	30	33	35	37	38	39	40	—
	11	33	36	38	40	42	43	44	—
	12	36	39	41	43	45	46	48	—
	13	39	42	44	47	49	50	51	52
	14	41	45	47	50	52	53	55	56
	15	44	48	50	53	55	57	59	60
	16	47	50	53	57	59	60	62	63
	17	50	53	57	60	62	64	66	67
	18	52	56	60	63	66	67	69	71
	19	55	59	63	67	69	71	73	74
	20	58	62	66	70	72	75	77	78
	21	61	65	69	73	76	78	80	82
	22	63	68	72	77	79	82	84	85
	23	66	71	75	80	83	85	88	89
	24	69	74	79	83	86	89	91	93
	25	72	77	82	87	90	92	95	97
	26	74	80	85	90	93	96	98	100
	27	77	83	88	93	96	99	102	104
	28	80	86	91	96	100	103	106	108
	29	83	89	94	100	103	106	109	111
	30	85	92	97	103	107	110	113	115
	31	88	95	100	106	110	113	117	119
	32	91	98	104	110	114	117	120	122
	33	94	101	107	113	117	120	124	126
	34	96	104	110	116	120	124	127	130
	35	99	107	113	120	124	127	131	133
	36	102	110	116	123	127	131	135	137
	37	105	113	119	126	131	134	138	141
	38	107	116	122	130	134	138	142	144
	39	110	118	125	133	137	141	145	148
4	40	113	121	129	136	141	145	149	152
5	5	20	21	23	24	25	—	—	—
	6	23	25	27	28	29	30	—	—
	7	24	29	30	32	34	35	—	—
	8	30	32	34	36	38	39	40	—
	9	33	36	38	40	42	43	44	45
	10	37	39	42	44	46	47	49	50

Table C-2 Critical Values for Mann Whitney U Test (U_α) (24).(cont.)

n_1	n_2	$\alpha(2)$: 0.20 $\alpha(1)$: 0.10	0.10 0.05	0.05 0.025	0.02 0.01	0.01 0.005	0.005 0.0025	0.002 0.001	0.001 0.0005
5	11	40	43	46	48	50	52	53	54
	12	43	47	49	52	54	56	58	59
	13	47	50	53	56	58	60	62	63
	14	50	54	57	60	63	64	67	68
	15	53	57	61	64	67	69	71	72
	16	57	61	65	68	71	73	75	77
	17	60	65	68	72	75	77	80	81
	18	63	68	72	76	79	81	84	86
	19	67	72	76	80	83	86	88	90
	20	70	75	80	84	87	90	93	95
	21	73	79	83	88	91	94	97	99
	22	77	82	87	92	96	98	102	104
	23	80	86	91	96	100	103	106	108
	24	84	90	95	100	104	107	110	113
	25	87	93	98	104	108	111	115	117
	26	90	97	102	108	112	115	119	121
	27	94	100	106	112	119	120	123	126
	28	97	104	110	116	120	124	128	130
	29	100	107	113	120	124	128	132	135
	30	104	111	117	124	128	132	136	139
	31	107	115	121	128	133	136	141	144
	32	110	118	125	132	137	141	145	148
	33	114	122	128	136	141	145	150	153
	34	117	125	132	140	145	149	154	157
	35	120	129	136	144	149	153	158	161
	36	124	132	140	148	153	158	163	166
	37	127	136	144	152	157	162	167	170
	38	130	140	147	156	161	166	171	175
	39	134	143	151	160	165	170	176	179
5	40	137	147	155	164	169	174	180	184
6	6	27	29	31	33	34	35	—	—
	7	29	34	36	38	39	40	42	—
	8	35	38	40	42	44	45	47	48
	9	39	42	44	47	49	50	52	53
	10	43	46	49	52	54	55	57	58
	11	47	50	53	57	59	60	62	64
	12	51	55	58	61	63	65	68	69
	13	55	59	62	66	68	70	73	74
	14	59	63	67	71	73	75	78	79
	15	63	67	71	75	78	80	83	85
	16	67	71	75	80	83	85	88	90
	17	71	76	80	84	87	90	93	95
	18	74	80	84	89	92	95	98	100
	19	78	84	89	94	97	100	103	106
	20	82	88	93	98	102	105	108	111
	21	86	92	97	103	107	110	114	116
	22	90	96	102	108	111	115	119	121
	23	94	101	106	112	116	120	124	126
	24	98	105	111	117	121	125	129	132
6	25	102	109	115	121	126	130	134	137

Table C-2 Critical Values for Mann Whitney U Test (U_α) (24).(cont.)

n_1	n_2	α(2): 0.20 α(1): 0.10	0.10 0.05	0.05 0.025	0.02 0.01	0.01 0.005	0.005 0.0025	0.002 0.001	0.001 0.0005
6	26	106	113	119	126	131	134	139	142
	27	110	117	124	131	135	139	144	147
	28	114	122	128	135	140	144	149	152
	29	118	126	132	140	145	149	154	157
	30	122	130	137	145	150	154	159	163
	31	125	134	141	149	154	159	164	168
	32	129	138	146	154	159	164	169	173
	33	133	142	150	158	164	169	174	178
	34	137	147	154	163	169	174	179	183
	35	141	151	159	168	173	179	185	188
	36	145	155	163	172	178	184	190	194
	37	149	159	167	177	183	188	195	199
	38	153	163	172	182	188	193	200	204
	39	157	167	176	186	193	198	205	209
6	40	161	172	181	191	197	203	210	214
7	7	36	38	41	43	45	46	48	49
	8	40	43	46	49	50	52	54	55
	9	45	48	51	54	56	58	60	61
	10	49	53	56	59	61	63	65	67
	11	54	58	61	65	67	69	71	73
	12	58	63	66	70	72	75	77	79
	13	63	67	71	75	78	80	83	85
	14	67	72	76	81	83	86	89	91
	15	72	77	81	86	89	92	95	97
	16	76	82	86	91	94	97	101	103
	17	81	86	91	96	100	103	106	109
	18	85	91	96	102	105	108	112	115
	19	90	96	101	107	111	114	118	120
	20	94	101	106	112	116	120	124	126
	21	99	106	111	117	122	125	129	132
	22	103	110	116	123	127	131	135	138
	23	108	115	121	128	132	136	141	144
	24	112	120	126	133	138	142	147	150
	25	117	125	131	139	143	148	153	156
	26	121	129	136	144	149	153	158	162
	27	126	134	141	149	154	159	164	168
	28	130	139	146	154	160	164	170	174
	29	135	144	151	160	165	170	176	179
	30	139	149	156	165	170	176	181	185
	31	144	153	161	170	176	181	187	191
	32	148	158	166	175	181	187	193	197
	33	153	163	171	181	187	192	199	203
	34	157	168	176	186	192	198	204	209
	35	162	172	181	191	198	203	210	215
	36	166	177	186	196	203	209	216	221
	37	171	182	191	202	208	215	222	227
	38	175	187	196	207	214	220	227	232
	39	180	191	201	212	219	226	233	238
7	40	184	196	206	217	225	231	239	244
8	8	45	49	51	55	57	58	60	62
	9	50	54	57	61	63	65	67	68
8	10	56	60	63	67	69	71	74	75

Table C-2 Critical Values for Mann Whitney U Test (U_α) (24).(cont.)

n_1	n_2	$\alpha(2)$: 0.20	0.10	0.05	0.02	0.01	0.005	0.002	0.001
		$\alpha(1)$: 0.10	0.05	0.025	0.01	0.005	0.0025	0.001	0.0005
8	11	61	65	69	73	75	77	80	82
	12	66	70	74	79	81	84	87	89
	13	71	76	80	84	87	90	93	95
	14	76	81	86	90	94	96	100	102
	15	81	87	91	96	100	103	106	109
	16	86	92	97	102	106	109	113	115
	17	91	97	102	108	112	115	119	122
	18	96	103	108	114	118	122	126	129
	19	101	108	114	120	124	128	132	135
	20	106	113	119	126	130	134	139	142
	21	112	119	125	132	136	140	145	148
	22	117	124	131	138	142	147	152	155
	23	122	130	136	144	149	153	158	162
	24	127	135	142	150	155	159	165	168
	25	132	140	147	155	161	165	171	175
	26	137	146	153	161	167	172	177	181
	27	142	151	159	167	173	178	184	188
	28	147	156	164	173	179	184	190	195
	29	152	162	170	179	185	190	197	201
	30	157	167	175	185	191	197	203	208
	31	162	172	181	191	197	203	210	214
	32	167	178	187	197	203	209	216	221
	33	172	183	192	203	209	215	223	227
	34	177	188	198	208	215	222	229	234
	35	182	194	203	214	221	228	235	241
	36	188	199	209	220	228	234	242	247
	37	193	205	215	226	234	240	248	254
	38	198	210	220	232	240	247	255	260
	39	203	215	226	238	246	253	261	267
8	40	208	221	231	244	252	259	268	273
9	9	56	60	64	67	70	72	74	76
	10	62	66	70	74	77	79	82	83
	11	68	72	76	81	83	86	89	91
	12	73	78	82	87	90	93	96	98
	13	79	84	89	94	97	100	103	106
	14	85	90	95	100	104	107	111	113
	15	90	96	101	107	111	114	118	120
	16	96	102	107	113	117	121	125	128
	17	101	108	114	120	124	128	132	135
	18	107	114	120	126	131	135	139	142
	19	113	120	126	133	138	142	146	150
	20	118	126	132	140	144	149	154	157
	21	124	132	139	146	151	155	161	164
	22	130	138	145	153	158	162	168	172
	23	135	144	151	159	164	169	175	179
	24	141	150	157	166	171	176	182	186
	25	147	156	163	172	178	183	189	193
	26	152	162	170	179	185	190	196	201
	27	158	168	176	185	191	197	203	208
	28	164	174	182	192	198	204	211	215
	29	169	179	188	198	205	211	218	222
9	30	175	185	194	205	212	218	225	230

Table C-2 Critical Values for Mann Whitney U Test (U_α) (24).(cont.)

n_1	n_2	α(2): 0.20	0.10	0.05	0.02	0.01	0.005	0.002	0.001
		α(1): 0.10	0.05	0.025	0.01	0.005	0.0025	0.001	0.0005
9	31	180	191	201	211	218	224	232	237
	32	186	197	207	218	225	231	239	244
	33	192	203	213	224	232	238	246	251
	34	197	209	219	231	238	245	253	259
	35	203	215	226	237	245	252	260	266
	36	209	221	232	244	252	259	267	273
	37	214	227	238	250	258	266	275	280
	38	220	233	244	257	265	273	282	288
	39	225	239	250	263	272	280	289	295
9	40	231	245	257	270	279	286	296	302
10	10	68	73	77	81	84	87	90	92
	11	74	79	84	88	92	94	98	100
	12	81	86	91	96	99	102	106	108
	13	87	93	97	103	106	110	113	116
	14	93	99	104	110	114	117	121	124
	15	99	106	111	117	121	125	129	132
	16	106	112	118	124	129	133	137	140
	17	112	119	125	132	136	140	145	148
	18	118	125	132	139	143	148	153	156
	19	124	132	138	146	151	155	161	164
	20	130	138	145	153	158	163	168	172
	21	137	145	152	160	166	170	176	180
	22	143	152	159	167	173	178	184	188
	23	149	158	166	175	180	186	192	196
	24	155	165	173	182	188	193	200	204
	25	161	171	179	189	195	201	207	212
	26	168	178	186	196	202	208	215	220
	27	174	184	193	203	210	216	223	228
	28	180	191	200	210	217	223	231	236
	29	186	197	207	217	224	231	238	244
	30	192	204	213	224	232	238	246	252
	31	199	210	220	232	239	246	254	259
	32	205	217	227	239	246	253	262	267
	33	211	223	234	246	254	261	269	275
	34	217	230	241	253	261	268	277	283
	35	223	236	247	260	268	276	285	291
	36	229	243	254	267	276	284	293	299
	37	236	249	261	274	283	291	300	307
	38	242	256	268	281	290	299	308	315
	39	248	262	275	289	298	306	316	323
10	40	254	269	281	296	305	314	324	331
11	11	81	87	91	96	100	103	106	109
	12	88	94	99	104	108	111	115	117
	13	95	101	106	112	116	119	123	126
	14	102	108	114	120	124	128	132	135
	15	108	115	121	128	132	136	141	144
	16	115	122	129	135	140	144	149	152
	17	122	130	136	143	148	152	158	161
	18	129	137	143	151	156	161	166	170
	19	136	144	151	159	164	169	175	178
11	20	142	151	158	167	172	177	183	187

APPENDIX D

Definition

- k refers to the emptying rate in one minutes (1/minute).
- β is the extrapolated y-intercept from the terminal portion of the modified power exponential curve.
- Lag phase time (TLAG) is the time the stomach consumes to digest food until it can pass through the pylorus.
- Constant emptying time (T_{RE}) is the emptying rate which is being constant.
- Emptying half time ($T_{1/2}$) is the time the stomach has emptied half of the food in the stomach.

BIOGRAPHY

NAME	Miss. Atchara Promdaung
DATE OF BIRTH	18 December 1982
PLACE OF BIRTH	Phatthalung, Thailand
INSTITUTIONS ATTENDED	Mahidol University, 2006 Bachelor of Science (Radiological Technology) Mahidol University, 2011 Master of Science (Medical Physics)
HOME ADDRESS	The Room Condo Ratchada-Ladprao, 518/1 Building A, Ladprao Road, Chandrakasem, Jatujak, Bangkok, Thailand 10900